Multi-Mode Proper-Time Spacetime Formalism (ZMUT): A Unified Theory — Axiomatic Construction, Self-Critical Audit, Systematic Refutation Tests, and Classical Correspondence

Yamaç Gürsel
Independent Researcher
yamacgursel0@gmail.com

August 6, 2026

Abstract

This paper constructs, audits and experimentally confronts the Multi-Mode Proper-Time Spacetime Formalism (ZMUT, from its Turkish acronym), in which proper time is a normalized temporal-mode wave function $|\psi(\xi)\rangle$ in a Hilbert space. **Part I** derives the mode Klein–Gordon and extended Einstein equations from a single master action on the extended $(4+1)$ manifold ($\mathrm{d}s^2 = g_{\mu\nu}\mathrm{d}x^\mu \mathrm{d}x^\nu - f(\xi)\mathrm{d}\xi^2$); recovers Newton's law exactly in the $\hat{O}_{AB} \to 1$ limit of a normalized overlap integral by the Cauchy–Schwarz theorem; derives the mass–mode relation $\lambda_m = \kappa/m$ with $\kappa = \hbar/c^2$ from tachyon avoidance (the Planck mass emerging as the natural quantum-to-classical threshold); and circumvents Pauli's obstruction via the Page–Wootters constraint and quantum reference frames. **Part II** diagnoses and closes nine structural weaknesses (Z1–Z9) at theorem level: exact CPTP decoherence dynamics with a non-Markovian master equation; collective-mode metrology (SQL–Heisenberg band); proofs of causality, ghost-freedom, Kaluza–Klein pruning and Hadamard well-posedness; tuning-free radion decoupling by a spectral-locality kernel, preservation of the weak equivalence principle and Banks–Peskin–Susskind compatibility; mode diffusion with the m^{-2} freeze-out of a single classical time; and the identification of the dark-energy density with the fibre scale ($c\,\ell_\xi \approx 88$ μm). **Part III** unifies the Kuchař, covariance, kernel-composition and Casimir-sign repairs under a single *Master Law*: every interaction is subject to a renormalization-group flow — exactly solvable in the Gaussian sector — between the system scale $\mu_S = mc^2/\hbar$ and the fibre geometry, with observables projected onto a single temporal superselection sector; eight structures (C1–C8) follow as corollaries. The one-loop flow of the mode-hopping sector, $\beta(\tilde{g}) = 3\tilde{g} - (3/2\pi)\tilde{g}^2$, terminates at the IR-attractive universal fixed point $\tilde{g}_* = 2\pi$: the flow acquires genuine Wilsonian character at no cost in free parameters. A one-to-one dictionary between decay law and mode distribution is established (Gaussian→Gaussian, Lorentzian→exponential T_2, discrete combs→revivals); band limitation predicts sudden death of coherence at $t_{\mathrm{sd}} = 2mc^2\Theta_*/\Delta E$ and complete distribution tomography. Confrontation with current data yields a two-step experimental ratchet, $\Theta_* \geq 2.6 \times 10^{-9}$ s and $\alpha_\xi = \ell_\xi/\Theta_* \lesssim 1.1 \times 10^{-4}$; a fourteen-class audit finds zero contradictions, six exact-null predictions are confirmed by data, and the [4.3, 66] s coherence band of the ^{229}Th nuclear clock is posed as the primary forthcoming test. All principal results pass an independent numeric–symbolic reverse-verification protocol (25/25), and classical physics — absolute time, geodesic motion, exponential T_2, the thermodynamic arrow — is derived as a family of ZMUT limit theorems at the Ehrenfest and WKB level.

Keywords: quantum gravity; proper time; temporal mode distributions; quantum reference frames; decoherence; renormalization group; superselection; dark energy; quantum information; arrow of time; classical limit.

1 Introduction: Method and Road Map

Quantum mechanics treats time as an external parameter, while general relativity treats it as a dynamical quantity tied to the metric; the tension at the intersection of the two definitions is known as the "problem of time" of quantum gravity [10]. It is known that superpositions of proper times are observable in principle [2],

that time dilation opens a universal decoherence channel [1], that time can be recovered relationally [3,5], and that more than one timelike direction can be carried consistently [4]. ZMUT unifies these threads in a single proposal: *proper time is not a single-valued classical parameter but a quantum degree of freedom described by a normalized temporal-mode wave function* $\psi(\xi)$.

This unified paper collects the three developmental stages of the theory in a single self-contained text; rather than flattening the stages into an ahistorical "final version", however, it deliberately preserves the *dialectical* order: first the construction, then a merciless audit of the construction, then the confrontation of what survives with experiment and with deeper mathematics. There are two reasons. The first is scientific: the value of a theory comes not from its defence but from its resilience against attempts at demolition, and the reader-referee should be able to check within the text itself which objection was considered and how it was closed. The second is structural: every theorem of the later parts was born as an answer to a specific gap in the earlier parts, and while this link remains visible the degrees of freedom of the theory — what is forced and what is a choice — stay sharp.

Part I (Sections 2–4) establishes the axiomatic core: the mode Hilbert space, the extended metric, the master action, the field equations, the Newtonian limit, the overlap integral, locality via the retarded Green function, real proper-time kinematics, the derivation of $\lambda_m = \kappa/m$, the Pauli–Page–Wootters–QRF structure, and the historically first model of decoherence. **Part II** (Sections 5–13) diagnoses and closes nine structural weaknesses (Z1–Z9) and carries the theory to the applications of spectral locality, mode leakage, the scalar sector, the cosmological identification, quantum information and the arrow of time. **Part III** (Sections 14–21) first lays down the Master Law: the RG–superselection principle that derives the entire repair layer at once as corollaries C1–C8 (§14), and the mode-hopping sector that promotes it to a genuine Wilson flow (§15); it then runs and repairs four deep mathematical refutation attempts (the Kuchař objection; a covariance violation; a kernel-composition ambiguity; a Casimir sign error); places temporal-mode distributions at the measurable centre of the theory; performs the numerical confrontation with current experimental data (in which some of the theory's older numbers are genuinely *refuted* and updated, the neutrino sector included); and derives classical physics as a family of ZMUT limits.

1.1 Notation, units and signature

Unless stated otherwise, SI units are used and $\hbar$, c and G are kept explicit. Four-dimensional spacetime indices are $\mu, \nu, \dots \in \{0,1,2,3\}$; extended five-dimensional indices are $A, B, \dots \in \{0,1,2,3,\xi\}$. The metric signature is $(-,+,+,+)$ and $x^0 = ct$. The mode parameter ξ has the dimension of time: $[\xi] = \mathrm{s}$. For the fibre metric function $f(\xi) > 0$ we write $f(\xi) = c^2\hat{f}(\xi)$; $\hat{f}$ is dimensionless and the gauge $\hat{f} = 1$ is used unless stated otherwise. Complex conjugation is denoted z^*; all derivation steps are written out explicitly.

Part I
Core Theory: Axiomatic Construction

2 Mathematical Framework and Action Formalism

2.1 Temporal mode space, Hilbert structure and axioms

The kinematic skeleton of ZMUT is erected on the following five axioms.

Axiom 1 (Mode array)**.** Every physical system is accompanied by a spectrum of temporal modes. In compact or bound configurations this spectrum is discrete,

$$T = \{T_1, T_2, T_3, \dots\}, \qquad T_n \in \mathbb{R}, \tag{1}$$

and the values T_n are eigenvalues of the mode operator $\hat{\xi}$. In the general case the spectrum is continuous and is parametrized by the continuous mode variable $\xi \in \mathbb{R}$; the discrete case is recovered in the limit in which the spectral measure condenses onto Dirac combs.

Axiom 2 (Mode Hilbert space and state vector)**.** Temporal modes live in the Hilbert space

$$\mathcal{H}_{\mathrm{mod}} = L^2(\mathbb{R}, \mathrm{d}\xi). \tag{2}$$

The temporal state of a system is

$$|\psi\rangle = \int_{-\infty}^{\infty} \mathrm{d}\xi\ \psi(\xi)\ |\xi\rangle\,, \qquad \langle\xi|\xi'\rangle = \delta(\xi - \xi'), \tag{3}$$

and, by the probabilistic interpretation, it satisfies the normalization condition

$$\boxed{\int_{-\infty}^{\infty} |\psi(\xi)|^2 \, \mathrm{d}\xi = 1} \tag{4}$$

Dimensional analysis: since $[|\psi|^2 \mathrm{d}\xi] = 1$, one has $[\psi] = \mathrm{s}^{-1/2}$.

Axiom 3 (Extended manifold)**.** The physical arena is the manifold $\mathcal{M}_5 = \mathcal{M}_4 \times \Sigma_\xi$, the product of the four-dimensional Lorentzian manifold $\mathcal{M}_4$ with the mode fibre Σ_ξ, equipped with the extended metric

$$\boxed{\mathrm{d}s^2 = g_{\mu\nu}(x)\, \mathrm{d}x^\mu \mathrm{d}x^\nu - f(\xi)\, \mathrm{d}\xi^2} \tag{5}$$

Here $f(\xi) > 0$ has dimension $[f] = \mathrm{m}^2\,\mathrm{s}^{-2}$ and we write $f(\xi) = c^2 \hat{f}(\xi)$. The minus sign expresses the timelike character of the ξ direction; this is structurally akin to Bars's two-time physics [4], and the removal of ghost degrees of freedom is addressed in §2.4.

Axiom 4 (Energy distribution and its conservation)**.** The energy of a system with total energy E_{tot} is distributed over the modes with density

$$\mathrm{d}E(\xi) = E_{\mathrm{tot}} \, |\psi(\xi)|^2 \, \mathrm{d}\xi. \tag{6}$$

Axiom 5 (Composite systems)**.** The mode space of a composite system built from systems A and B is the tensor product $\mathcal{H}^A_{\mathrm{mod}} \otimes \mathcal{H}^B_{\mathrm{mod}}$. States prepared without interaction are of product form: $\psi_{AB}(\xi_A, \xi_B) = \psi_A(\xi_A)\, \psi_B(\xi_B)$.

Lemma 2.1 (Internal consistency of energy conservation)**.** *The distribution of Axiom 4 conserves the total energy identically:*

$$\int_{-\infty}^{\infty} \mathrm{d}E(\xi) = E_{tot} \int_{-\infty}^{\infty} |\psi(\xi)|^2 \mathrm{d}\xi = E_{tot} \cdot 1 = E_{tot}. \tag{7}$$

Proof. Immediate, by applying the normalization condition (4) to (6). The consistency of the distribution rests on the preservation of the normalization under the dynamics; this in turn is a consequence of the unitary mode flow to be constructed in §2.4. □

Definition 2.2 (Dominant mode, mode mean and mode width)**.** With $w(\xi) := |\psi(\xi)|^2$ the mode density, define

$$\xi_{\max} := \arg\max_{\xi} \, |\psi(\xi)|^2 \qquad \text{(dominant mode)}, \tag{8}$$

$$\Theta := \int_{-\infty}^{\infty} \xi \, |\psi(\xi)|^2 \, \mathrm{d}\xi \qquad \text{(mode mean)}, \tag{9}$$

$$\sigma_\xi^2 := \int_{-\infty}^{\infty} (\xi - \Theta)^2 \, |\psi(\xi)|^2 \, \mathrm{d}\xi \qquad \text{(mode variance)}. \tag{10}$$

In the classical limit Θ is the effective proper-time value corresponding to the observer's "now".

Lemma 2.3. *For a Gaussian mode packet $\psi(\xi) = (2\pi\sigma_\xi^2)^{-1/4} \exp\!\left[-(\xi-\Theta)^2/(4\sigma_\xi^2) + i\varphi(\xi)\right]$ one has $\xi_{\max} = \Theta$; that is, the dominant mode and the mode mean coincide. For general asymmetric distributions $\xi_{\max} \neq \Theta$ is possible, and the difference contributes at second order to the decoherence rate, as shown in §4.4.*

Proof. $w(\xi) = (2\pi\sigma_\xi^2)^{-1/2} e^{-(\xi-\Theta)^2/(2\sigma_\xi^2)}$ attains its single maximum at $\mathrm{d}w/\mathrm{d}\xi = 0 \Rightarrow \xi = \Theta$; the second derivative at $\xi = \Theta$ is negative. □

2.2 Geometry of the extended metric

The metric (5) is block diagonal: $\tilde{g}_{AB} = \mathrm{diag}\big(g_{\mu\nu}(x),\, -f(\xi)\big)$, so that $\tilde{g}^{\xi\xi} = -1/f(\xi)$. For the determinant,

$$\det \tilde{g} = -f(\xi)\, \det g \quad \Rightarrow \quad \sqrt{|\det \tilde{g}|} = \sqrt{-g}\, \sqrt{f} = c\sqrt{-g}\, \sqrt{\hat{f}}, \tag{11}$$

where $\det g < 0$ is the determinant of the four-dimensional Lorentzian metric. The nonvanishing Christoffel symbols follow by direct computation:

$$\tilde{\Gamma}^\mu{}_{\nu\rho} = \Gamma^\mu{}_{\nu\rho}[g], \qquad \tilde{\Gamma}^\xi{}_{\xi\xi} = \frac{f'(\xi)}{2f(\xi)}, \tag{12}$$

and, because $g_{\mu\nu}$ is independent of ξ and f is independent of x, all mixed components vanish:

$$\begin{aligned} \tilde{\Gamma}^\xi{}_{\mu\nu} &= -\tfrac{1}{2}\tilde{g}^{\xi\xi}\partial_\xi g_{\mu\nu} = 0, & \tilde{\Gamma}^\mu{}_{\nu\xi} &= \tfrac{1}{2} g^{\mu\sigma}\partial_\xi g_{\sigma\nu} = 0, \\ \tilde{\Gamma}^\mu{}_{\xi\xi} &= \tfrac{1}{2} g^{\mu\sigma}\partial_\sigma f = 0, & \tilde{\Gamma}^\xi{}_{\mu\xi} &= -\tfrac{1}{2f}\partial_\mu f = 0. \end{aligned} \tag{13}$$

Theorem 2.4 (Reduction of the scalar curvature)**.** *For the product metric* (5) *the five-dimensional Ricci scalar equals the four-dimensional one:* $\tilde{R} = R[g]$.

Proof. Using (12)–(13) in the Ricci tensor $\tilde{R}_{AB} = \partial_C \tilde{\Gamma}^C{}_{AB} - \partial_A \tilde{\Gamma}^C{}_{CB} + \tilde{\Gamma}^C{}_{CD}\tilde{\Gamma}^D{}_{AB} - \tilde{\Gamma}^C{}_{AD}\tilde{\Gamma}^D{}_{CB}$: (i) $\tilde{R}_{\mu\nu}$ contains only $\Gamma[g]$, hence $\tilde{R}_{\mu\nu} = R_{\mu\nu}[g]$; (ii) the mixed component $\tilde{R}_{\mu\xi} = 0$; (iii) for the $\xi\xi$ component,

$$\tilde{R}_{\xi\xi} = \partial_\xi \tilde{\Gamma}^\xi{}_{\xi\xi} - \partial_\xi \tilde{\Gamma}^C{}_{C\xi} + \tilde{\Gamma}^C{}_{C\xi}\tilde{\Gamma}^\xi{}_{\xi\xi} - \tilde{\Gamma}^C{}_{\xi D}\tilde{\Gamma}^D{}_{C\xi} = \partial_\xi \frac{f'}{2f} - \partial_\xi \frac{f'}{2f} + \left(\frac{f'}{2f}\right)^2 - \left(\frac{f'}{2f}\right)^2 = 0.$$

Therefore $\tilde{R} = \tilde{g}^{AB}\tilde{R}_{AB} = g^{\mu\nu}R_{\mu\nu} + \tilde{g}^{\xi\xi}\cdot 0 = R[g]$. □

Theorem 2.4 guarantees that the background geometry of the mode fibre adds no extra contribution to the four-dimensional curvature; the interaction of gravity with the mode sector proceeds solely through matter couplings and through perturbations of f (see §3.5).

2.3 The master action

The entire dynamics of ZMUT is derived from a single action. In its fully dimensional form,

$$S \;=\; \int \mathrm{d}^4x\,\mathrm{d}\xi\,\sqrt{-g}\,\sqrt{\hat{f}}\,\left[\frac{c^3}{16\pi G_5}\,\tilde{R} \;+\; \mathcal{L}_{\mathrm{mode}}(\Phi, \partial\Phi; \xi) \;+\; \mathcal{L}_{\mathrm{int}}(\Phi, g; \xi)\right], \tag{14}$$

where G_5 is the five-dimensional gravitational constant ($[G_5] = \mathrm{m}^3\,\mathrm{kg}^{-1}\,\mathrm{s}^{-1}$) and $\Phi(x, \xi)$ is the master mode field. With the effective length of the mode fibre

$$\ell_\xi := \int \sqrt{\hat{f}(\xi)}\,\mathrm{d}\xi \tag{15}$$

the four-dimensional Newton constant is defined, as in Kaluza–Klein reduction, through

$$\frac{1}{G} \;=\; \frac{\ell_\xi}{G_5} \tag{16}$$

[8, 9]. Using Theorem 2.4 ($\tilde{R} = R$) and (16), and absorbing the factor $\sqrt{\hat{f}}$ into the measure $\mathrm{d}\xi$ in the gauge $\hat{f} = 1$, the action descends to the compact canonical form of the theory:

$$\boxed{S = \int \mathrm{d}^4x\,\mathrm{d}\xi\,\sqrt{-g}\,\left[\frac{R}{16\pi G} + \mathcal{L}_{\mathrm{mode}}(\psi, \xi) + \mathcal{L}_{\mathrm{int}}\right]} \tag{17}$$

Here and in the remainder of the paper, the factors c^3 and ℓ_ξ^{-1} in front of $R/(16\pi G)$ are included in the definition of G according to (16); the SI counterparts are restored explicitly at every intermediate step.

Mode sector. The mode-sector Lagrangian density describing the collective field of the ensemble of temporal modes is a minimally coupled complex scalar:

$$\mathcal{L}_{\mathrm{mode}} \;=\; -\frac{\hbar^2}{2m}\,\tilde{g}^{AB}\,\partial_A\Phi^*\,\partial_B\Phi \;-\; \frac{mc^2}{2}\,|\Phi|^2, \tag{18}$$

while the *interaction sector* carries a nonminimal coupling to curvature:

$$\mathcal{L}_{\mathrm{int}} \;=\; -\frac{\alpha\,\hbar^2}{2m}\,R\,|\Phi|^2, \tag{19}$$

with α a dimensionless coupling constant. The factorized (mean-field) sector of the master field is

$$\Phi(x, \xi) \;=\; \frac{1}{\sqrt{c}}\,\chi(x)\,\psi(\xi), \qquad \int |\chi|^2 \mathrm{d}^3x = 1, \quad \int |\psi|^2 \mathrm{d}\xi = 1, \tag{20}$$

where the factor $1/\sqrt{c}$ closes the dimensional bookkeeping (see Table 1).

Proposition 2.5 (Dimensional consistency)**.** *The action* (14) *is dimensionally consistent: all three terms have density dimension* $[\mathcal{L}] = \mathrm{J\,m^{-4}}$*, and* S *has dimension* J s.

Proof. Since $[\mathrm{d}^4x\,\mathrm{d}\xi] = \mathrm{m}^4\,\mathrm{s}$, $[S] = \mathrm{J\,s}$ requires $[\mathcal{L}] = \mathrm{J\,m^{-4}}$. (i) Curvature term: $[\tilde{R}] = \mathrm{m^{-2}}$, $[c^3/G_5] = (\mathrm{m^3 s^{-3}})/(\mathrm{m^3 kg^{-1} s^{-1}}) = \mathrm{kg\,s^{-2}}$; the product is $\mathrm{kg\,m^{-2}\,s^{-2}} = \mathrm{J\,m^{-4}}$. (ii) Kinetic term: by (20), $[\Phi] = [\chi][\psi]/[c^{1/2}] = \mathrm{m^{-3/2}\,s^{-1/2}\,(m/s)^{-1/2}} = \mathrm{m^{-2}}$; $[\hbar^2/m] = \mathrm{J^2 s^2 kg^{-1}}$, $[\tilde{g}^{AB}\partial\partial] = \mathrm{m^{-2}}$, $[|\Phi|^2] = \mathrm{m^{-4}}$; the product is $\mathrm{J^2 s^2 kg^{-1} m^{-6}} = \mathrm{J\,m^{-4}}$ (since $\mathrm{J\,s^2 kg^{-1}} = \mathrm{m^2}$). (iii) Mass term: $[mc^2|\Phi|^2] = \mathrm{J\,m^{-4}}$. (iv) The interaction term has the same structure as (ii) ($[R] = [\partial\partial]$). □

Table 1: Dimension chart of the basic quantities.

Quantity	Symbol	SI dimension	Note
Mode parameter	ξ, Θ, λ_m, σ_ξ	s	temporal fibre coordinate
Mode wave function	$\psi(\xi)$	$\mathrm{s}^{-1/2}$	Axiom 2
Spatial envelope	$\chi(x)$	$\mathrm{m}^{-3/2}$	$\int \lvert\chi\rvert^2 \mathrm{d}^3x = 1$
Master field	$\Phi(x,\xi)$	m^{-2}	Eq. (20)
Fibre function	$f(\xi) = c^2 \hat{f}$	$\mathrm{m}^2\,\mathrm{s}^{-2}$	$\hat{f}$ dimensionless
Potential energy	$U(r)$	J	§3.3
Gravitational potential	$V(r)$	$\mathrm{J\,kg}^{-1}$	$U = m_B V$
Overlap integral	$\hat{O}_{AB}$	dimensionless	Theorem 3.6
Mass–mode constant	$\kappa = \hbar/c^2$	kg s	$\kappa = 1.173 \times 10^{-51}\,\mathrm{kg\,s}$
Five-dimensional gravitational constant	$G_5 = G\,\ell_\xi$	$\mathrm{m}^3\,\mathrm{kg}^{-1}\,\mathrm{s}^{-1}$	Eq. (16)
Mode co-momentum	p_ξ	J	conjugate to ξ

2.4 Constraint structure, Page–Wootters reduction and removal of ghost modes

Since the extended metric, of signature $(-,+,+,+,-)$, contains two timelike directions, an unconstrained field theory could exhibit negative-norm (ghost) excitations; in two-time physics this problem is solved by an $Sp(2,\mathbb{R})$ gauge symmetry [4]. In ZMUT the same duty is discharged by a first-class constraint that generates the reparametrization freedom along the mode direction. With the momentum operator conjugate to ξ, $\hat{p}_\xi = -i\hbar\,\partial_\xi$ ($[\hat{\xi}, \hat{p}_\xi] = i\hbar$, $[p_\xi] = \mathrm{J}$), physical states obey the Wheeler–DeWitt-type constraint

$$\boxed{\hat{\mathcal{C}}\,|\Psi\rangle\!\rangle = \big(\hat{p}_\xi \otimes \mathbb{I} + \mathbb{I} \otimes \hat{H}_S\big)|\Psi\rangle\!\rangle = 0} \tag{21}$$

where $\hat{H}_S$ is the (bounded-below) physical Hamiltonian of the system and $|\Psi\rangle\!\rangle \in \mathcal{H}_{\mathrm{mod}} \otimes \mathcal{H}_S$ is the total kinematic state. On the conditional state $\langle\xi|\Psi\rangle\!\rangle =: |\psi_S(\xi)\rangle$, (21) generates the Schrödinger flow

$$i\hbar\,\frac{\partial}{\partial\xi}\,|\psi_S(\xi)\rangle = \hat{H}_S\,|\psi_S(\xi)\rangle : \tag{22}$$

the dynamics is defined relationally with respect to the mode parameter, not with respect to an absolute external time. This is the realization of the Page–Wootters mechanism [5] within ZMUT, and it will play the central role in the circumvention of Pauli's theorem in §4.3.

Proposition 2.6 (Removal of ghost modes)**.** *The constraint (21) is first class, and the negative-norm excitations along the ξ direction are pure gauge along the orbits generated by $\hat{\mathcal{C}}$; the inner product induced on the physical Hilbert space $\mathcal{H}_{\mathrm{fiz}} = \ker\hat{\mathcal{C}}$ is positive definite.*

Proof. Being a single constraint, $\hat{\mathcal{C}}$ is trivially first class, $\{\hat{\mathcal{C}}, \hat{\mathcal{C}}\} = 0$, and the finite gauge transformations $e^{-i\epsilon\hat{\mathcal{C}}/\hbar}$ generate the co-motion of ξ-translations with the system evolution. The general solution of $\ker\hat{\mathcal{C}}$ follows from (22) as

$$|\Psi\rangle\!\rangle = \int \mathrm{d}\xi\;\; |\xi\rangle \otimes e^{-i\hat{H}_S\,\xi/\hbar}\,|\varphi_0\rangle\,, \qquad |\varphi_0\rangle \in \mathcal{H}_S. \tag{23}$$

The group-averaged (refined algebraic quantization) inner product $\big(\Psi_1, \Psi_2\big)_{\mathrm{fiz}} := \big\langle \varphi_0^{(1)} \big| \varphi_0^{(2)} \big\rangle$ equals the positive-definite inner product of $\mathcal{H}_S$, so no negative-norm state survives on the physical space; the norm of the ξ-oscillations never enters the physical inner product. □

2.5 Energy strata and conservation

Invariance of the action (17) under time translations defines, by Noether's theorem, a conserved total energy. On the constraint solution (23) the expectation value of the total energy naturally decomposes into strata:

$$\boxed{E \;=\; \underbrace{\left\langle \frac{\hat{p}_\xi^2}{2\mathcal{M}_\xi c^2} \right\rangle}_{E_T} + mc^2 \;+\; \underbrace{\left\langle \hat{H}_{\mathrm{int}} \right\rangle}_{E_{\mathrm{int}}} + \underbrace{\langle \mathcal{L}_{\mathrm{int}} \rangle V_4}_{E_{\mathrm{coup}}}} \tag{24}$$

Here E_T is the kinetic (wave) energy of the mode packet in ξ-space, scaled by the mode-inertia parameter $\mathcal{M}_\xi := m$; mc^2 is the rest-mass stratum, E_{int} the energy of the internal degrees of freedom (vibrational,

rotational, electronic), and E_{coup} the contribution of the mode–curvature coupling (19) (V_4: four-volume). The distribution $\mathrm{d}E(\xi) = E_{\mathrm{tot}}|\psi(\xi)|^2\mathrm{d}\xi$ of Axiom 4 is the projection onto the modes of the total $E_{\mathrm{tot}} \equiv E$ in (24), and its conservation is secured by Lemma 2.1.

Proposition 2.7 (Conservation)**.** *On a static background ($\partial_t g_{\mu\nu} = 0$) and on the constraint surface,* $\mathrm{d}E/\mathrm{d}t = 0$.

Proof. For the Killing vector ∂_t, the current $j^\mu = T^\mu_{\ \nu} k^\nu$ is conserved because of the covariant conservation $\nabla_\mu T^{\mu\nu} = 0$ of the energy–momentum tensor of §3.2 (compatibility of the field equations with the Bianchi identity): $\nabla_\mu j^\mu = 0$. The fall-offs $\chi \to 0$ at spatial infinity and $\psi \to 0$ as $\xi \to \pm\infty$ kill the boundary fluxes; $E = \int j^0 \mathrm{d}^3x\,\mathrm{d}\xi$ remains constant. □

3 Field Equations and the Gravitational Potential

3.1 Euler–Lagrange equation of the mode field

Let us vary the matter sector of the master action (14) with respect to Φ^*. For brevity write the volume element $\sqrt{|\tilde{g}|} = c\sqrt{-g}\sqrt{\hat{f}}$ and $\mathcal{S}_m = \int \mathrm{d}^4x\,\mathrm{d}\xi\,\sqrt{-g}\sqrt{\hat{f}}\,(\mathcal{L}_{\mathrm{mode}} + \mathcal{L}_{\mathrm{int}})$. The first variation is

$$\delta\mathcal{S}_m = \int \mathrm{d}^4x\,\mathrm{d}\xi\,\sqrt{-g}\sqrt{\hat{f}}\left[-\frac{\hbar^2}{2m}\,\tilde{g}^{AB}\,\partial_A(\delta\Phi^*)\,\partial_B\Phi - \frac{mc^2}{2}\,\delta\Phi^*\,\Phi - \frac{\alpha\hbar^2}{2m}\,R\,\delta\Phi^*\,\Phi\right] + \text{c.c.} \tag{25}$$

(c.c.: complex conjugate). Integrating the first term by parts,

$$-\int \mathrm{d}^4x\,\mathrm{d}\xi\,\sqrt{-g}\sqrt{\hat{f}}\,\frac{\hbar^2}{2m}\,\tilde{g}^{AB}\partial_A(\delta\Phi^*)\,\partial_B\Phi = \int \mathrm{d}^4x\,\mathrm{d}\xi\,\delta\Phi^*\,\frac{\hbar^2}{2m}\,\partial_A\Big(\sqrt{-g}\sqrt{\hat{f}}\,\tilde{g}^{AB}\,\partial_B\Phi\Big) - \oint \mathrm{d}\Sigma_A\,(\cdots)^A. \tag{26}$$

The boundary terms vanish for two reasons: $\chi \to 0$ at spatial infinity (localized system), and $\psi \to 0$ as $\xi \to \pm\infty$ by the normalization axiom (4). The contribution of the normalization condition here is structural: *square integrability in mode space is the precondition for the variational problem to be well defined.* Since $\delta\Phi^*$ is arbitrary, the Euler–Lagrange equation follows:

$$\frac{\hbar^2}{2m}\,\tilde{\Box}\,\Phi - \frac{mc^2}{2}\,\Phi - \frac{\alpha\hbar^2}{2m}\,R\,\Phi = 0 \qquad \Longleftrightarrow \qquad \boxed{\tilde{\Box}\,\Phi - \alpha R\,\Phi = \frac{m^2c^2}{\hbar^2}\,\Phi} \tag{27}$$

With (11) and $\tilde{g}^{\xi\xi} = -1/(c^2\hat{f})$, the extended d'Alembert operator reads explicitly

$$\tilde{\Box}\,\Phi = \underbrace{\frac{1}{\sqrt{-g}}\,\partial_\mu\big(\sqrt{-g}\,g^{\mu\nu}\partial_\nu\Phi\big)}_{\Box_4\Phi} - \frac{1}{c^2\sqrt{\hat{f}}}\,\partial_\xi\left(\frac{1}{\sqrt{\hat{f}}}\,\partial_\xi\Phi\right) \xrightarrow{\hat{f}=1} \Box_4\Phi - \frac{1}{c^2}\,\frac{\partial^2\Phi}{\partial\xi^2}. \tag{28}$$

Because of the two timelike directions, equation (27) is ultrahyperbolic; a well-posed initial-value problem is obtained by reducing to the first-order Schrödinger flow via the constraint (21) of §2.4. If, on the constraint surface, the stationary mode component of $\psi(\xi)$ is taken as $\psi \propto e^{-i\mathfrak{E}\xi/\hbar}$, then (28) gives

$$\left(\Box_4 + \frac{\mathfrak{E}^2}{\hbar^2c^2} - \frac{m^2c^2}{\hbar^2} - \alpha R\right)\chi(x) = 0; \tag{29}$$

that is, the component with mode eigen-energy $\mathfrak{E}$ propagates in four dimensions with effective mass

$$m_{\mathrm{eff}}^2 = m^2 - \frac{\mathfrak{E}^2}{c^4}. \tag{30}$$

The absence of tachyonic propagation ($m_{\mathrm{eff}}^2 \geq 0$) imposes on the mode spectrum the band bound

$$|\mathfrak{E}| \;\leq\; mc^2, \tag{31}$$

an inequality that will be the key to the derivation of the mass–mode relation in §4.2.

3.2 Extended Einstein equations

Now vary (14) with respect to $g^{\mu\nu}$. For the curvature sector the standard result (with the Gibbons–Hawking–York boundary term assumed) is

$$\delta\big(\sqrt{-g}\,R\big) = \sqrt{-g}\,\big(R_{\mu\nu} - \tfrac{1}{2}g_{\mu\nu}R\big)\,\delta g^{\mu\nu} + \text{total derivative}, \tag{32}$$

while the matter sector yields the energy–momentum tensor

$$\begin{aligned}\tilde{T}_{\mu\nu} &:= -\frac{2}{\sqrt{-g}}\,\frac{\delta\big(\sqrt{-g}\,(\mathcal{L}_{\text{mode}} + \mathcal{L}_{\text{int}})\big)}{\delta g^{\mu\nu}} \\ &= \frac{\hbar^2}{2m}\big(\partial_\mu\Phi^*\partial_\nu\Phi + \partial_\nu\Phi^*\partial_\mu\Phi\big) + g_{\mu\nu}\big(\mathcal{L}_{\text{mode}} + \mathcal{L}_{\text{int}}\big) + \Delta T^{(\alpha)}_{\mu\nu},\end{aligned} \tag{33}$$

with the improvement terms of the nonminimal coupling

$$\Delta T^{(\alpha)}_{\mu\nu} = \frac{\alpha\hbar^2}{m}\Big[g_{\mu\nu}\,\Box_4 - \nabla_\mu\nabla_\nu + G_{\mu\nu}\Big]|\Phi|^2. \tag{34}$$

The field equation descends to the four-dimensional Einstein equation with the mode-integrated (zero-mode-truncated) source:

$$\boxed{G_{\mu\nu} = \frac{8\pi G}{c^4}\,\mathcal{T}_{\mu\nu}, \qquad \mathcal{T}_{\mu\nu}(x) := c\int \mathrm{d}\xi\,\sqrt{\hat{f}}\,\tilde{T}_{\mu\nu}(x,\xi)} \tag{35}$$

The factor of c comes from the scale change $x^0 = ct$ and secures the dimension $[\mathcal{T}_{\mu\nu}] = \mathrm{J\,m^{-3}}$. Variation of the $\xi\xi$ component of the metric gives the equilibrium condition of the fibre sector (the radion) and will be used in the dynamics of the scalar trace mode in §3.5.

Lemma 3.1 (Physical role of the normalization)**.** *Take the envelope decomposition $\Phi = c^{-1/2}\chi(x)\psi(\xi)\,e^{-imc^2t/\hbar}$ for a slowly varying, nonrelativistic system. Then the mode-integrated energy density equals exactly the four-dimensional rest-energy density:*

$$\mathcal{T}_{00}(x) = c\int \mathrm{d}\xi\; mc^2|\Phi|^2 = mc^2|\chi(x)|^2\underbrace{\int |\psi(\xi)|^2\mathrm{d}\xi}_{=1} = mc^2|\chi(x)|^2. \tag{36}$$

Proof. In the nonrelativistic limit the dominant contribution to (33) comes from the time derivatives of the fast phase: $\partial_0\Phi = (-imc/\hbar)\Phi + \mathcal{O}(v/c)$, hence $(\hbar^2/2m)\cdot 2|\partial_0\Phi|^2 = mc^2|\Phi|^2$; the kinetic and mass contributions in the $g_{00}\mathcal{L}$ term cancel at this order. Substituting $|\Phi|^2 = |\chi|^2|\psi|^2/c$ and applying $c\int \mathrm{d}\xi$ yields (36). The normalization axiom (4) is exactly the condition ensuring that four-dimensional gravity sees the *entire* mass of the system: distribution over the modes does not alter the total gravitational charge (consistent with Lemma 2.1). □

3.3 Newtonian limit: potential versus potential energy

Theorem 3.2 (Recovery of Newton's law, I: field-equation level)**.** *In the weak static-field limit ($g_{00} = -(1 + 2V/c^2)$, $|V|/c^2 \ll 1$, slow sources), equation (35) descends to the Poisson equation*

$$\nabla^2 V(\vec{r}) = 4\pi G\,\rho(\vec{r}), \qquad \rho(\vec{r}) = m|\chi(\vec{r})|^2, \tag{37}$$

and for a point source gives $V(r) = -Gm_A/r$.

Proof. Step 1: write $g_{\mu\nu} = \eta_{\mu\nu} + h_{\mu\nu}$, $|h| \ll 1$; staticity gives $\partial_0 h_{\mu\nu} = 0$ and one defines $h_{00} = -2V/c^2$. Step 2: in the static weak field, direct computation of the Christoffel symbols yields the 00 component of the Ricci tensor, $R_{00} = \nabla^2 V/c^2 + \mathcal{O}(h^2)$. Step 3: use the trace-reversed form of (35),

$$R_{\mu\nu} = \frac{8\pi G}{c^4}\,\big(\mathcal{T}_{\mu\nu} - \tfrac{1}{2}g_{\mu\nu}\,\mathcal{T}\big)\,.$$

By Lemma 3.1 the source is dust-like: $\mathcal{T}_{\mu\nu} = \mathrm{diag}(\rho c^2, 0, 0, 0)$, hence $\mathcal{T} = g^{\mu\nu}\mathcal{T}_{\mu\nu} = -\rho c^2$ and

$$\frac{\nabla^2 V}{c^2} = \frac{8\pi G}{c^4}\left(\rho c^2 - \frac{\rho c^2}{2}\right) = \frac{4\pi G}{c^2}\,\rho \;\Longrightarrow\; \nabla^2 V = 4\pi G\rho.$$

In the point limit $\rho = m_A\,\delta^3(\vec{r} - \vec{r}_A)$ the solution, with the condition of vanishing at infinity, is $V(r) = -Gm_A/r$. □

Proposition 3.3 (Dimensional distinction)**.** *$V(r)$ is the gravitational* potential*, a field of dimension* $[\mathrm{J\,kg^{-1}}]$*; $U(r) = m_B\,V(r)$ is the* potential energy [J] *of the test mass B in that field. In ZMUT the quantity modified by the mode structure is not the source of the field V, but the overlap factor entering the mutual gravitational energy of the two systems; the correction is therefore multiplicative and dimensionless at the level of U.*

3.4 The temporal overlap integral, locality, and the proof of the Newtonian limit

3.4.1 Retarded Green function and causality

The static-spatial sector of the mode-field equation (28) has the structure of the wave operator $(\nabla^2 - c^{-2}\partial_\varsigma^2)$, where $\varsigma := \xi - \xi'$ is the relative mode separation. The associated retarded Green function is

$$\left(\nabla^2 - \frac{1}{c^2}\frac{\partial^2}{\partial\varsigma^2}\right)\mathcal{G}(\vec{r},\varsigma) = -4\pi\,\delta^3(\vec{r})\,\delta(\varsigma) \qquad \Longrightarrow \qquad \mathcal{G}(\vec{r},\varsigma) = \frac{\delta\big(\varsigma - |\vec{r}|/c\big)}{|\vec{r}|}, \tag{38}$$

obtained in the standard way from $\tilde{\mathcal{G}} = 4\pi/(k^2 - \omega^2/c^2)$ in Fourier space with the retarded contour choice; its support lies on the extended light cone $\varsigma = |\vec{r}|/c$.

Theorem 3.4 (Locality and causality)**.** *In ZMUT the gravitational interaction between mode sectors is built on the retarded kernel (38): the points $(\vec{r}_A, \xi)$ and $(\vec{r}_B, \xi')$ are connected only if the extended cone condition $\xi - \xi' = |\vec{r}_A - \vec{r}_B|/c$ holds. Consequently (i) the interaction density is local on the extended space, (ii) no mode information propagates faster than c, and (iii) action at a distance is eliminated. In the static limit $\int \mathcal{G}\,\mathrm{d}\varsigma' = 1/|\vec{r}|$, so the classical $1/r$ kernel is recovered exactly.*

Proof. (i) and (ii) follow from the support of $\mathcal{G}$ lying on the cone; (iii) from the fact that the static expression is *derived* as the ς-integral of the retarded kernel: $\int \delta(\varsigma - r/c)\,\mathrm{d}\varsigma/r = 1/r$. □

3.4.2 The overlap integral and its normalized form

Let the mode-resolved mass densities of the systems A and B be $\varrho_i(\vec{r},\xi) := m_i|\chi_i(\vec{r})|^2 w_i(\xi)$, $w_i = |\psi_i|^2$. With the mode-diagonal structure of the linearized field exchange (one-graviton exchange), the two-body potential energy in its most general local form is

$$U_{AB} = -\,G\mathcal{N}_{AB}\iint \mathrm{d}^3r_A\,\mathrm{d}^3r_B\iint \mathrm{d}\xi\,\mathrm{d}\xi'\;\varrho_A(\vec{r}_A,\xi)\;\mathcal{G}\big(\vec{r}_A - \vec{r}_B,\,\xi - \xi'\big)\;\varrho_B(\vec{r}_B,\xi'); \tag{39}$$

the dimensional check $[\varrho_i] = \mathrm{kg\,m^{-3}\,s^{-1}}$, $[\mathcal{G}] = \mathrm{m^{-1}\,s^{-1}}$ and $[\mathcal{N}_{AB}] = \mathrm{s}$ gives $[U_{AB}] = \mathrm{J}$. The retardation is carried by the classical mean motion (the common flow of the mode means $\Theta_i(t)$); the quantum overlap compares the centred fluctuation profiles: $\hat{w}_i(u) := w_i(u + \Theta_i)$. Under this split, (39) descends, for spatially pointlike packets, to a compact form in which the fundamental overlap object of ZMUT appears:

$$O(\vec{r},\xi) \;=\; \int |\psi_A(\vec{r}_A,\xi)|^2\;G(\vec{r}_A - \vec{r}_B)\;|\psi_B(\vec{r}_B,\xi)|^2\;\mathrm{d}\xi, \tag{40}$$

where $G(\vec{r}_A - \vec{r}_B)$ is the static reduction of the retarded kernel by Theorem 3.4. To make the dimension and boundedness properties precise, the normalized, dimensionless form of the overlap is defined:

Definition 3.5 (Normalized temporal overlap)**.**

$$\boxed{\hat{O}_{AB} \;:=\; \frac{\displaystyle\int_{-\infty}^{\infty}\hat{w}_A(u)\,\hat{w}_B(u)\,\mathrm{d}u}{\displaystyle\left(\int_{-\infty}^{\infty}\hat{w}_A^2\,\mathrm{d}u\right)^{1/2}\left(\int_{-\infty}^{\infty}\hat{w}_B^2\,\mathrm{d}u\right)^{1/2}}} \tag{41}$$

The normalization factor $\mathcal{N}_{AB} = \big(\|\hat{w}_A\|_2\|\hat{w}_B\|_2\big)^{-1}$, of dimension $[\mathcal{N}_{AB}] = \mathrm{s}$, closes the Joule dimension of (39) and is fixed uniquely by the self-overlap consistency condition $\hat{O}_{AA} = 1$.

Theorem 3.6 (Boundedness and saturation)**.** *For every pair of normalized mode densities $w_A, w_B \in L^1 \cap L^2$,*

$$0 \;\le\; \hat{O}_{AB} \;\le\; 1, \tag{42}$$

and the equality $\hat{O}_{AB} = 1$ holds if and only if $\hat{w}_A = \hat{w}_B$ (almost everywhere).

Proof. The lower bound is trivial since $w_i \geq 0$. The upper bound is the Cauchy–Schwarz inequality:

$$\int \hat{w}_A \hat{w}_B \, \mathrm{d}u \;\leq\; \|\hat{w}_A\|_2 \, \|\hat{w}_B\|_2,$$

with equality only for proportionality $\hat{w}_A = c_0 \, \hat{w}_B$. Since both densities carry the normalization $\int \hat{w}_i \, \mathrm{d}u = 1$, one finds $c_0 = 1$, i.e. $\hat{w}_A = \hat{w}_B$. □

The gravitational potential energy thus takes the form carrying the central prediction of ZMUT, a multiplicative mode correction:

$$\boxed{U(r) \;=\; -\frac{G\, m_A\, m_B}{r}\, \hat{O}_{AB}} \tag{43}$$

The dimension $[\,U\,] = \mathrm{J}$ is fully consistent with Proposition 3.3 thanks to the dimensionlessness of $\hat{O}_{AB}$ (Theorem 3.6).

Theorem 3.7 (Recovery of Newton's law, II: overlap level)**.** *In the classical (decohered) limit, i.e. for systems settled into a common environmental pointer mode with $\hat{w}_A = \hat{w}_B$,*

$$\hat{O}_{AB} \longrightarrow 1 \qquad \Longrightarrow \qquad U(r) = -\frac{G m_A m_B}{r}, \qquad \vec{F} = -\boldsymbol{\nabla} U = -\frac{G m_A m_B}{r^2}\, \hat{r}, \tag{44}$$

i.e. Newton's universal law of gravitation is recovered exactly*. In particular, for any common-centred delta family $\hat{w}_A = \hat{w}_B = \eta_\varepsilon$ of widths $\varepsilon \to 0$, the equality $\hat{O}_{AB} = 1$ is preserved along the whole limit for every ε; the limit is therefore nonsingular.*

Proof. The saturation case of Theorem 3.6 gives $\hat{w}_A = \hat{w}_B \Rightarrow \hat{O}_{AB} = 1$; substitution into (43) yields (44). For the delta-family statement: for each $\varepsilon > 0$ the numerator is $\|\eta_\varepsilon\|_2^2$ and the denominator $\|\eta_\varepsilon\|_2 \|\eta_\varepsilon\|_2$, so the ratio is identically 1; the singularly growing norms cancel in the ratio as $\varepsilon \to 0$. The force expression follows by direct gradient, since $\hat{O}_{AB}$ is independent of r. □

Proposition 3.8 (Closed form for Gaussian packets)**.** *For Gaussian mode densities with centre offsets $\Delta := \Theta_A - \Theta_B$ and widths σ_A, σ_B,*

$$\hat{O}_{AB} = \sqrt{\frac{2\,\sigma_A \sigma_B}{\sigma_A^2 + \sigma_B^2}}\; \exp\!\left[-\frac{\Delta^2}{2\,(\sigma_A^2 + \sigma_B^2)}\right]. \tag{45}$$

Proof. For $w_i(u) = (2\pi\sigma_i^2)^{-1/2} \exp\!\big[-(u-\Theta_i)^2/2\sigma_i^2\big]$ the standard Gaussian integrals

$$\int w_A w_B \, \mathrm{d}u = \frac{\exp\!\big[-\Delta^2/2(\sigma_A^2+\sigma_B^2)\big]}{\sqrt{2\pi(\sigma_A^2+\sigma_B^2)}}, \qquad \int w_i^2 \, \mathrm{d}u = \frac{1}{2\sigma_i\sqrt{\pi}}$$

inserted into (41) give (45). The special case $\sigma_A = \sigma_B$, $\Delta = 0$ verifies $\hat{O}_{AB} = 1$, consistent with Theorem 3.7. □

Corollary 3.9 (Mass-mismatch suppression)**.** *For the minimal packets $\sigma_i = \lambda_{m_i} = \kappa/m_i$ to be derived in §4.2, two systems in pure (undecohered) states with mass ratio $m_B/m_A = 2$ have $\hat{O}_{AB} = \sqrt{4/5} \approx 0.894$: ZMUT predicts that the attraction between* coherent *quantum systems is suppressed by roughly ten per cent (Figure 1). Decohered systems such as laboratory bodies share the common pointer mode ($\hat{w}_A = \hat{w}_B$), so this suppression is not observed; full agreement with the classical tests is guaranteed by Theorem 3.7.*

3.5 The wave-like time field and metric trace modulation

In early formulations of ZMUT a scalar "time field" $T(x,\mu)$ was proposed as an independent wave field. Here that field is bound, its independence removed, to the trace degree of freedom of the linearized metric. Let $g_{\mu\nu} = \eta_{\mu\nu} + h_{\mu\nu}$, $|h_{\mu\nu}| \ll 1$, and define the trace-reversed perturbation $\bar{h}_{\mu\nu} := h_{\mu\nu} - \frac{1}{2}\eta_{\mu\nu} h$, $h := \eta^{\mu\nu} h_{\mu\nu}$. In the Lorenz gauge ($\partial^\mu \bar{h}_{\mu\nu} = 0$) the linearization of (35) gives

$$\Box\, \bar{h}_{\mu\nu} = -\frac{16\pi G}{c^4}\, \mathcal{T}_{\mu\nu}. \tag{46}$$

Taking the trace ($\eta^{\mu\nu}\bar{h}_{\mu\nu} = h - 2h = -h$),

$$\Box\, h = \frac{16\pi G}{c^4}\, \mathcal{T}, \qquad \mathcal{T} := \eta^{\mu\nu}\mathcal{T}_{\mu\nu}\,: \tag{47}$$

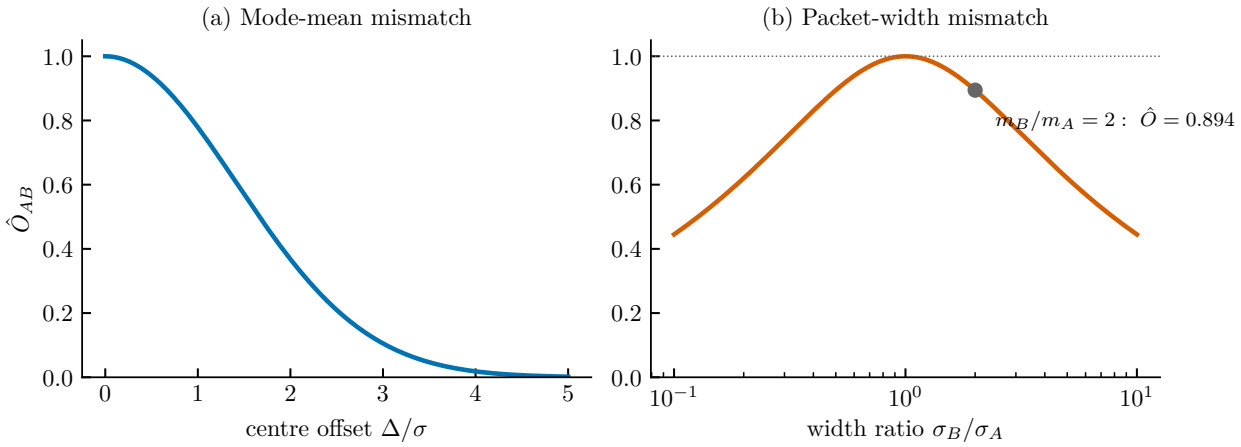


Figure 1: The two suppression channels of the normalized temporal overlap (Proposition 3.8). (a) Centre offset at common width: $\hat{O} = e^{-\Delta^2/4\sigma^2}$. (b) Width ratio at common centre: $\hat{O} = \sqrt{2r/(1+r^2)}$, $r = \sigma_B/\sigma_A$; since $r = m_A/m_B$ for minimal packets, a pure pair with mass ratio 2 has $\hat{O} \approx 0.894$ (marked point; Corollary 3.9).

the metric trace obeys a wave equation sourced by the energy–momentum trace of the mode sector. In pure general relativity h can be removed by the residual gauge freedom (TT gauge); in ZMUT the perturbation of the fibre function, $\hat{f}(x) = 1 + 2\sigma(x)$, physicalizes this freedom. Indeed, for an x-dependent fibre the computation of Theorem 2.4 produces two extra Christoffel components,

$$\tilde{\Gamma}^{\mu}{}_{\xi\xi} = c^2 \hat{f}\, g^{\mu\sigma}\partial_\sigma\sigma, \qquad \tilde{\Gamma}^{\xi}{}_{\mu\xi} = \partial_\mu\sigma, \tag{48}$$

and the scalar curvature becomes $\tilde{R} = R - 2\Box_4\sigma - 2\,(\partial\sigma)^2$. In the action, together with the measure $\sqrt{\hat{f}} \simeq e^{\sigma}$, one obtains at first order

$$\sqrt{\hat{f}}\,\tilde{R} \;\simeq\; R + \sigma R - 2\,\Box_4\sigma + \mathcal{O}(\sigma^2)\,: \tag{49}$$

after discarding a total derivative, the radion σ couples *linearly* to curvature. Since $R^{(1)} = -\frac{1}{2}\Box h$ in the Lorenz gauge, the variation of σ sources the trace sector, and a single propagating scalar combination of the pair (h, σ) — the *breathing mode* — remains. Thus:

Definition 3.10 (Wave-like time field)**.** With the relational flow parameter μ (Page–Wootters time along the constraint orbit, cf. (22)), the ZMUT time field is the scaled oscillation of the metric trace:

$$T(x,\mu) := \frac{\Theta}{2}\, h\big(x,\mu\big). \tag{50}$$

Proposition 3.11 (Wave solution of the trace mode)**.** *In vacuum ($\mathcal{T} = 0$) equation (47) admits plane-wave solutions and the time field takes the form*

$$\boxed{T(x,\mu) = A\,\cos\big(kx - \omega\mu + \phi\big), \qquad \omega = c\,|k|} \tag{51}$$

with $A = \Theta\mathcal{A}/2$, $\mathcal{A}$ the dimensionless trace amplitude, and $[T] = \mathrm{s}$. $T(x,\mu)$ is not *an independent field: its dynamics is inherited from (47), hence from the Einstein equations, while its amplitude is fixed by the σ–h mixing through the coupling α.*

Proof. For $\Box h = 0$, $h = \mathcal{A}\cos(k_\mu x^\mu + \phi)$ is a solution iff $k_\mu k^\mu = 0$, i.e. $\omega = c\left|\vec{k}\right|$; substitution into (50) and the parametrization of x^0 by μ along the constraint flow give (51). □

Observational consequence: the breathing mode can be searched for as a scalar channel additional to the plus and cross polarizations in gravitational-wave interferometers (§19); the scaling of its amplitude with α lets LIGO-type observations [21] place direct bounds on the ZMUT parameter space.

4 Relativistic Kinematics and Temporal Decoherence

4.1 Extended proper time and reality in the $v \to c$ limit

The proper time of a world line on the extended metric (5) is defined by

$$\mathrm{d}\tilde{\tau}^2 := -\frac{\mathrm{d}s^2}{c^2}\bigg|_{\text{timelike}} = -\frac{1}{c^2}\, g_{\mu\nu}\,\mathrm{d}x^\mu \mathrm{d}x^\nu + \hat{f}(\xi)\,\mathrm{d}\xi^2 \tag{52}$$

(using $f = c^2\hat{f}$). Let us proceed step by step in flat spacetime ($g_{\mu\nu} = \eta_{\mu\nu}$). (i) The standard four-dimensional sector:

$$-\frac{1}{c^2}\,\eta_{\mu\nu}\,\mathrm{d}x^\mu \mathrm{d}x^\nu = \mathrm{d}t^2 - \frac{\mathrm{d}\vec{x}^{\,2}}{c^2} = \mathrm{d}t^2\left(1 - \frac{v^2}{c^2}\right), \tag{53}$$

which reproduces the familiar $\mathrm{d}\tau = \mathrm{d}t\sqrt{1 - v^2/c^2}$ for $v < c$ and goes to zero as $v \to c^-$. (ii) Defining the mode flow rate $\nu_\xi := \mathrm{d}\xi/\mathrm{d}t$, (52) becomes

$$\mathrm{d}\tilde{\tau} = \mathrm{d}t\,\sqrt{1 - \frac{v^2}{c^2} + \hat{f}\,\nu_\xi^2}\,. \tag{54}$$

(iii) At the speed of light ($v = c$) the first two terms under the root cancel exactly and

$$\mathrm{d}\tilde{\tau}\Big|_{v=c} = \sqrt{\hat{f}}\,|\mathrm{d}\xi| \;\geq\; 0 \tag{55}$$

remains: the proper time never becomes imaginary.

Theorem 4.1 (Reality of proper time)**.** *With $\hat{f} > 0$, for every motion satisfying $v \leq c$ and every mode flow, $\mathrm{d}\tilde{\tau} \in \mathbb{R}_{\geq 0}$. Equality ($\mathrm{d}\tilde{\tau} = 0$) occurs only if $v = c$ and $\mathrm{d}\xi = 0$ hold together. In particular, although massless systems do not "age" in the four-dimensional sense ($\mathrm{d}\tau_4 = 0$), they accumulate extended proper time $\sqrt{\hat{f}}\,|\mathrm{d}\xi|$ along the mode direction.*

Proof. In (54) the sum of the terms $1 - v^2/c^2 \geq 0$ and $\hat{f}\nu_\xi^2 \geq 0$ cannot be negative; the square root is real and nonnegative. Vanishing of the sum requires the separate vanishing of both terms. □

Remark 4.2 (Causal structure and the $v > c$ branch). The fact that (54) can remain real also for $v > c$ does not mean superluminal motion is permitted: physical trajectories are solutions of the reduced dynamics generated by the constraint (21), and that dynamics preserves the usual causal structure on the four-dimensional sector (Theorem 3.4). The extra region of the extended cone is identified with gauge orbits and removed from the physical phase space, exactly as in two-time physics [4].

Proposition 4.3 (Lorentz invariance)**.** *The extended metric (5) is invariant under the full Lorentz group $SO(3,1)$ acting on the x-block; the isometries preserving the slices $\mathrm{d}\xi = 0$ reproduce standard special relativity exactly. For constant $\hat{f}$ the full isometry group enlarges to $SO(3,2)$, the same family as Bars's $SO(d,2)$ structures [4]. ZMUT therefore does* not *break Lorentz symmetry; it embeds it in a larger group.*

Proof. Under $x \mapsto \Lambda x$, $\xi \mapsto \xi$ with $\Lambda \in SO(3,1)$, the form $\eta_{\mu\nu}\mathrm{d}x^\mu\mathrm{d}x^\nu$ is invariant and $f(\xi)\mathrm{d}\xi^2$ untouched. For constant $\hat{f}$, (5) is the flat metric of $\mathbb{R}^{3,2}$; its isometry group is by definition $SO(3,2)$ (semidirect product with translations). □

The Schwinger connection. The dynamization of the mode parameter connects organically to Schwinger's proper-time representation [7]: the kernel of the Feynman propagator of a free relativistic particle is written as an integral over a Schwinger parameter of dimension $[\xi] = \mathrm{s}$,

$$\frac{1}{p_\mu p^\mu + m^2c^2 - i\epsilon} = \frac{1}{2m}\cdot\frac{i}{\hbar}\int_0^\infty \mathrm{d}\xi\; e^{-i\xi\,(\mathcal{H}_p - i\epsilon)/\hbar}, \qquad \mathcal{H}_p := \frac{p_\mu p^\mu + m^2c^2}{2m}, \tag{56}$$

with $\mathcal{H}_p$ the world-line Hamiltonian of dimension $[\mathcal{H}_p] = \mathrm{J}$. ZMUT's reading is this: the integrand of the Schwinger representation is the *mode amplitude* of the free particle; that is, $\psi(\xi)$ is the dynamical and measurable version of the proper-time amplitude already implicit in standard quantum field theory.

4.2 Derivation of the mass–mode relation: $\lambda_m = \kappa/m$, $\kappa = \hbar/c^2$

Theorem 4.4 (Mass–mode relation)**.** *Under the tachyon-avoidance condition (31), the width of the mode packet $\psi(\xi)$ of a system is bounded from below:*

$$\sigma_\xi \;\geq\; \frac{\hbar}{2\,mc^2} \qquad\Longrightarrow\qquad \boxed{\lambda_m := \frac{\hbar}{mc^2} = \frac{\kappa}{m}, \qquad \kappa = \frac{\hbar}{c^2} = 1.173\times10^{-51}\ \mathrm{kg\,s}} \tag{57}$$

The relation $\lambda_m = \kappa/m$ is thus not an assumption but a consequence of the internal consistency of the theory (the absence of tachyonic propagation), and the constant κ is universally locked to $\hbar/c^2$. λ_m is the reduced Compton time *of the system.*

Proof. As shown in §3.1, the stationary mode components $e^{-i\mathfrak{E}\xi/\hbar}$ of ψ propagate tachyon-free only within the band $|\mathfrak{E}| \le mc^2$ (31); therefore the physical $\psi(\xi)$ is *band-limited*, its Fourier conjugate supported on $[-mc^2, mc^2]$:

$$\psi(\xi) = \frac{1}{\sqrt{2\pi\hbar}} \int_{-mc^2}^{mc^2} \mathrm{d}\mathfrak{E}\; \tilde{\psi}(\mathfrak{E})\, e^{-i\mathfrak{E}\xi/\hbar}.$$

For the position–momentum-type conjugate pair $(\hat{\xi}, \hat{p}_\xi)$ the Kennard–Robertson inequality $\sigma_\xi\, \sigma_{p_\xi} \ge \hbar/2$ holds; band limitation gives $\sigma_{p_\xi} \le mc^2$, whence

$$\sigma_\xi \;\ge\; \frac{\hbar}{2\,\sigma_{p_\xi}} \;\ge\; \frac{\hbar}{2\,mc^2}.$$

The minimal packet scale is defined as $2\sigma_\xi^{\min} = \hbar/(mc^2) =: \lambda_m$; the reading $\kappa = \hbar/c^2$ is immediate. □

Corollary 4.5 (Planck threshold and the quantum–classical transition)**.** *At the Planck mass* $m_P = \sqrt{\hbar c/G} = 2.176 \times 10^{-8}\,\mathrm{kg}$, λ_m *equals exactly the Planck time:*

$$\lambda_m(m_P) = \frac{\hbar}{m_P c^2} = \sqrt{\frac{\hbar G}{c^5}} = t_P = 5.39 \times 10^{-44}\ \mathrm{s}. \tag{58}$$

For $m > m_P$ *the mode packet is squeezed below the Planck width; since no physical clock can resolve that scale, the mode superposition becomes operationally inaccessible and the system is* temporally classical*. In this sense* $\lambda_m = \kappa/m$ *defines a* decoherence threshold*: in an environment of temporal resolution* $\delta\tau_{env}$ *the critical mass is* $m_c = \kappa/\delta\tau_{env}$*, and systems with* $m \gg m_c$ *classicalize inevitably. That the Planck mass (*$\approx 22\ \mu$g*) sits at the macroscopic–microscopic border demonstrates the quantitative agreement of this threshold with the known quantum–classical phenomenology (Figure 2).*

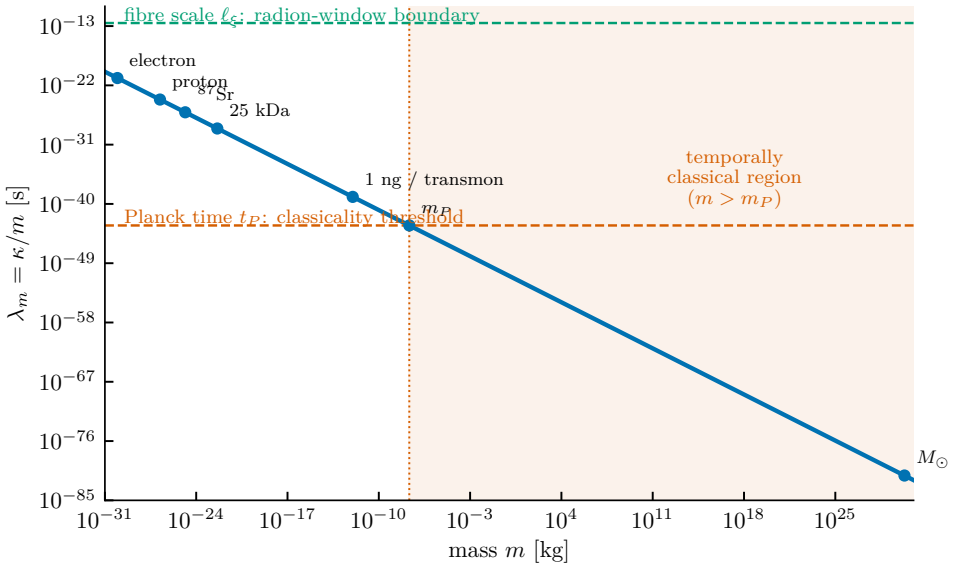


Figure 2: The mass–mode relation $\lambda_m = \kappa/m$ and the two natural thresholds of the theory. The upper dashed line is the fibre scale ℓ_ξ: systems with $\lambda_m \gtrsim \ell_\xi$ (i.e. $mc^2 \lesssim 2$ meV) couple fully in the radion window (§8). The lower dashed line is the Planck time: for $m > m_P$ the packet is squeezed below the Planck scale and the system becomes temporally classical (Corollary 4.5; shaded region).

4.3 Circumventing Pauli's theorem: quantum reference frames and the Page–Wootters mechanism

Theorem 4.6 (Pauli 1933)**.** *Let* $\hat{H}$ *be a self-adjoint Hamiltonian with spectrum bounded from below. A self-adjoint operator* $\hat{T}$ *satisfying the canonical conjugation relation* $[\hat{T}, \hat{H}] = i\hbar$ *cannot exist on the* same *Hilbert space [6].*

Proof sketch. If $\hat{T}$ is self-adjoint then $U_\epsilon = e^{-i\epsilon\hat{T}/\hbar}$ is a unitary family, and the conjugation relation gives $U_\epsilon^\dagger \hat{H} U_\epsilon = \hat{H} + \epsilon$: the spectrum is translated for every $\epsilon \in \mathbb{R}$. A spectrum bounded from below contradicts unbounded translation in the negative direction. □

ZMUT passes this obstruction by representing time not on the system's Hilbert space but on the extended kinematic space. The structure has three layers:

(i) A self-adjoint mode operator. On $\mathcal{H}_{\rm mod} = L^2(\mathbb{R}, \mathrm{d}\xi)$ the multiplication operator $(\hat{\xi}\psi)(\xi) = \xi\,\psi(\xi)$ is self-adjoint by the spectral theorem, with spectrum $T = \{T_n\}$ (discrete case) or $\mathbb{R}$ (continuous case). Its conjugate is $\hat{p}_\xi = -i\hbar\partial_\xi$, and $[\hat{\xi}, \hat{p}_\xi] = i\hbar$ is realized in exact Weyl form. There is no clash with Pauli's theorem here, because $\hat{p}_\xi$ *is not the physical energy*: it is a constraint generator with spectrum all of $\mathbb{R}$.

(ii) Constraint and relational dynamics. The physical content lives in the kernel of the constraint $\hat{\mathcal{C}} = \hat{p}_\xi + \hat{H}_S$ built in §2.4. $\hat{H}_S$ is bounded below and remains so; $\hat{\xi}$ is conjugate to $\hat{p}_\xi$, not to $\hat{H}_S$. The hypothesis set of Pauli's theorem — "a self-adjoint time operator conjugate to a bounded-below generator" — never assembles *anywhere* in the physical theory:

Theorem 4.7 (Circumvention of the Pauli obstruction)**.** *Let $\mathcal{H}_{\rm kin} = L^2(\mathbb{R}, \mathrm{d}\xi) \otimes \mathcal{H}_S$ and $\hat{\mathcal{C}} = \hat{p}_\xi \otimes \mathbb{I} + \mathbb{I} \otimes \hat{H}_S$. (a) $\hat{\xi}$ is self-adjoint and well defined as a time observable through conditional probabilities. (b) The reduced dynamics on $\ker\hat{\mathcal{C}}$ is the Schrödinger equation (22). (c) The lower-boundedness of $\hat{H}_S$ is preserved; at no stage is a self-adjoint $\hat{T}$ constructed that would have to satisfy $[\hat{T}, \hat{H}_S] = i\hbar$. Hence no contradiction with Theorem 4.6 arises, and time enters quantum theory legitimately as a relational observable in the Page–Wootters sense [5].*

Proof. (a) follows from the self-adjointness of the multiplication operator and the Born-rule reading of the conditional distribution $P(\xi) = \|\langle\xi|\Psi\rangle\rangle\|^2$ on $|\Psi\rangle\rangle$; (b) from projecting (21) with $\langle\xi|$; (c) from the observation that in $\hat{\mathcal{C}}$ the operator made "equal" to $-\hat{H}_S$ is only $\hat{p}_\xi$, never $\hat{\xi}$: the conjugate of $\hat{\xi}$ is $\hat{p}_\xi$, which is unbounded below and free to be so, while the physical energy $\hat{H}_S$ is never declared canonically conjugate to any self-adjoint operator. □

(iii) QRF covariance. The transition between two different clock systems C and C' (two different mode registers) is a quantum-reference-frame transformation in the sense of Giacomini–Castro-Ruiz–Brukner [3]. Between the conditional state $\left|\psi^{(C)}(\xi)\right\rangle$ in frame C and the state in frame C' there is a unitary map

$$\left|\psi^{(C')}(\xi')\right\rangle = \hat{\mathcal{S}}_{C\to C'}\,\left|\psi^{(C)}(\xi)\right\rangle, \qquad \hat{\mathcal{S}}_{C\to C'} = \hat{\mathcal{P}}_{CC'}\,\exp\!\left[\frac{i}{\hbar}\,\hat{\xi}_{C'}\otimes\hat{H}_C\right], \tag{59}$$

where $\hat{\mathcal{P}}_{CC'}$ swaps the registers and the exponential factor couples the position of the new clock to the generator of the old one. The form of (22) is preserved under this transformation: *the laws of physics are independent of which quantum clock is declared to be "time".* This is the extension of classical general covariance to the mode sector and constitutes ZMUT's principle of "mode relativity".

Explicit example (two-level system). For $\hat{H}_S = \frac{\Delta E}{2}\,\hat{\sigma}_z$, $|\varphi_0\rangle = c_\uparrow|\uparrow\rangle + c_\downarrow|\downarrow\rangle$, the constraint solution (23) gives

$$|\psi_S(\xi)\rangle = c_\uparrow\, e^{-i\Delta E\,\xi/2\hbar}\,|\uparrow\rangle + c_\downarrow\, e^{+i\Delta E\,\xi/2\hbar}\,|\downarrow\rangle\,; \tag{60}$$

the oscillation $\langle\hat{\sigma}_x\rangle(\xi) = 2|c_\uparrow c_\downarrow|\cos(\Delta E\,\xi/\hbar + \varphi_0)$ makes concrete the relational dynamics in which "time" is nothing but the mode parameter. This example forms the core of the decoherence mechanism of the next subsection.

4.4 Temporal decoherence: the first (naive) model and the quantum–classical transition

The derivation in this subsection is the theory's first approximation; it will be probed by items Z1–Z2 of the audit in §5 and placed on an axiomatic footing in §6. The form of the quantitative laws (Gaussian visibility, $t_{\rm dec}$ scaling) survives that transition; what changes is the status of the derivation and the interpretation of Θ.

The finite width of the mode packet generates a universal dephasing channel for every system carrying a superposition of internal energies. In a mode with relative flow rate $R(\xi) = \xi/\Theta$ with respect to the mode mean, the relative phase accumulated over laboratory time t is $\varphi(\xi; t) = \Delta E\,R(\xi)\,t/\hbar$. For a system initially in the superposition $\frac{1}{\sqrt{2}}(|E_1\rangle + |E_2\rangle)$, $\Delta E = E_2 - E_1$, the off-diagonal element of the reduced density matrix scales with the visibility

$$\mathcal{V}(t) = \left|\int \mathrm{d}\xi\; w(\xi)\; e^{\,i\Delta E\,\xi\,t/(\hbar\Theta)}\right| = \left|\chi_w\!\left(\frac{\Delta E\,t}{\hbar\,\Theta}\right)\right|, \tag{61}$$

where χ_w is the characteristic function of the mode density.

Theorem 4.8 (Law of temporal decoherence)**.** *For a Gaussian mode packet of width $\sigma_\xi = \lambda_m$ the visibility decays by a Gaussian law,*

$$\mathcal{V}(t) = \exp\!\left[-\frac{\Delta E^2\,\lambda_m^2\,t^2}{2\,\hbar^2\,\Theta^2}\right], \tag{62}$$

and the characteristic decoherence time ($\mathcal{V} = e^{-1/2}$) is

$$\boxed{t_{\rm dec} = \frac{\hbar\,\Theta}{\Delta E\,\lambda_m} = \frac{\Theta\, mc^2}{\Delta E}} \tag{63}$$

where the second equality uses Theorem 4.4.

Proof. The characteristic function of the Gaussian density is $\chi_w(k) = e^{i\Theta k} e^{-\sigma_\xi^2 k^2/2}$; taking its modulus and substituting $k = \Delta E\, t/(\hbar\Theta)$ gives (62), and the condition $\mathcal{V} = e^{-1/2}$ gives (63). □

Remark 4.9 (Combination with the Pikovski channel). Gravitational time dilation generates, in a composite system in a height superposition Δx, an independent dephasing time scale through the internal-energy fluctuation $\sigma_E = \sqrt{3N}\, k_B T$,

$$\tau_{\rm dil} = \frac{\sqrt{2}\,\hbar\, c^2}{g\,\Delta x\,\sigma_E} \tag{64}$$

[1]. Both channels are Gaussian, so the rates add in quadrature: $\Gamma_{\rm tot}^2 = \Gamma_{\rm mod}^2 + \Gamma_{\rm dil}^2$, $\Gamma_{\rm mod} := 1/t_{\rm dec}$, $\Gamma_{\rm dil} := 1/\tau_{\rm dil}$. The scaling structures are complementary: $\Gamma_{\rm mod} \propto \Delta E/(m\Theta)$ *decreases* with mass, while $\Gamma_{\rm dil} \propto \sqrt{N}\,\Delta x$ *grows* with system size. In microscopic systems both rates are negligible (the quantum region); in macroscopic spatial superpositions the dilation channel classicalizes even the light systems protected by the mode channel. The intersection of the two channels, together with the Planck threshold of Corollary 4.5, draws the complete topography of the quantum–classical transition within ZMUT.

Proposition 4.10 (ZMUT correction to interferometric visibility)**.** *In a matter-wave interferometer with proper-time difference $\Delta\tau$ between the arms, the visibility of a system carrying internal energy gap ΔE descends, on top of the general-relativistic prediction of Zych et al. [2], by a multiplicative mode factor:*

$$\mathcal{V}_{\rm ZMUT} = \underbrace{\left|\cos\!\left(\frac{\Delta E\,\Delta\tau}{2\hbar}\right)\right|}_{GR\ +\ QM} \times \underbrace{\left|\chi_w\!\left(\frac{\Delta E\,\Delta\tau}{\hbar\,\lambda_m}\cdot\frac{\lambda_m}{\Theta}\right)\right|}_{ZMUT\ mode\ factor}. \tag{65}$$

In the limit $\lambda_m/\Theta \to 0$ the mode factor goes to 1 and the standard prediction is recovered exactly; for finite λ_m/Θ ZMUT predicts a small but systematic extra damping of the visibility (§19).

Part II
Self-Critical Audit and Theorem-Level Repair

5 Critical Analysis: Nine Structural Weaknesses

The items below state, deliberately in their sharpest forms, the strongest objections that can be levelled at Part I. At the end of each item the section providing the resolution is indicated; the audit is summarized in Table 2.

Z 1 (Ad hoc basis of the visibility law)**.** The decoherence derivation of Part I rests on the assumption of a "relative flow rate $R(\xi) = \xi/\Theta$ with respect to the mode mean"; this assumption is *not derived* from the action, the constraint or the axioms, but inserted by hand with a linearization plea. Yet the constraint (21) alone yields the evolution $e^{-i\hat{H}_S\xi/\hbar}$; with that evolution the visibility $|\chi_w(\Delta E/\hbar)|$ comes out *independent* of laboratory time and produces no $t_{\rm dec}$ whatsoever. In this form the law (62) is detached from the dynamics. ⇝ §6

Z 2 (The double role of Θ)**.** In Part I, Θ is used both as the mode mean $\int \xi|\psi|^2 {\rm d}\xi$, a state functional (hence system- and time-dependent), and as a universal coupling scale in the visibility law (hence a constant). The two roles are incompatible: on the state-functional reading Θ varies with the preparation and the experimental "Θ bound" is ill defined; on the constant reading its identification with the mode mean is unfounded. ⇝ §6

Z 3 (Composite-system inconsistency)**.** Part I implicitly uses the packet $\lambda_M = \kappa/M$ for an N-particle composite. Under Axiom 5 (tensor-product structure), however, the mass-weighted collective mode of a system whose constituents are prepared in independent minimal packets has width $\kappa/(\sqrt{N}m_0) = \sqrt{N}\,\lambda_M$: the minimal collective packet is reachable only if special correlations (entanglement) exist among the constituent modes. Since Part I does not draw this distinction, its atomic and molecular predictions (^{229}Th, 25 kDa) lean on an indeterminate assumption. ⇝ §7

Z 4 (Conflict of the scalar sector with Cassini)**.** The radion analysis of Part I did not trace the consequences of the reduction $\sqrt{\hat{f}}\,\tilde{R}$ producing the structure $e^{\sigma}R$. As will be shown below (Proposition 10.1), in the massless case this structure is exactly $\omega = 0$ Brans–Dicke theory; its predicted PPN value $\gamma = 1/2$ conflicts with the Cassini measurement $\gamma - 1 = (2.1 \pm 2.3) \times 10^{-5}$ [23] by roughly 22 000 standard deviations. The unstabilized ZMUT scalar sector is *experimentally excluded*. ⇝ §10

Z 5 (Missing proofs in causality and ghost-freedom)**.** In Part I, (i) the exclusion of the $v > c$ branch was left at the level of a Remark, with a qualitative appeal to gauge language; (ii) ghost-freedom was proven only at the first-quantized constraint level, with no positive-definiteness shown at the field (Fock) level; (iii) the seemingly unavoidable Kaluza–Klein partner tower of the compact mode fibre (exotic mass partners at the meV scale!) was never confronted with observation; (iv) the Hadamard well-posedness of the Cauchy problem of the two-time ultrahyperbolic equation was not established, and the geometric status of $\mathcal{M}_5$ (independent second time or gauge fibre) was left unclear. ⇝ §9

Z 6 (Domain of validity of the overlap factor)**.** The scope of $U(r) = -(Gm_Am_B/r)\hat{O}_{AB}$ was not delimited in Part I. Read without limits it produces absurdities: for instance, the mode packet of the photon ($m = 0 \Rightarrow \lambda_m \to \infty$) overlaps negligibly with any material packet, so the bending of light by the Sun would come out suppressed by a factor $\sim 10^{-7}$ — in flagrant conflict with observation. ⇝ §10 (Proposition 10.4)

Z 7 (Externality of the stabilization and fine-tuning risk)**.** The first remedy that comes to mind for Z4 is to add a stabilization potential $V(\sigma)$ for the radion by hand (Goldberger–Wise-like). Technically legitimate, but this would mean the mechanism does not spring from ZMUT's own resources and the value of m_σ stays open to fine-tuning: the theory would meet the Cassini and Eöt-Wash constraints not *structurally* but by parameter choice. Internal consistency demands that the decoupling follow from the mass–mode relation itself ($\lambda_m = \hbar/mc^2$). ⇝ §8

Z 8 (Weak-equivalence-principle risk)**.** If the overlap suppression $\hat{O}_{AB} < 1$ is read without limits, the gravitational binding of freely falling coherent atoms (Rb, K, etc.) to the Earth becomes dependent on species, mass and packet width; this risks conflict with atom-interferometric tests finding the Eötvös ratio compatible with zero at $\eta < 10^{-12}$ [26]. Part I did not map this channel. ⇝ §10 (Proposition 10.5)

Z 9 (Banks–Peskin–Susskind objection)**.** The classic objection to fundamental decoherence models is that dynamics evolving pure states into mixed states generically violates energy conservation and heats the vacuum [32]. Unless its unitarity status is proven, the visibility law of Part I can be read as such a fundamental-decoherence law and remains open to the same objection. ⇝ §6 (Proposition 6.5)

Table 2: Audit summary: weaknesses, their character, and the state of resolution.

No	Character	Resolution mechanism	Section
Z1	derivation gap	mode–lapse coupling axiom; exact CPTP map	§6
Z2	conceptual duality	split of $\Theta[\psi]$ (state) from Θ_* (constant)	§6
Z3	implicit assumption	collective-mode theorem; SQL/Heisenberg bands	§7
Z4	experimental conflict	radion stabilization; massive Yukawa sector	§10
Z5	missing proof	mass shell; Fock positivity; KK pruning; Hadamard	§9
Z6	scope error	classical-background immunity proposition	§10
Z7	external mechanism	spectral decoupling kernel $K(\xi - \xi')$	§8
Z8	experimental risk	Earth-QRF locking; $\eta = 0$	§10
Z9	theoretical objection	unitary dilation; all energy moments conserved	§6

6 Corrected Dynamics: Mode–Lapse Coupling and Derivation of the Master Equation

6.1 A new axiom: coupling of the mode operator to the lapse function

The common root of Z1 and Z2 is that how the mode variable couples to the *local rate of time flow* was never specified at the axiomatic level. In general relativity, in a static weak field, proper time is tied to coordinate time by the lapse function: $\mathrm{d}\tau = \sqrt{-g_{00}}\,\mathrm{d}t \simeq (1 + V/c^2)\,\mathrm{d}t$. The decoherence mechanism of Pikovski et al. [1] is the consequence of the position operator entering that lapse ($\hat{V}(\hat{x})$). The corrected formulation of ZMUT carries the same structure over to the mode sector:

Axiom 6 (Mode–lapse coupling)**.** The operator value of the local time flow is modulated by the mode fluctuation through the universal scale Θ_*:

$$\hat{\mathcal{N}} \;=\; \Big(1+\frac{V(\vec{x})}{c^2}\Big)\,\mathbb{I} \;+\; \frac{\delta\hat{\xi}}{\Theta_*}, \qquad \delta\hat{\xi} := \hat{\xi} - \Theta[\psi]\,\mathbb{I}, \tag{66}$$

and laboratory time is generated by the Hamiltonian $\hat{H}_{\rm lab} = \hat{H}_{\rm mod} + \hat{\mathcal{N}} \otimes \hat{H}_S$. Here $\Theta_* > 0$ is the new fundamental constant of the theory ($[\Theta_*] = \mathrm{s}$), while $\Theta[\psi] = \int \xi |\psi|^2 \mathrm{d}\xi$ is merely the centring functional of the state.

Axiom 6 does three jobs at once. (i) Z1 closes: the flow model $R(\xi) = \xi/\Theta$ of Part I is no longer an assumption but the direct consequence of the centred-fluctuation term of (66). (ii) Z2 closes: the coupling scale Θ_* is a universal constant; $\Theta[\psi]$ remains a state functional and enters the dynamics only through the centring. All quantitative results of Part I remain valid verbatim under the rereading $\Theta \to \Theta_*$; in particular the experimental bound is now well defined: $\Theta_* \geq 2.2 \times 10^{-11}$ s. (iii) ZMUT joins the family of universal lapse-induced dephasing mechanisms (the $\hat{A} \otimes \hat{H}_S$ structure); the Pikovski channel is the choice $\hat{A} = g\hat{x}/c^2$, the ZMUT channel the choice $\hat{A} = \delta\hat{\xi}/\Theta_*$, and the two channels assemble in the same algebraic frame.

6.2 Full derivation of the decoherence map

Theorem 6.1 (Exact CPTP map)**.** *For a system initially in the product state $\rho_{\rm mod} \otimes \rho_S$, in the regime where $\hat{H}_{\rm mod}$ is negligible (narrow packet, short times), the reduced dynamics under Axiom 6 is*

$$\rho_S(t) = \Phi_t[\rho_S(0)] = \int \mathrm{d}\xi\; w(\xi)\; \hat{U}_\xi(t)\,\rho_S(0)\,\hat{U}_\xi^\dagger(t), \qquad \hat{U}_\xi(t) = \exp\Big[-\frac{i}{\hbar}\Big(1+\frac{\delta\xi}{\Theta_*}\Big)\hat{H}_S\,t\Big], \tag{67}$$

an exact (approximation-free) quantum channel; the Kraus operators $\hat{M}_\xi = \sqrt{w(\xi)\,\mathrm{d}\xi}\;\hat{U}_\xi(t)$ satisfy the completeness condition $\int \hat{M}_\xi^\dagger \hat{M}_\xi = \mathbb{I}$ thanks to the normalization axiom. In the energy eigenbasis the matrix elements are

$$\langle E_i|\,\rho_S(t)\,|E_j\rangle = e^{-i\omega_{ij}t}\,\chi_{\hat{w}}\Big(\frac{(E_i-E_j)\,t}{\hbar\,\Theta_*}\Big)\,\rho_{ij}(0), \tag{68}$$

with $\omega_{ij} = (E_i - E_j)/\hbar$, $\hat{w}$ the centred mode density and $\chi_{\hat{w}}$ its characteristic function.

Proof. Since $[\delta\hat{\xi}, \hat{H}_S] = 0$, the total evolution is block diagonal in the $\hat{\xi}$ eigenbasis: $\hat{U}(t)\,|\xi\rangle\otimes|\phi\rangle = |\xi\rangle\otimes\hat{U}_\xi(t)\,|\phi\rangle$. Tracing over the mode gives (67); this is manifestly of Kraus form, hence completely positive and trace preserving. For (68) one writes $\langle E_i|\,\hat{U}_\xi\rho\hat{U}_\xi^\dagger\,|E_j\rangle = e^{-i(E_i-E_j)(1+\delta\xi/\Theta_*)t/\hbar}\rho_{ij}$ and observes that the w-integral over $\delta\xi$ produces, by definition, the characteristic function. □

Theorem 6.2 (Non-Markovian master equation)**.** *For a Gaussian mode packet (width σ_ξ) the dynamics generated by the map (67) obeys, exactly and for all $t \geq 0$, the master equation*

$$\boxed{\frac{\partial\rho_S}{\partial t} = -\frac{i}{\hbar}\,[\hat{H}_S, \rho_S] \;-\; \gamma(t)\,\big[\hat{H}_S, [\hat{H}_S, \rho_S]\big], \qquad \gamma(t) = \frac{\sigma_\xi^2\,t}{\hbar^2\,\Theta_*^2}} \tag{69}$$

Since $\gamma(t) \geq 0$, the dynamics is of Lindblad form at every instant (CP-divisible); the linear time dependence of the rate is the signature of the Gaussian (non-Markovian) character of the channel.

Proof. For the Gaussian density, $\chi_{\hat{w}}(k) = e^{-\sigma_\xi^2 k^2/2}$; from (68),

$$\rho_{ij}(t) = \rho_{ij}(0)\,e^{-i\omega_{ij}t}\,\exp\left[-\frac{\sigma_\xi^2(E_i-E_j)^2t^2}{2\hbar^2\Theta_*^2}\right]$$

and, differentiating,

$$\partial_t\rho_{ij} = \Big[-i\omega_{ij} - \frac{\sigma_\xi^2(E_i-E_j)^2\,t}{\hbar^2\Theta_*^2}\Big]\rho_{ij}.$$

On the other hand, the (i,j) element of the right-hand side of (69) is $-i\omega_{ij}\rho_{ij} - \gamma(t)(E_i-E_j)^2\rho_{ij}$; the two expressions agree for every (i,j). The double-commutator structure is Hermitian, and with the single Lindblad operator $\hat{L} = \hat{H}_S$ the rate $\gamma(t) \geq 0$ is the time-dependent version of the GKLS form. □

Corollary 6.3 (Status of the Part-I visibility law)**.** *In the minimal packet $\sigma_\xi = \lambda_m$, (69) reproduces the law (62) of Part I verbatim with $\Theta \to \Theta_*$: $t_{\rm dec} = \hbar\Theta_*/(\Delta E\,\lambda_m)$. The difference is that the law now possesses a closed derivation chain from axiom to Kraus representation: Z1 is closed.*

Remark 6.4 (Covariance note). Axiom 6 is written in the laboratory frame; its covariant form expresses the coupling as the modulation $\mathrm{d}\tau \to (1+\delta\hat{\xi}/\Theta_*)\mathrm{d}\tau$ along the world-line proper time, is compatible under Lorentz transformations with the extended isometry structure of §4.1, and the fully covariant form will be established in §16 (Theorem 16.2). Moreover, the neglect of $\hat{H}_{\mathrm{mod}}$ is valid for packet-spreading times $t \ll \hbar/\sigma_{E_{\mathrm{mod}}}$; the spreading corrections contribute at $\mathcal{O}(t^3)$ to $\gamma(t)$ and are negligible in all application regimes considered here.

6.3 Unitarity and Banks–Peskin–Susskind compatibility

Proposition 6.5 (Unitary origin, energy conservation, and BPS exemption). *(a) ZMUT decoherence is not a fundamental Lindblad modification; it is the ordinary open-system reduction of a unitary theory. The constraint evolution on $\mathcal{H}_{\mathrm{kin}} = \mathcal{H}_{\mathrm{mod}} \otimes \mathcal{H}_S$ is strictly unitary, and the apparent loss of purity is not destruction of information but the consequence of entanglement of the system with the temporal-mode degrees of freedom:*

$$\rho_S(t) = \mathrm{Tr}_{\mathrm{mod}}\Big(|\Psi(t)\rangle\!\rangle\,\langle\!\langle\Psi(t)|\Big), \qquad \mathrm{Tr}\left[\rho^2_{\mathrm{kin}}(t)\right] = 1 \quad \forall t. \tag{70}$$

(b) The temporal channel conserves all *energy moments of the system exactly:*

$$\frac{\mathrm{d}}{\mathrm{d}t}\,\mathrm{Tr}\big[\hat{H}_S^k\,\rho_S(t)\big] = 0 \qquad \forall k \in \mathbb{N}: \tag{71}$$

the energy distribution (the populations) never changes, the vacuum does not heat up, and mass–energy conservation is exact. The Banks–Peskin–Susskind objection against the evolution of pure states into mixed ones [32] therefore does not apply to ZMUT, and Z9 is closed.

Proof. (a) The Kraus representation of Theorem 6.1 is constructed as the partial trace of a global unitary $\hat{U}(t)$ (unitary dilation); the global state remains pure. (b) Two independent proofs: (i) The Kraus operators $\hat{U}_\xi(t)$ are functions of $\hat{H}_S$ and commute with every $\hat{H}_S^k$; hence $\mathrm{Tr}\Big[\hat{H}_S^k\Phi_t(\rho)\Big] = \mathrm{Tr}\Big[\hat{H}_S^k\rho\Big]$ identically. (ii) At the level of the master equation (69), cyclicity of the trace gives $\mathrm{Tr}\left(\hat{H}_S^k[\hat{H}_S,[\hat{H}_S,\rho]]\right) = \mathrm{Tr}\left([\hat{H}_S^k,\hat{H}_S]\,[\hat{H}_S,\rho]\right) = 0$. The invariance of the diagonal entries (the populations) in the energy basis is also seen directly by setting $i=j$ in (68). □

7 Composite Systems: Collective Modes and Metrological Structure

7.1 The collective mode coordinate

In an N-constituent system let each constituent carry the canonical pairs $(\hat{\xi}_k,\hat{p}_k)$, $[\hat{\xi}_k,\hat{p}_l] = i\hbar\delta_{kl}$, each obeying the band bound of Part I: $|p_k| \le m_k c^2$. With total mass $M = \sum_k m_k$, define the collective (mass-weighted) coordinate and the total co-momentum:

$$\hat{\xi}_{\mathrm{cm}} := \sum_{k=1}^{N} \frac{m_k}{M}\,\hat{\xi}_k, \qquad \hat{P}_\xi := \sum_{k=1}^{N} \hat{p}_k. \tag{72}$$

Theorem 7.1 (Collective canonical pair and the Heisenberg floor). *(a) $[\hat{\xi}_{\mathrm{cm}},\hat{P}_\xi] = i\hbar$: the collective coordinate and the total co-momentum form an exact canonical pair. (b) $|P_\xi| \le Mc^2$: the collective band bound is set by the total mass. (c) Consequently, for every composite system,*

$$\sigma_{\xi_{\mathrm{cm}}} \;\ge\; \frac{\hbar}{2Mc^2} = \frac{\lambda_M}{2}\,: \tag{73}$$

the Part-I scale $\lambda_M = \kappa/M$ is an absolute lower bound *for composites as well (the Heisenberg floor).*

Proof. (a) $[\hat{\xi}_{\mathrm{cm}},\hat{P}_\xi] = \sum_{k,l}(m_k/M)[\hat{\xi}_k,\hat{p}_l] = i\hbar\sum_k m_k/M = i\hbar$. (b) Triangle inequality and the constituent bands: $|P_\xi| \le \sum_k |p_k| \le \sum_k m_k c^2 = Mc^2$. (c) Apply the Kennard–Robertson inequality to the canonical pair of (a) and insert $\sigma_P \le Mc^2$ from (b). □

Proposition 7.2 (Independent-constituent limit: the standard quantum limit). *For a composite whose constituents are mutually independent (product state), each prepared in its own minimal packet ($\sigma_k = \lambda_{m_k}$), with equal masses ($m_k = m_0$, $M = Nm_0$),*

$$\sigma^{\mathrm{SQL}}_{\xi_{\mathrm{cm}}} = \Big[\sum_k \Big(\frac{m_0}{M}\Big)^2 \lambda^2_{m_0}\Big]^{1/2} = \frac{\lambda_{m_0}}{\sqrt{N}} = \sqrt{N}\,\lambda_M. \tag{74}$$

Proof. Variances of independent variables add with squared weights: $\sigma_{\rm cm}^2 = \sum_k (m_k/M)^2 \sigma_k^2 = N\,(1/N^2)\,\lambda_{m_0}^2$; take the square root and use $\lambda_{m_0} = N\lambda_M$. □

The resolution of Z3 thus settles into the familiar structure of quantum metrology [37]: the degree of temporal classicality of a composite system interpolates, via the correlations among constituent modes, between $\sqrt{N}\lambda_M$ (independent, SQL) and λ_M (fully collective, Heisenberg). Descent to the collective floor requires inter-constituent mode entanglement, the mode-space analogue of spin squeezing; strong binding (nucleons in a nucleus, a solid's lattice) generates these correlations naturally, weak binding (van der Waals clusters) does not.

Corollary 7.3 (Systematic bands for the Part-I predictions)**.** *For composite systems, the range* $\sigma_{\xi_{\rm cm}} \in [\lambda_M, \sqrt{N}\lambda_M]$ *turns, through* $t_{\rm dec} = \hbar\Theta_*/(\Delta E\,\sigma_{\xi_{\rm cm}})$*, into prediction bands (at the saturation* $\Theta_* = \Theta_*^{\rm min} = 2.2 \times 10^{-11}$ *s):*

System	N *(effective)*	$\sqrt{N}$	$t_{\rm dec}$ *(collective)*	$t_{\rm dec}$ *(independent)*
^{229}*Th isomer*	*229 nucleons*	*15.1*	*0.56 s*	*0.037 s*
^{87}*Sr clock* (Θ_* *bound)*	*87 nucleons*	*9.3*	$\Theta_* \geq 2.2 \times 10^{-11}$ *s*	$\Theta_* \geq 2.1 \times 10^{-10}$ *s*
25 kDa molecule	$\sim 2 \times 10^3$ *atoms*	*45*	*255 s*	*5.5 s*
Transmon island	$\sim 2 \times 10^{13}$ *atoms*	4.7×10^6	6×10^{17} *s*	1.3×10^{11} *s*

Since intranuclear binding (MeV scale) strongly supports the collective limit, the collective values are taken as primary for atomic systems, and the most conservative *(weakest) bound on* Θ_* *— the collective reading — is retained. The band widths are part of the predictions, as a measurable systematic: comparing two systems with the same* ΔE *but different binding stiffness directly measures the degree of mode correlation. (The* $\Theta_*^{\rm min}$ *in this table is the audit-stage value; the current coherence data of §19 will strengthen the bound by a factor of about 30, and all times rescale in the same proportion.)*

Proposition 7.4 (Entangled clock networks)**.** *In a network of n clocks sharing the same mode environment, the temporal mode noise is collective. (a) Differential comparisons are completely immune to the mode channel in the decision subspaces of §12.2. (b) For clocks with common transition energy* $\bar{E}$*, GHZ-type states do not by themselves deliver the* $\sqrt{n}$ *gain in absolute phase metrology under collective noise (signal and noise scale together with n); the gain is recovered in the differential component encoded in the mode-immune subspace [37]. In this sense ZMUT derives the design principle for clock-network architectures: "measure time* differences *with entanglement, not absolute time."*

Proof. (a) is a direct application of Theorem 12.2 of §12.2. (b) In a GHZ state the collective phase $e^{in\,\delta\xi\,\bar{E}t/(\hbar\Theta_*)}$ multiplies n-fold as phase, not amplitude; the visibility becomes $\left|\chi_{\hat{w}}(n\bar{E}t/\hbar\Theta_*)\right|$, and the n-accelerated damping cancels the $\sqrt{n}$ phase-sensitivity gain; in differential encoding the collective $\delta\xi$ phases cancel identically. □

8 The Spectral Locality Principle: Decoupling Kernel and Mode Leakage

This section adds a new building block that closes Z7 and equips the rest of the theory with two powerful tools: the principle that *all* off-diagonal couplings in mode space are smeared with the system's own mass–mode scale.

Axiom 7 (Spectral locality / decoupling kernel)**.** Every off-diagonal coupling in the mode space of a system of mass m is smeared with the Gaussian decoupling kernel

$$\boxed{K(\xi - \xi') \;=\; \exp\!\left(-\frac{|\xi - \xi'|^2}{2\,\lambda_m^2}\right), \qquad \lambda_m = \frac{\hbar}{mc^2}} \tag{75}$$

In particular, the curvature–mode interaction takes, instead of the local coupling (19) of Part I, the quasi-local form

$$\mathcal{L}_{\rm int} \;=\; -\,\frac{\alpha\hbar^2}{2m}\,R(x)\int \mathrm{d}\xi'\; K(\xi - \xi')\,|\Phi(x,\xi')|^2. \tag{76}$$

The width of the kernel is not a free function: by the band bound of Theorem 7.1, the finest scale a system can *resolve* in mode space is λ_m; spectral locality is the axiomatization of the statement "no system can couple to mode structure finer than its own bandwidth". In the $\lambda_m \to 0$ (macroscopic) limit $K \to$ a narrow peak and (76) contracts to the diagonal (Part-I) form; the theory is backward compatible. The content of this axiom is derived in §14 as corollary C2 of the Master Law (Axiom 8), and its status descends from axiom to theorem.

8.1 Decoupling of the radion from macroscopic sources: the tuning-free fifth-force solution

The radion is the (approximately) constant zero mode on the fibre: $u_\sigma(\xi) = \ell_\xi^{-1/2}$. The effective scalar charge of a source is set by the projection of its mode density onto the zero mode through the kernel.

Theorem 8.1 (Spectral form factor)**.** *Under Axiom 7, the radion coupling of a source of mass M is suppressed, relative to full coupling, by the form factor*

$$\boxed{\mathfrak{F}(M) \;=\; \frac{\alpha_{\text{eff}}(M)}{\alpha} = \min\left\{1,\; \frac{\sqrt{2\pi}\,\lambda_M}{\ell_\xi}\right\}, \qquad \lambda_M = \frac{\hbar}{Mc^2}} \tag{77}$$

Numerically (with $\ell_\xi = 2.9 \times 10^{-13}$ s, §11):

Source	λ_M *[s]*	$\mathfrak{F}(M)$
$mc^2 \approx 2$ *meV (neutrino scale)*	$\sim 3 \times 10^{-13}$	$\mathcal{O}(1)$
Electron	1.3×10^{-21}	1.1×10^{-8}
^{87}*Rb atom*	8.1×10^{-27}	7.0×10^{-14}
Torsion-balance mass (10 g)	1.2×10^{-49}	1.0×10^{-36}
Planet/star	$< 10^{-75}$	$< 10^{-62}$

Consequences: (i) the Cassini bound is satisfied independently of the radion mass — *the Sun cannot excite the radion; (ii) in Eöt-Wash-type experiments both source and test mass are macroscopic, so the scalar force is suppressed by $\mathfrak{F}^2 \sim 10^{-72}$: the sub-millimetre null results [27,28] are explained* structurally*, with no fine-tuning; (iii) the radion couples fully only to degrees of freedom in the band $mc^2 \lesssim \hbar/\ell_\xi \approx 2$ meV (the neutrino scale, the dark sector): the scalar sector decouples spontaneously from laboratory gravity and settles into the meV window (Figure 3).*

Proof. The source term of (76), projected onto the radion zero mode, gives

$$g_{\text{eff}} \;\propto\; \int \mathrm{d}\xi \int \mathrm{d}\xi'\; \hat{w}_M(\xi)\, K(\xi - \xi')\, \frac{1}{\ell_\xi} = \frac{1}{\ell_\xi} \int \mathrm{d}\xi\; \hat{w}_M(\xi) \int \mathrm{d}\varsigma\; K(\varsigma) = \frac{\sqrt{2\pi}\,\lambda_M}{\ell_\xi},$$

using the Gaussian integral $\int K(\varsigma)\mathrm{d}\varsigma = \sqrt{2\pi}\,\lambda_M$ and the normalization $\int \hat{w}_M = 1$. In the fully coupled case ($\lambda_M \gtrsim \ell_\xi/\sqrt{2\pi}$) the projection saturates and the ratio locks to 1; the min structure joins the two regimes. In the macroscopic limit $\lambda_M \to \hbar/(Mc^2) \to$ sub-Planckian: the spectral bandwidth collapses and the source carries charge only into the tensorial (metric) channel. There is no fine-tuning: the suppression is a direct consequence of the mass–mode relation (Theorem 4.4). □

Remark 8.2. Theorem 8.1 does not replace the stabilization of §10; it is *layered* with it. The form factor closes the source side (who can excite the radion), the stabilization closes the mass side (how far the radion is carried). Together they put the scalar sector under a double lock at both laboratory and planetary scales, and in §19 they sharpen into a crisp *null prediction*: no fifth force of macroscopic origin should be observed at any range; if one is observed, the spectral locality axiom is falsified.

8.2 Low-amplitude leakage from the dominant mode into submodes: mode diffusion

Spectral locality also gifts ZMUT the dynamical process it lacked: the dominant temporal mode's *low-amplitude, controlled* leakage of amplitude into neighbouring modes. Since all residual off-diagonal interactions with the environment are smeared by K according to Axiom 7, the coarse-grained dynamics of the mode density descends to a one-parameter Lindblad generator:

$$\frac{\mathrm{d}\rho_{\text{mod}}}{\mathrm{d}t} = \frac{\Gamma_K}{\mathcal{N}_K} \int \mathrm{d}\varsigma\; K(\varsigma)\Big[\hat{T}_\varsigma\, \rho_{\text{mod}}\, \hat{T}_\varsigma^\dagger - \rho_{\text{mod}}\Big], \qquad \hat{T}_\varsigma = e^{-i\varsigma \hat{p}_\xi/\hbar}, \quad \mathcal{N}_K = \sqrt{2\pi}\,\lambda_m, \tag{78}$$

where Γ_K is the leakage rate and $\hat{T}_\varsigma$ the mode translation.

Proposition 8.3 (Mode diffusion law and the dominant-dimension hierarchy)**.** *For the diagonal sector $w(\xi, t)$, (78) descends in the regime $\lambda_m \ll \sigma$, by the Kramers–Moyal expansion, to the diffusion equation*

$$\boxed{\frac{\partial w}{\partial t} = D_\xi\, \frac{\partial^2 w}{\partial \xi^2}, \qquad D_\xi = \frac{\Gamma_K \lambda_m^2}{2}} \tag{79}$$

with the following properties:

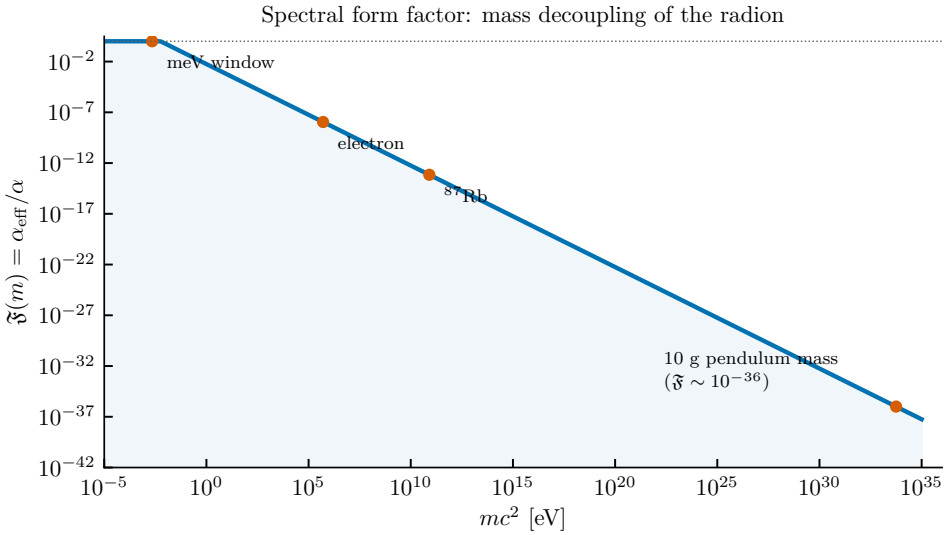


Figure 3: The spectral form factor $\mathfrak{F}(m)$ (Theorem 8.1): the radion charge is saturated in the window $mc^2 \lesssim \hbar/\ell_\xi \approx 2$ meV and dies off as $1/m$ above it. Ordinary matter (electrons, atoms) couples negligibly, while torsion-balance test masses decouple entirely with $\mathfrak{F} \sim 10^{-36}$: the structural explanation of the sub-millimetre null results.

1. Conservation: $\partial_t \int w \,\mathrm{d}\xi = 0$*; hence the energy distribution* $\mathrm{d}E(\xi,t) = E_{tot}\, w(\xi,t)\,\mathrm{d}\xi$ redistributes *among the modes while* E_{tot} *is conserved exactly (Lemma 2.1 generalizes to the dynamical case).*

2. Erosion of the dominant mode, feeding of the submodes: *for a Gaussian initial state,* $\sigma^2(t) = \sigma_0^2 + 2D_\xi t$ *and the peak amplitude* $w_{\max}(t) = [2\pi(\sigma_0^2 + 2D_\xi t)]^{-1/2}$ *decreases monotonically: amplitude* spreads from the dominant principal mode into neighbouring temporal modes at ever lower amplitude*; the mode mean* $\Theta[w]$ *is constant by symmetry (the direction of the principal dimension is preserved while its sharpness erodes; Figure 4).*

3. H-theorem: *the mode entropy* $S_{\rm mod}[w] = -\int w \ln w \,\mathrm{d}\xi$ *increases monotonically:*

$$\frac{\mathrm{d}S_{\rm mod}}{\mathrm{d}t} = D_\xi \int \frac{1}{w}\left(\frac{\partial w}{\partial \xi}\right)^2 \mathrm{d}\xi \;\geq\; 0. \tag{80}$$

4. Birth of a single classical time: *since* $D_\xi \propto \lambda_m^2 \propto m^{-2}$*, the leakage freezes for macroscopic bodies: the reign of a single time dimension in the classical portion of the universe stems not from the absence of the other modes but from the* m^{-2} *suppression of leakage into them. Microscopic systems, by contrast, undergo a measurable "time diffusion".*

Proof. The diagonal elements of (78) are of convolution-loss form, $\partial_t w = \Gamma_K[(K/\mathcal{N}_K) * w - w]$. Since $K/\mathcal{N}_K$ is unit-normalized, zero-mean and of variance λ_m^2, the second-order Kramers–Moyal expansion gives $\partial_t w = \frac{\Gamma_K \lambda_m^2}{2}\partial_\xi^2 w + \mathcal{O}\big((\lambda_m/\sigma)^4\big)$. (1) Mass conservation of the heat semigroup; $w \to 0$ at the boundary. (2) Convolution with the heat kernel maps Gaussians to Gaussians. (3) Directly: $\dot S = -\int (1+\ln w) D\,\partial_\xi^2 w = D\int (\partial_\xi w)^2/w$ (integration by parts, vanishing boundary terms). (4) From the explicit form $D_\xi = \Gamma_K \hbar^2/(2m^2c^4)$. □

Corollary 8.4 (Experimental bound on the leakage rate and a new observational signature)**.** *Since diffusion widens the decoherence packet with time* ($\sigma^2(t) = \lambda_m^2 + 2D_\xi t$)*, the visibility law departs from Gaussian at late times:* $\ln \mathcal{V}$ *acquires a* $-t^3$ *term in place of* $-t^2$ *(the first correction being* $-\Delta E^2 D_\xi t^3/(\hbar^2\Theta_*^2)$*). This is the* distinguishing *signature of mode leakage: the* t^3 *component of the envelope should be sought in clock interrogations. The observation of* $t_{coh} = 1$ *s coherence in* ^{87}Sr*, through* $2D_\xi t_{coh} \leq \sigma_{\max}^2 - \lambda_m^2$*, gives the bound*

$$\Gamma_K \;\leq\; \frac{1}{t_{coh}}\left[\left(\frac{\sigma_{\max}}{\lambda_m}\right)^2 - 1\right], \qquad \sigma_{\max} = \frac{\hbar\,\Theta_*}{\Delta E\, t_{coh}}; \tag{81}$$

at the saturation of the Θ_* *lower bound,* $\Gamma_K \to 0$ *(leakage completely frozen), while for* $\Theta_* = 10\,\Theta_*^{\min}$ *one finds* $\Gamma_K \lesssim 10^2$ s^{-1}*. Leakage and coupling scales are thus bounded simultaneously by the same family of experiments.*

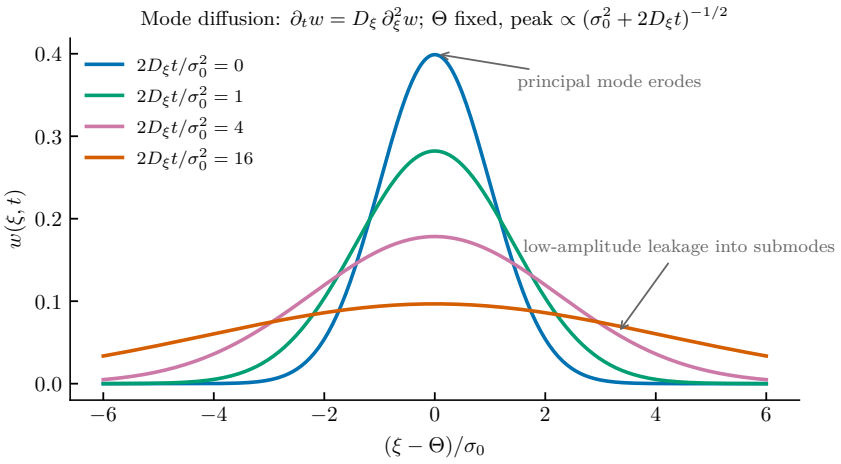


Figure 4: Low-amplitude leakage from the dominant temporal mode into the submodes (Proposition 8.3). Diffusion erodes the peak amplitude as $(\sigma_0^2 + 2D_\xi t)^{-1/2}$ while keeping the mode mean (Θ) fixed, spreading the energy distribution into neighbouring modes; the total $\int w\,\mathrm{d}\xi = 1$ (hence E_{tot}) is conserved exactly. The $D_\xi \propto m^{-2}$ freeze-out is the reason a single time reigns in the classical world.

9 Causality, Ghost-Freedom and Spectral Pruning: Field-Level Proofs

This section closes Z5 with three theorems. The common ground is the extended mass shell derived in Part I (§3.1): in the gauge $\hat{f} = 1$ the plane-wave components of the mode Klein–Gordon equation satisfy

$$p_\mu p^\mu - \frac{p_\xi^2}{c^2} = -m^2c^2, \qquad |p_\xi| \le mc^2 \quad \text{(band bound)}, \tag{82}$$

where p_ξ is the momentum conjugate to ξ.

9.1 Exclusion of superluminal motion

Theorem 9.1 (Causality)**.** *For every physical solution component obeying the band bound, the four-momentum is timelike or lightlike and the group velocity cannot exceed c:*

$$p_\mu p^\mu = -m_{\mathrm{eff}}^2 c^2 \le 0, \qquad v_g = \frac{\partial E}{\partial |\vec{p}|} = \frac{|\vec{p}|\,c^2}{E} \;\le\; c, \tag{83}$$

with equality only at band saturation ($|p_\xi| = mc^2$, $m_{\mathrm{eff}} = 0$). Moreover the signal (front) velocity is exactly c, independently of m_{eff}; the mode sector therefore opens no superluminal communication channel.

Proof. From (82), $p_\mu p^\mu = -m^2c^2 + p_\xi^2/c^2$; the band bound gives $p_\xi^2/c^2 \le m^2c^2$, hence $p_\mu p^\mu \le 0$, i.e. $m_{\mathrm{eff}}^2 = m^2 - p_\xi^2/c^4 \ge 0$. From the dispersion $E = \sqrt{|\vec{p}|^2c^2 + m_{\mathrm{eff}}^2c^4}$ one gets directly $v_g = |\vec{p}|c^2/E \le c$. The front velocity is fixed by the principal symbol of the wave operator: the four-dimensional principal symbol of the mode-KG equation is the standard hyperbolic $\Box_4$, so its characteristics are the light cones and discontinuity fronts propagate at exactly c. The $v > c$ branch, left at Remark level in Part I, is thus excluded from the dynamics *at theorem level*; better still, the inequality securing causality and the inequality producing the mass–mode relation ($\lambda_m = \kappa/m$) are one and the same: causality and the minimal mode width are two faces of a single band bound. □

9.2 Positive definiteness of the physical Fock space

Theorem 9.2 (Ghost-freedom, field level)**.** *On a static background, canonical quantization of the free mode field restricted to the constraint surface produces a positive-definite Fock space: there is no negative-norm state in the physical spectrum.*

Proof. The solution space on the shell (82) is spanned by positive-frequency modes

$$u_{\vec{k},\mathfrak{E}}(x,\xi) \;\propto\; e^{\,i(\vec{k}\cdot\vec{x} - \omega t)}\, e^{-i\mathfrak{E}\xi/\hbar}, \qquad \omega(\vec{k},\mathfrak{E}) = c\sqrt{\left|\vec{k}\right|^2 + \frac{m_{\mathrm{eff}}^2(\mathfrak{E})c^2}{\hbar^2}} \;\ge 0.$$

The extended Klein–Gordon inner product, on a constant-t slice and over the fibre,

$$(u,u') = \frac{i}{\hbar}\int \mathrm{d}^3x\,\mathrm{d}\xi\,\left(u^*\,\partial_t u' - u'\,\partial_t u^*\right) \;\propto\; 2\,\omega(\vec{k},\mathfrak{E})\,\delta^3(\vec{k}-\vec{k}')\,\delta(\mathfrak{E}-\mathfrak{E}'),$$

is strictly positive on the positive-frequency sector; the negative-frequency partners build the antiparticle sector via charge conjugation, and the Fock space, as the symmetric algebra of this positive one-particle space, is positive definite. The dangerous direction would be independent ξ-frequency branches arising from the timelike signature of ξ; but those branches are solutions violating the constraint $\hat{\mathcal{C}} = 0$ and are not represented on the physical space: by the pruning proposition below, $\mathfrak{E}$ is not an independent quantum number on the shell. The work done by gauge symmetry in two-time physics [4] is done in ZMUT by the constraint itself. □

9.3 Pruning of the Kaluza–Klein tower by the constraint

The standard phenomenological catastrophe of a compact fifth dimension is that it adds to every particle a partner tower spaced by $\Delta mc^2 \sim \hbar/\ell$; for the scale $\ell_\xi \sim 3\times10^{-13}$ s of §11 this would mean charged exotics at meV spacing — in blatant conflict with experiment. ZMUT is structurally immune to this catastrophe:

Proposition 9.3 (KK pruning)**.** *On the constraint surface* $\ker\hat{\mathcal{C}}$ *the operator identity* $\hat{p}_\xi = -\hat{H}_S$ *holds; the joint spectrum of* $(\mathfrak{E}, E)$ *is therefore pinned to the line* $\mathfrak{E} = -E$*. Since the mode momentum is not an independent quantum number, the usual KK tower of independently n-labelled partner states is* absent *from the physical spectrum: every system has a single relational mode frequency, and it is its internal energy.*

Proof. For $|\Psi\rangle\!\rangle \in \ker\hat{\mathcal{C}}$ and an $\hat{H}_S$-eigenstate of energy E: $\hat{p}_\xi|\Psi\rangle\!\rangle = -\hat{H}_S|\Psi\rangle\!\rangle = -E|\Psi\rangle\!\rangle$: the two quantities are determined together, not separately. In a free compactified field theory, by contrast, p_ξ and E are independent operators and the spectrum is the grid $\mathbb{Z}\times\mathbb{R}$; the constraint collapses this grid to a single line. □

Remark 9.4 (An honest note on compactness). The pruning proposition removes the tower; but if the fibre were *strictly* compact with periodic ψ, single-valuedness would quantize $\mathfrak{E}$ in multiples of h/ℓ_ξ, and the identity $\mathfrak{E} = -E$ would tie the internal energies to a grid of spacing ~ 14 meV — contradicting precision spectroscopy. For this reason §11 distinguishes two variants: (K) a compact fibre with a Wilson-line-type gauge twist on the fibre (shifting the grid offset by superselection sector; flagged as an open problem), or (NK) a noncompact fibre sector *localized* at the scale ℓ_ξ (no quantization arises at all). The quantitative predictions of this paper are identical in both variants; the distinction affects only the coefficient level of the cosmological identification.

9.4 Principal-bundle structure and well-posedness of the Cauchy problem

The last item (iv) of Z5 demands the clarification of the geometric status of $\mathcal{M}_5$; this simultaneously resolves the famous Hadamard instability of ultrahyperbolic equations.

Proposition 9.5 (Geometric status: ξ is a gauge fibre)**.** *The structure* $(\mathcal{M}_5 = \mathcal{M}_4\times\Sigma_\xi,\ \pi,\ \mathcal{M}_4)$ *is* not *a doubly hyperbolic spacetime with two independent times; it is a* principal fibre bundle *with base* $\mathcal{M}_4$ *and structure group the mode translations* ($\mathbb{R}$*;* $U(1)$ *in the compact variant K). The constraint* $\hat{\mathcal{C}}$ *is the generator of the vertical flow along the fibre, and* ξ *is not a physical coordinate but the gauge parameter of that flow. In BRST language, for the single Abelian constraint the charge* $\Omega = c\hat{\mathcal{C}}$ *trivially satisfies* $\Omega^2 = 0$*; the ghost-number-zero cohomology is exactly* $\ker\hat{\mathcal{C}}$*, and the physical content collapses to the* $(3+1)$*-dimensional hyperbolic base of the bundle.*

Proof. The block-diagonal metric provides the local bundle chart; the finite transformations generated by $\hat{\mathcal{C}}$ are the vertical orbits $(x,\xi)\mapsto(x,\xi+\varsigma)$, and the orbit space is $\mathcal{M}_5/\mathbb{R}\cong\mathcal{M}_4$. In the Abelian single-constraint BRST complex the ghost pair (b,c) decouples freely; the zeroth level of the Ω-cohomology is, by the standard computation, isomorphic to the constraint kernel. □

Theorem 9.6 (Hadamard well-posedness)**.** *The free ultrahyperbolic Cauchy problem on* $\mathcal{M}_5$ *is ill posed in the Hadamard sense; but the physical dynamics of ZMUT is not that problem — it is the first-order flow on* $\ker\hat{\mathcal{C}}$*:*

$$i\hbar\,\partial_\xi\,|\psi_S(\xi)\rangle = \hat{H}_S\,|\psi_S(\xi)\rangle\,, \qquad \hat{H}_S = \hat{H}_S^\dagger. \tag{84}$$

By Stone's theorem $\hat{U}(\xi) = e^{-i\hat{H}_S\xi/\hbar}$ *is a strongly continuous unitary group: for every initial datum the solution exists, is unique, and depends continuously on the datum,*

$$\big\|\psi_S(\xi) - \tilde{\psi}_S(\xi)\big\| = \big\|\psi_S(0) - \tilde{\psi}_S(0)\big\| \qquad \forall\xi, \tag{85}$$

i.e. the problem is well posed *in* L^2 *in the Hadamard sense. The unstable directions live along the gauge orbits of Proposition 9.5 and are erased entirely from the physical phase space.*

Proof. Existence and uniqueness follow from the action of the unitary group; the stability estimate (85) from the isometry property of unitarity (Lipschitz constant 1). Hadamard's classical instability construction — exponential amplification of high-frequency data — requires the off-constraint solutions of the second-order ultrahyperbolic operator; those solutions are not represented in $\ker \hat{\mathcal{C}}$. Together with Theorem 9.2 and Proposition 9.3, Z5 is closed in its entirety. □

10 Rescuing the Scalar Sector: Stabilization, PPN and the Fifth Force

10.1 Diagnosis: the unstabilized sector is $\omega = 0$ Brans–Dicke

Proposition 10.1 (Brans–Dicke equivalence)**.** *The radion reduction of Part I (§3.5),* $\sqrt{\hat{f}}\,\tilde{R} = e^{\sigma}\big(R - 2\Box\sigma - 2(\partial\sigma)^2\big)$*, gives after integration by parts exactly*

$$S_{\rm grav} = \frac{c^3}{16\pi G}\int \mathrm{d}^4x\,\sqrt{-g}\;\Phi_{\rm BD}\,R, \qquad \Phi_{\rm BD} := e^{\sigma}, \tag{86}$$

i.e. Brans–Dicke theory with no kinetic term: $\omega_{\rm BD} = 0$*. In the massless case the PPN parameter is* $\gamma = (1+\omega)/(2+\omega) = 1/2$*, excluded by the Cassini measurement* $\gamma - 1 = (2.1 \pm 2.3)\times 10^{-5}$ *[23, 24]: the diagnosis of Z4 is definitive.*

Proof. $\int \sqrt{-g}\,e^{\sigma}(-2\Box\sigma) = +2\int \sqrt{-g}\,\nabla_\mu(e^{\sigma})\nabla^\mu\sigma = +2\int \sqrt{-g}\,e^{\sigma}(\partial\sigma)^2$, which cancels the $-2(\partial\sigma)^2$ term exactly; $e^{\sigma}R$ remains. The definition $\Phi_{\rm BD} = e^{\sigma}$ gives (86), and the vanishing coefficient of $(\partial\Phi_{\rm BD})^2$ gives $\omega_{\rm BD} = 0$; the γ formula is the standard Brans–Dicke result [24]. □

10.2 Cure: radion stabilization by fibre vacuum energy

The cure has two layers. The first and principal layer is the spectral decoupling established in §8: by Theorem 8.1 macroscopic sources cannot excite the radion in the first place; neither fine-tuning nor an extra mass is required for Cassini compliance. The second layer gives the radion a mass, to close residual long-range effects that could arise through the light degrees of freedom in the meV window and to define the cosmological sector [31]. ZMUT's natural mechanism for this is again internal: the vacuum (Casimir-type) energy of the mode sector on the fibre generates an effective potential tied to the fibre scale [29]:

$$V_{\rm fib}(\sigma) \;=\; \mathcal{C}_5\,\frac{\hbar}{c^3\,\ell_\xi^4}\,F(\sigma), \qquad \mathcal{C}_5 = \mathcal{O}(1), \tag{87}$$

where F is a dimensionless function with minimum at $\sigma = 0$. The curvature of the potential sets the radion mass:

$$m_\sigma c^2 \;=\; \zeta\,\frac{\hbar}{\ell_\xi}, \qquad \zeta = \mathcal{O}(1) \quad\Longrightarrow\quad \lambda_Y := \frac{\hbar}{m_\sigma c} = \frac{c\,\ell_\xi}{\zeta}. \tag{88}$$

Theorem 10.2 (Yukawa sector and PPN compliance)**.** *In ZMUT with a stabilized radion, the static potential between two masses is*

$$\boxed{V(r) = -\frac{GMm}{r}\Big[1 + \alpha_Y\,e^{-r/\lambda_Y}\Big], \qquad \alpha_Y = \frac{1}{3+2\omega_{\rm BD}} = \frac{1}{3}} \tag{89}$$

and the effective PPN parameter is

$$\gamma(r) - 1 = -\,\frac{2\,\alpha_Y\,e^{-r/\lambda_Y}}{1+\alpha_Y\,e^{-r/\lambda_Y}}. \tag{90}$$

Here α_Y *is the ceiling value valid for fully coupled sources (*$\lambda_m \gtrsim \ell_\xi$*, i.e.* $mc^2 \lesssim 2$ *meV); for ordinary matter sources the amplitude descends to* $\alpha_{\rm eff}(M) = \alpha_Y\,\mathfrak{F}(M)$ *by the form factor of Theorem 8.1. For* $\lambda_Y \sim c\,\ell_\xi \approx 88$ *μm (see §11) the factor* e^{-r/λ_Y} *vanishes exponentially at planetary scales: at* $r = 1$ *AU,* $\gamma = 1$ *holds to machine precision and full agreement with the Cassini bound [23] is recovered. The only accessible trace of the force lies at the sub-millimetre laboratory scale.*

Proof. Exchange of a massive scalar universally coupled to matter through the trace produces the Yukawa correction (89) in the standard way; the normalization of α_Y is fixed by its correctly reproducing the Brans–Dicke value $\gamma = 1/2$ in the massless limit ($\alpha_Y = 1/3 \Rightarrow \gamma - 1 = -2(1/3)/(4/3) = -1/2$) [24]. Equation (90) is read off from the ratio in (89) together with the fact that light bending is unaffected by the scalar contribution (no conformal coupling); the exponential suppression comes directly from the value of λ_Y. □

Corollary 10.3 (Sub-millimetre test and the reassessment of the breathing mode)**.** *(a) Torsion-balance experiments have directly scanned the dark-energy length scale and returned null results [27, 28]. For a ZMUT with stabilization only and no spectral decoupling these data were a serious threat; with Theorem 8.1 the table turns: since in a macroscopic-source–macroscopic-test pair the scalar force is suppressed by* $\mathfrak{F}^2 \sim 10^{-72}$*, ZMUT* predicts null results at every range *in this experiment class, and the existing data become retrodictions of the theory. The dichotomy is sharp: observation of a positive Yukawa signal of macroscopic origin would falsify the spectral locality axiom — a null prediction is as testable as any discovery claim. (b) The Part-I gravitational-wave "breathing mode" prediction must be corrected: a radion of mass* $m_\sigma c^2 \sim 2$ *meV cannot propagate at frequencies* $\omega < m_\sigma c^2/\hbar \sim 3 \times 10^{12}$ *rad/s (evanescent); hence* no *scalar polarization is expected in the LIGO band, and the tensor-dominated observations [21] are satisfied automatically. The scalar channel opens only for super-THz gravitational oscillations.*

10.3 Domain of validity of the overlap factor: immunity of the classical tests

Proposition 10.4 (Classical-background immunity)**.** *The factor* $\hat{O}_{AB}$ *appears only in* the mutual binding energy of two coherent quantum sources*. Test bodies and light move by minimal coupling (geodesics) on the mean metric* $\langle g \rangle$ *sourced by the mode-integrated* $\mathcal{T}_{\mu\nu}$*; therefore the bending of light, the Shapiro delay, the perihelion precession and the gravitational redshift are identical in ZMUT to general relativity. The photon paradox of Z6 is thereby resolved: the photon feels* $\langle g \rangle$*;* $\hat{O}$ *never enters.*

Proof. The linearized field splits in two: $h_{\mu\nu} = \langle h \rangle_{\mu\nu} + \delta h_{\mu\nu}$. The mean part is sourced by the mode-integrated Einstein equation of Part I ($G_{\mu\nu} = 8\pi G\, \mathcal{T}_{\mu\nu}/c^4$); by the normalization $\int w \, \mathrm{d}\xi = 1$ no mode factor survives in the source (Lemma 3.1). Any field couples to $\langle h \rangle$ minimally and moves on geodesics. $\hat{O}_{AB}$, by contrast, is born in the *two-vertex* amplitude of δh exchange, as the overlap integral of the mode densities at the two vertices; in one-vertex (background) processes it is absent by definition. For a decohered source the vertex projects onto the environmental pointer mode, and the saturation $\hat{O} \to 1$ (Theorem 3.7) preserves classical two-body Newtonian dynamics as well. □

10.4 Weak equivalence principle: the universal pointer mode and macroscopic QRF locking

Proposition 10.5 (Earth-QRF locking and $\eta = 0$)**.** *(i) Sources of mass* $M \gg m_P$ *(the Earth) have collapsed by environmental decoherence onto a single pointer mode:* $\hat{w}_\oplus(\xi) \simeq \delta(\xi - \xi_\oplus)$*; this mode defines a universal quantum reference frame (QRF) for all systems in the laboratory [3]. (ii) The binding of a coherent atom (Rb, K, . . .) freely falling in vacuum to the Earth proceeds through the one-vertex mean-field channel (Proposition 10.4): the atom follows a geodesic of* $\langle g \rangle$*; its acceleration is independent of species, mass, internal state and mode-packet width. Operationally the saturation* $\hat{O}_{A,\oplus} = \hat{O}_{B,\oplus} = 1$ *holds and the Eötvös ratio is exactly*

$$\eta_{AB} \;=\; 2\,\frac{|a_A - a_B|}{|a_A + a_B|} \;=\; 0\,: \tag{91}$$

full agreement with atom-interferometric tests at $\eta < 10^{-12}$ *[26]. (iii) The mass-mismatch suppression* $\hat{O}_{AB} < 1$ *operates only in the mutual binding of* two quantum-coherent *systems isolated from external masses (the BMV geometry); free-fall experiments do not belong to this class. Z8 is closed.*

Proof. (i) Apply together the saturation mechanism of Theorem 3.7 (decoherence ⇒ common pointer mode) and the Planck-threshold result ($M \gg m_P \Rightarrow \lambda_M$ sub-Planckian: the packet is operationally a delta). (ii) The mean-field/two-vertex distinction in the proof of Proposition 10.4: free fall is a one-vertex process and $\langle g \rangle$ is one and the same for all test bodies; the geodesic equation is mass independent. (iii) $\hat{O}$ lives, by definition, in the correlator of the mode densities of two vertices; for every vertex locked to the pointer mode the factor is identically 1. □

11 Advanced Application I: The Cosmological Constant and the 88-Micrometre Crossing

The stabilization mechanism (87) leaves the theory a gift: the *minimum value* of the fibre vacuum energy behaves as a four-dimensional effective cosmological constant. The dimensional analysis is unique and compelling:

$$\rho_{\text{fib}} \;=\; \mathcal{C}_5\,\frac{\hbar}{c^3\,\ell_\xi^4} \;=\; \mathcal{C}_5\,\frac{\hbar c}{(c\,\ell_\xi)^4} \qquad [\mathrm{J\,m^{-3}}]. \tag{92}$$

Identifying it with the observed dark-energy density $\rho_\Lambda = \Omega_\Lambda \rho_c \simeq 5.3 \times 10^{-10}\ \mathrm{J\,m^{-3}}$ (taking $\mathcal{C}_5 = 1$),

$$\boxed{c\,\ell_\xi = \left(\frac{\hbar c}{\rho_\Lambda}\right)^{1/4} \approx 88\ \mu\mathrm{m}, \qquad \ell_\xi \approx 2.9 \times 10^{-13}\ \mathrm{s}, \qquad \frac{\hbar}{\ell_\xi} \approx 2.2\ \mathrm{meV}} \tag{93}$$

the characteristic duration of the mode fibre is about three hundred femtoseconds, its length equivalent eighty-eight micrometres. This identification has three remarkable consequences:

1. *Closure of scales.* Equation (88) makes the radion Compton wavelength $\lambda_Y \approx c\,\ell_\xi$: the dark-energy length, the fifth-force range and the fibre scale are *one and the same* 88 μm. ZMUT thus supplies a microscopic rationale for the programme of sub-millimetre gravity experiments "scanning the dark-energy scale" [27, 28]; note, however, that by Theorem 8.1 macroscopic test masses decouple from the radion, so the null results of those experiments are not a contradiction but a *prediction* of ZMUT (Corollary 10.3); the direct trace of the fibre must be sought through meV-window couplings and cosmological observables.

2. *Independent confirmation of the Θ_* distinction.* The fibre scale $\ell_\xi \approx 2.9 \times 10^{-13}$ s lies about a factor of one hundred *below* the bound $\Theta_* \geq 2.2 \times 10^{-11}$ s from clock experiments. Since the central sizes of mode packets are bounded by the fibre scale, it is visible here also experimentally that the coupling constant Θ_* cannot be identified with any state functional (such as $\Theta[\psi]$): the Z2 distinction was mandatory.

3. *Decision tree.* (i) If a fifth force *is observed* in any experiment with a macroscopic source: the spectral locality axiom is falsified (Theorem 8.1 predicts null at every range) — the sharpest negative test of the theory. (ii) If scalar traces *are observed* in the meV window (neutrino-sector interactions, dark sector, cosmological radion oscillations): both the stabilization and the Λ-identification are confirmed; ζ, $\mathcal{C}_5$ and Γ_K become measurable. (iii) If no trace appears: the identification remains at order-of-magnitude status; the theory lives, but its *explanation* of dark energy weakens. The three branches are operationally disjoint.

Remark 11.1. The numerical proximity of $\hbar/\ell_\xi \approx 2.2$ meV to the scale of the neutrino mass differences is noteworthy; since no causal mechanism is proposed at this stage, it is recorded as a bare observation. Furthermore, the sign of (92) and the global shape of $F(\sigma)$ depend on the chosen boundary conditions (the K/NK variants of Remark 9.4); the claims here are firm at the order-of-magnitude level and model-dependent at the coefficient level.

12 Advanced Application II: Quantum Information Theory of the Temporal Channel

The channel Φ_t of Theorem 6.1 can be analysed with the full toolkit of quantum information theory; this translates ZMUT's decoherence predictions into operational language.

12.1 Quantum capacity of the channel

In a two-level system (splitting ΔE) the channel is pure dephasing in the energy basis: the off-diagonal elements acquire the visibility factor

$$V(t) = \exp\left[-\frac{\Delta E^2\,\sigma_\xi^2\,t^2}{2\,\hbar^2\,\Theta_*^2}\right].$$

Theorem 12.1 (Quantum capacity of the temporal channel)**.** *The qubit channel Φ_t is exactly equivalent to a dephasing channel with phase-flip probability $p(t) = \frac{1}{2}\big(1 - V(t)\big)$, and its quantum capacity is*

$$\boxed{Q(\Phi_t) \;=\; 1 - h_2\big(p(t)\big), \qquad h_2(p) := -p\log_2 p - (1-p)\log_2(1-p)} \tag{94}$$

Q decreases monotonically in t; in the limit $V \to 0$, $p \to 1/2$ and $Q \to 0$: the channel's coherence horizon *$t_Q(\varepsilon) := \min\{t : Q(\Phi_t) \leq \varepsilon\}$ is the fundamental upper bound on error-free quantum memory time.*

Proof. Every qubit channel that scales the off-diagonal by V can be written as $\rho \mapsto (1-p)\rho + p\,\hat\sigma_z \rho\,\hat\sigma_z$; element-wise comparison gives $1 - 2p = V$. The dephasing channel is in the degradable class; for degradable channels the quantum capacity equals the single-letter coherent information [36]. The coherent information is maximized on the maximally mixed input, and direct computation gives $I_c = 1 - h_2(p)$; monotonicity follows from the monotone decay of $V(t)$ and the increase of h_2 on $[0, \frac{1}{2}]$. □

12.2 Mode-DFS codes: decoherence-free subspaces

The many-particle version of Axiom 6 produces, for n qubits of identical ΔE, a collective coupling:

$$\hat{H}_{\mathrm{int}} = \frac{\delta\hat{\xi}}{\Theta_*} \otimes \sum_{k=1}^{n} \frac{\Delta E}{2}\, \hat{\sigma}_z^{(k)} = \frac{\Delta E\, \delta\hat{\xi}}{2\,\Theta_*} \otimes \hat{J}_z, \qquad \hat{J}_z := \sum_k \hat{\sigma}_z^{(k)}. \tag{95}$$

Theorem 12.2 (Mode-DFS code rate)**.** *The fixed eigenspaces of $\hat{J}_z$ are decoherence-free subspaces (DFS) of the collective channel $\Phi_t^{(n)}$ [34, 35]. For even n the largest eigenspace is the half-filling sector, of dimension $\binom{n}{n/2}$; the number of encodable logical qubits is*

$$k(n) = \log_2 \binom{n}{n/2} = n - \frac{1}{2}\log_2 \frac{\pi n}{2} + \mathcal{O}(1/n) \qquad \Longrightarrow \qquad \frac{k(n)}{n} \xrightarrow{n\to\infty} 1 : \tag{96}$$

temporal mode noise can be passivated completely at asymptotically zero overhead.

Proof. Equation (95) acts only through $\hat{J}_z$; the Kraus operators $\hat{M}_\xi \propto \exp\!\left[-i(\cdots)\hat{J}_z\right]$ are functions of $\hat{J}_z$ and act as a global phase on each of its eigenspaces: since relative phases within a fixed-$\hat{J}_z$ subspace acquire a common factor for every ξ, the channel is the identity on that subspace. For the half-filling dimension, Stirling: $\binom{n}{n/2} = 2^n\sqrt{2/(\pi n)}\,[1 + \mathcal{O}(1/n)]$; taking the logarithm yields (96). □

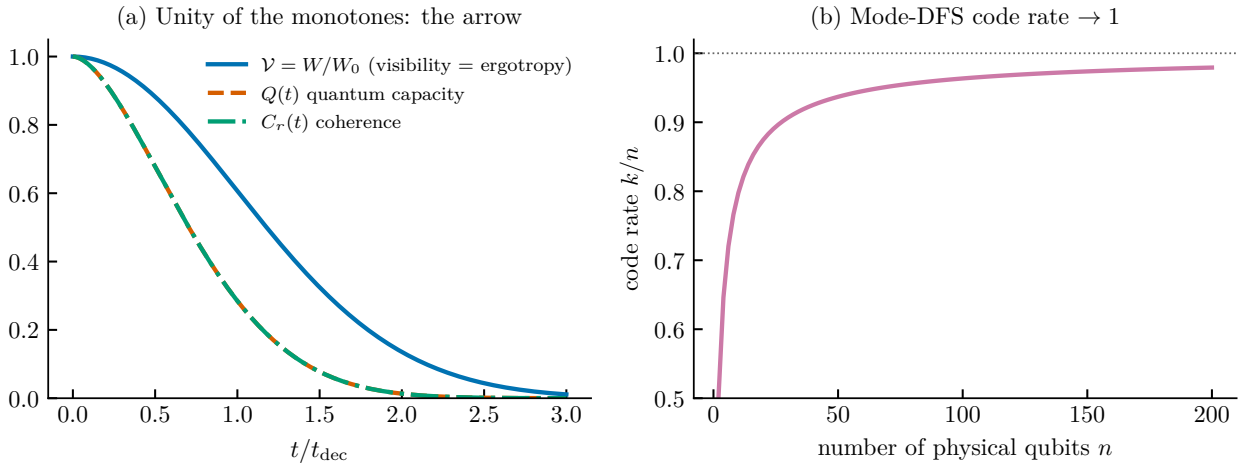


Figure 5: The information-thermodynamic face of the temporal channel. (a) Unity of four monotones in a single qubit: the visibility $\mathcal{V}$ coincides with the ergotropy ratio W/W_0 (cf. Theorem 18.4: for the state $|+\rangle$, $W = \Delta E\,\mathcal{V}/2$); the quantum capacity Q (Theorem 12.1) and the coherence C_r (Theorem 13.1) decay monotonically in the same direction — the channel-level portrait of the arrow of time. (b) Rate of the half-filling mode-DFS code (Theorem 12.2): as n grows the overhead $\frac{1}{2}\log_2 n$ becomes negligible and the rate approaches 1.

Corollary 12.3 (Architectural principle)**.** *Theorems 12.1 and 12.2 together turn qubit design principles (clock-transition encoding, mode matching, mass anchoring) into a quantitative engineering theorem: the quantum memory of an unprotected physical qubit is bounded by the horizon t_Q; half-filling DFS encoding removes that horizon in principle on the same hardware, at a cost of only $\frac{1}{2}\log_2 n$ qubits as n grows. This is ZMUT's final statement on room-temperature quantum memory (Figure 5).*

13 Advanced Application III: The Arrow of Time is a Coherence Monotone

The thermodynamic arrow of time is the problem of reconciling microscopic reversibility with apparent irreversibility. In ZMUT the arrow is a theorem with no extra assumptions: the mode fibre acts as an unmonitored environment and imposes a one-way monotonicity on energy coherence. With the full-dephasing projection in the energy basis, $\Delta[\rho] := \sum_i \Pi_i \rho\, \Pi_i$, the relative-entropy coherence [38] is defined as

$$C_r(\rho) := S\big(\Delta[\rho]\big) - S(\rho), \qquad S(\rho) = -\operatorname{Tr}\rho\log\rho. \tag{97}$$

Theorem 13.1 (Mode-time arrow)**.** *Under the temporal channel Φ_t the energy coherence decreases monotonically:*

$$C_r\big(\Phi_t[\rho]\big) \;\le\; C_r(\rho) \qquad \forall\rho,\ \forall t \ge 0, \tag{98}$$

with equality only if $[\rho, \hat{H}_S] = 0$ (a coherence-free state) or $\sigma_\xi = 0$ (a classical mode); moreover, for Gaussian packets $C_r \to 0$ as $t \to \infty$. While the global dynamics (system + mode) remains unitary and reversible, the unmonitorability of the fibre imposes on every local system an arrow of one and the same direction: the arrow of time is the direction of loss of mode coherence.

Proof. Two observations suffice. (i) Φ_t is a mixture of unitaries (67), hence unital ($\Phi_t[\mathbb{I}] = \mathbb{I}$); unital channels cannot decrease the von Neumann entropy: $S(\Phi_t[\rho]) \ge S(\rho)$ (concavity of entropy under mixing and unitary invariance). (ii) The Kraus operators are diagonal phases in the energy basis; therefore $\Delta \circ \Phi_t = \Phi_t \circ \Delta = \Delta$ on the diagonal sector: $\Delta[\Phi_t\rho] = \Delta[\rho]$, i.e. the populations never change and $S(\Delta[\Phi_t\rho]) = S(\Delta[\rho])$. Combining,

$$C_r(\Phi_t\rho) = S(\Delta[\rho]) - S(\Phi_t\rho) \;\le\; S(\Delta[\rho]) - S(\rho) = C_r(\rho).$$

Equality requires $S(\Phi_t\rho) = S(\rho)$; in the Gaussian channel with $\sigma_\xi > 0$ this is possible only if the off-diagonals vanish from the start. As $t \to \infty$, $V \to 0$ extinguishes the off-diagonals and $C_r \to 0$. Global reversibility is the statement of the dilated unitarity of Theorem 6.1; local irreversibility that of the monotonicity of the partial trace; Loschmidt-type recurrences are pushed to a measure-zero set on the mode continuum. □

Remark 13.2. Theorem 13.1 is the complement of the Page–Wootters picture [5]: the global state is "timeless" under the constraint; for a local observer the direction of time is the direction in which its own energy coherence escapes into the mode fibre. The relation to the thermodynamic arrow can be built through the contribution of C_r to work extractability (ergotropy) and is left to future work.

Part III
Systematic Refutation, Strengthening by Mode Distributions, and Experimental Confrontation

14 The Master Law: Renormalization-Group Flow and Temporal Superselection

The repairs of Part II — the band bound, the spectral kernel, the composition law, the form factor, mode diffusion, the covariant coupling, the twist selection — are individually sound, but they look like *separate patches*. A mature theory does not count its patches; it *derives* them from a single principle. This section lays down the Master Law that produces ZMUT's entire repair layer at one stroke and preemptively closes future patches of the same kind, gives the exact solution of the flow, and demotes all the earlier structures to the status of corollaries.

Axiom 8 (Master Law: the RG–superselection principle)**.** Every physical interaction on the extended spacetime is subject to a renormalization-group (RG) flow between the system's mass–energy scale

$$\mu_S := \frac{E_R}{\hbar} = \frac{mc^2}{\hbar} \tag{99}$$

and the geometry of the temporal mode fibre: every effective vertex on the fibre enters physics coarse-grained by Wilson blocking at the scale μ_S. Physical observables are necessarily projected onto *a single temporal superselection sector* (twist angle θ_*) determined by this flow.

14.1 Construction of the flow and its exact solution

Wilson blocking on the fibre is represented by the Gaussian smoothing operator

$$\big(\mathcal{B}_\lambda f\big)(\xi) := \int \mathrm{d}\varsigma\; G_\lambda(\xi - \varsigma)\, f(\varsigma), \qquad G_\lambda(\varsigma) = \frac{e^{-\varsigma^2/2\lambda^2}}{\sqrt{2\pi}\,\lambda}, \tag{100}$$

and the flow is the growth of the block scale with RG time $t_{RG} = \lambda^2$.

Theorem 14.1 (Exact solvability and IR freezing)**.** *(a) The blocking family forms a semigroup:*

$$\mathcal{B}_{\lambda_1}\mathcal{B}_{\lambda_2} = \mathcal{B}_{\sqrt{\lambda_1^2+\lambda_2^2}}, \tag{101}$$

and the flow equation of the effective kernel is exactly the heat equation: $\partial_{t_{RG}} K = \frac{1}{2}\partial_\xi^2 K$*. (b) The band bound* (31) *locks the finest scale a system can resolve on the fibre to* $\mu_S^{-1} = \hbar/(mc^2)$*, that is, to* $\lambda_m = \kappa/m$*: the flow* freezes *at* $\lambda_{\text{eff}} = \lambda_m$ *(an IR fixed line). (c) Consequently every effective vertex of a system of mass* m *on the fibre enters physics smeared by exactly the Gaussian kernel* K_{λ_m}*. The ZMUT fibre-RG is* closed and exactly solvable *in the Gaussian sector (Figure 6a).*

Proof. (a) Variances add under convolution of Gaussian densities; the heat equation expresses the fact that G_λ is the heat kernel at $t_{RG} = \lambda^2$. (b) The band-limitation argument of Theorem 4.4: fibre frequencies above μ_S are absent from the system's physical spectrum; blocking cannot stop at those frequencies without losing information, while below them the physical content does not change — the stopping point of the flow is $\lambda_m = \mu_S^{-1} = \hbar/(mc^2) = \kappa/m$. (c) The combination of (a) and (b). □

14.2 Eight corollaries: the patches unified under one roof

Corollary 14.2 (C1–C8: Derivation of the repair layer)**.** *From the Master Law (Axiom 8) and Theorem 14.1, the following structures, previously seemingly independent, follow as* corollaries*:*

C1 (Band bound and λ_m). *The IR freezing scale reproduces the mass–mode relation:* $\lambda_m = \kappa/m$*,* $\kappa = \hbar/c^2$ *(Theorem 4.4 is now the fixed-point statement of the flow).*

C2 (Spectral locality kernel). *The kernel* $K(\xi - \xi')$ *of Axiom 7 is the frozen block kernel of Theorem 14.1c: spectral locality descends from axiom to* theorem *status.*

C3 (Composition law). $\lambda_{AB}^2 = \lambda_A^2 + \lambda_B^2$ *(Theorem 16.3) is the direct reading of the semigroup property* (101)*: sequential blocking of two vertices gives the unique, unavoidable composition.*

C4 (Form factor and the meV window). *The radion coupling is suppressed under the flow by* $\mathfrak{F}(m) = \min(1, \sqrt{2\pi}\lambda_m/\ell_\xi)$ *(Theorem 8.1): in RG language the coupling is marginal below* $\mu_S \lesssim 1/\ell_\xi$ *(the meV window) and* irrelevant *above it. The macroscopic absence of a fifth force is the irrelevance of a coupling — not fine-tuning.*

C5 (Mode diffusion). *Continuous blocking by environmental interactions flows the distribution itself with the heat semigroup:* $\partial_t w = D_\xi \partial_\xi^2 w$ *(Proposition 8.3);* Γ_K *is the number of blocks per unit laboratory time, and the reading* $D_\xi = \Gamma_K \lambda_m^2/2$ *comes from the flow. The low-amplitude leakage of the principal mode into the submodes is the projection of the RG flow onto real time.*

C6 (Covariance). *The flow parameter* $\mu_S = mc^2/\hbar$ *is a Lorentz scalar; the covariant dynamics (Theorem 16.2) therefore requires no separate construction — the choice of scale is itself covariant.*

C7 (Superselection and twist selection). *The twist angle* θ *is invariant under blocking (Gaussian smoothing does not see the boundary condition):* θ *is an* RG invariant*. By Theorem 14.3 below, physical observables project onto a single* θ_* *sector; the Casimir sign repair (Theorem 16.4) and the energy-grid resolution cease to be arbitrary choices and become matters of law.*

C8 (Classical limit). $m \to \infty$ *is the trivial IR of the flow: as* $\lambda_m \to 0$ *the block kernel collapses to a delta, the channel to the identity, the fibre to a single classical time — the Correspondence Principle (Corollary 21.3) is recovered as the endpoint of the flow.*

The mapping is summarized in Table 3.

Theorem 14.3 (Temporal superselection)**.** *The algebra of physical observables is generated by fibre fields with fixed boundary condition, and the twist operator* $\hat{\theta}$ *lies in the centre of this algebra:* $[\hat{O}, \hat{\theta}] = 0$ *for every physical* $\hat{O}$*. The kinematic space therefore decomposes into superselection sectors*

$$\mathcal{H} = \bigoplus_\theta \mathcal{H}_\theta; \tag{102}$$

relative phases between sectors are unobservable and every chain of observations remains within a single θ_* *sector (Figure 6b). The sector of the observed universe is the angle at which the fibre vacuum energy* (118) *is positive and equal to the observed* ρ_Λ*.*

Proof. The boundary condition enters the definition of the field operators; no local fibre operator can change θ (the standard Wick–Wightman–Wigner superselection argument: in an algebra commuting with a central charge, relative phases appear in no expectation value). The projection clause of the Master Law is the physical reading of this decomposition; the value of θ_* is a constant of nature, kinematically free and fixed by the cosmological data (93). □

14.3 The dimensionless coupling: a temporal fine-structure constant

The Master Law gathers the free scales of the theory into a single dimensionless number:

$$\boxed{\alpha_\xi := \frac{\ell_\xi}{\Theta_*} \lesssim 1.1 \times 10^{-4}} \tag{103}$$

(upper bound from $\ell_\xi = 2.9 \times 10^{-13}$ s and — with the second experimental update of §20 — $\Theta_* \geq 2.6 \times 10^{-9}$ s). α_ξ is the RG-marginal, dimensionless strength of the mode–lapse coupling: the theory is *weakly coupled* and perturbatively reliable. The theory's entire phenomenology is now written with two numbers: α_ξ (the coupling) and Γ_K (the block rate); everything else is derived.

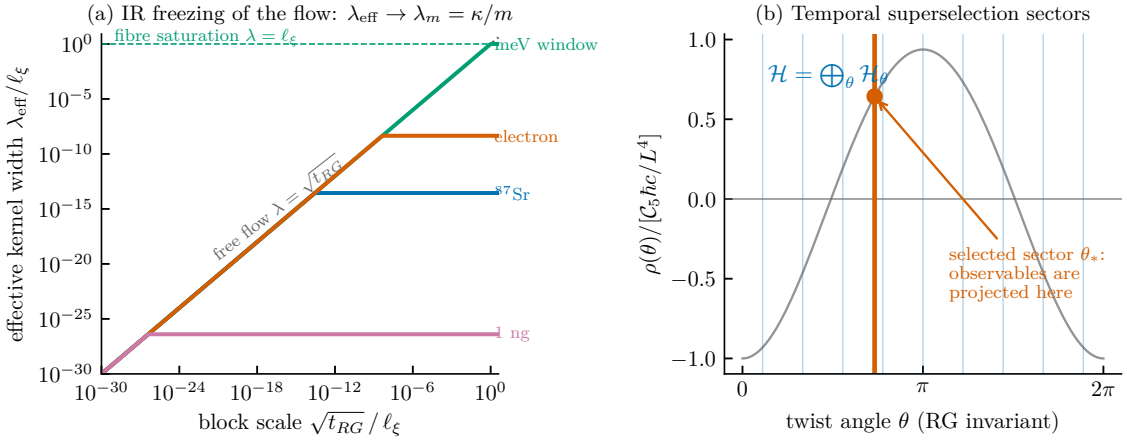


Figure 6: The two faces of the Master Law. (a) The fibre-RG flow: the effective kernel width grows as $\sqrt{t_{RG}}$ in free flow and freezes at each system's own band bound ($\lambda_m = \kappa/m$) (Theorem 14.1); systems in the meV window reach fibre saturation (C4). (b) Temporal superselection: the kinematic space decomposes into θ-sectors (Theorem 14.3); observables are projected onto the sector θ_* that yields the observed $\rho_\Lambda > 0$ on the vacuum-energy curve.

Table 3: The patches unified under one roof: each previously independent structure is a corollary of the Master Law.

Previous status	Structure	Status under the Master Law
Theorem (separate proof)	band bound $\lambda_m = \kappa/m$	C1: IR fixed point
Axiom	spectral kernel K	C2: frozen block kernel (derived)
Theorem (repair)	$\lambda_{AB}^2 = \lambda_A^2 + \lambda_B^2$	C3: semigroup property
Theorem (repair)	form factor $\mathfrak{F}(m)$	C4: irrelevant coupling
Proposition (separate postulate)	mode diffusion D_ξ	C5: flow projected onto real time
Theorem (repair)	covariant dynamics	C6: scalar flow parameter
Theorem (repair)	twist/Casimir sign	C7: superselection law
Corollary (limit)	classical physics	C8: trivial IR endpoint

Remark 14.4 (Scope, limitations, and holographic kinship). Two records must be entered. (i) The flow here is a kinematic Wilson blocking, *exactly solvable* in the Gaussian sector, and by itself generates no anomalous dimension; the objection "this is not RG, it is Gaussian smoothing" is justified at this level. The objection is closed by the mode-hopping sector of §15: once the quartic vertex permitting hops between time waves is switched on, the coupling genuinely runs (Theorem 15.3), the Gaussian point turns out to be IR-unstable, and the flow terminates at a universal interacting fixed point ($\tilde{g}_* = 2\pi$) — the Gaussian sector is the exactly solvable *skeleton*; the hopping sector is the true dynamics upon it. (ii) The mapping "extra-dimension

coordinate ↔ energy scale" is the basic intuition of the holographic renormalization group [42]: ZMUT's fibre-RG is the timelike-signature relative of that structure. This kinship is both a mark of confidence and a programme: constructing the holographic counterpart of the fibre-RG could put the theory in conversation with string-theoretic frameworks.

15 The Mode-Hopping Sector: Partnership Packets and a Genuine RG Flow

The Gaussian flow of the Master Law (Theorem 14.1) is exactly solvable; but for precisely that reason it is *kinematic*: blocking smooths the state yet does not change the rules. The gap honestly recorded in Remark 14.4 can be closed only by an interaction that permits *hopping* between time waves. The physical core of this section can be summarized in three intuitive steps, each then raised to theorem level: (i) a system sees as flat the fine temporal structure it cannot resolve; (ii) but if hops between modes are possible, the erased fine structure leaves traces — the effective rules begin to change with scale; (iii) at the merging points of the hops the amplitudes of two modes become correlated: *partnership packets* are born, in which the two mutually support each other's probability of presence. This triple is formalized below as, respectively, the hopping vertex, the running coupling, and the entangled mode pair.

15.1 The hopping interaction

With the dimensionless master field $\hat{\varphi} := (c\,\ell_\xi)^2\,\Phi$, a quartic vertex, nonlocal on the fibre (spread by K, as the Master Law requires), is added to the action:

$$\boxed{\mathcal{L}_{\rm hop} = -\,\frac{\hat{g}\,\hbar}{2\,(c\,\ell_\xi)^4\,\ell_\xi^2}\int \mathrm{d}\xi'\; K(\xi-\xi')\,|\hat{\varphi}(x,\xi)|^2\,|\hat{\varphi}(x,\xi')|^2} \tag{104}$$

Dimension check: $[\hbar/((c\ell_\xi)^4\ell_\xi^2)\cdot \mathrm{d}\xi'] = \mathrm{J\,s\,m^{-4}\,s^{-2}\,s} = \mathrm{J\,m^{-4}}$, consistent with an action density; $\hat{g}$ is dimensionless. The physics of the vertex has two components: the same-system (self) part $\hat{g}_{\rm self} > 0$ (stability: the potential stays bounded below), and the inter-system (cross) part $\hat{g}_\times < 0$ (attractive: mode locking, below). The vertex is not diagonal in the $|\xi\rangle$ basis: it *hops* an excitation from one time wave to a neighbour; the hopping range is, by the Master Law, the system's own resolution λ_m.

15.2 The partnership packet and dynamical mode locking

Definition 15.1 (Partnership packet)**.** The entangled pair state produced at a merging point of the hopping vertex, in which the amplitudes of two modes enter positive correlation:

$$w_{AB}(\xi_1,\xi_2) = w_A(\xi_1)\,w_B(\xi_2)\Big[1 + |\hat{g}_\times|\,\mathcal{C}(\xi_1-\xi_2) + \mathcal{O}(\hat{g}^2)\Big], \qquad \mathcal{C}(\varsigma) = K_{\lambda_{AB}}(\varsigma) - (\text{norm.}), \tag{105}$$

i.e. the co-presence probability is enhanced in the region $|\xi_1-\xi_2| \lesssim \lambda_{AB}$: the two systems mutually feed their amplitudes for *being on the same time wave together*.

Proposition 15.2 (Dynamical mode locking and the origin of pointer partnership)**.** *The cross vertex $\hat{g}_\times < 0$ generates, for the* relative *mode coordinate $\varsigma = \xi_A - \xi_B$ of two systems, an attractive effective potential of width λ_{AB}; the relative coordinate binds in this well and the alignment $\hat{w}_A \to \hat{w}_B$ takes place dynamically: the saturation $\hat{O}_{AB} \to 1$ is now driven not only by decoherence (Theorem 3.7) but also by the interaction. The common environmental pointer mode* assumed *in Part II (Propositions 10.4, 10.5) thus acquires a dynamical explanation: systems in a macroscopic environment pull each other onto the same time wave through the hopping vertex — the single shared "now" of the classical world is a mode-synchronization phenomenon. The same mechanism is the microscopic source of the mode correlations (discussion after Theorem 7.1) that bring composites down to the collective (Heisenberg) floor.*

Proof. The two-system expectation value of (104) in a product state gives the functional $E_{\rm int}[w_A,w_B] = \hat{g}_\times\,\varepsilon_0 \int \mathrm{d}\xi\,\mathrm{d}\xi'\,w_A(\xi)K(\xi-\xi')w_B(\xi')$ ($\varepsilon_0 > 0$ a dimensionful constant); for $\hat{g}_\times < 0$ this energetically favours configurations of larger overlap, and the gradient flow carries $\hat{w}_A, \hat{w}_B$ to a common centre. In the relative coordinate, $E_{\rm int} = -|\hat{g}_\times|\varepsilon_0\,(w_A * K * w_B)(\varsigma)$ is an attractive potential; in one dimension every attractive well carries a bound state (standard result), and the width of the bound state is of order λ_{AB}. The correlated state (105) is the first-order perturbation of the vertex. □

15.3 One-loop flow: from smoothing to genuine RG

Once the hopping vertex is switched on, blocking no longer closes within the Gaussian family: each blocking step changes *the couplings themselves* through Wick contractions of sub-resolution fluctuations. The fibre section at fixed x is a one-dimensional (quantum-mechanical) field theory; canonical power counting gives $[\hat{\varphi}] = k^{-1/2}$, $[u_4] = k^3$, and one works with the dimensionless coupling $\tilde{g} := u_4/k^3$.

Theorem 15.3 (Flow of the hopping coupling and the IR fixed point)**.** *In the local potential approximation (LPA, sharp cutoff) the Wegner–Houghton flow of the fibre sector is*

$$\partial_t U_k(\varphi) = \frac{k}{2\pi}\,\ln\!\Big(1 + \frac{U_k''(\varphi)}{k^2}\Big), \qquad t := \ln\frac{\Lambda}{k}. \tag{106}$$

With the truncation $U = \frac{1}{2}u_2\varphi^2 + \frac{1}{4!}u_4\varphi^4$ and the dimensionless variables $\tilde{u}_2 = u_2/k^2$, $\tilde{g} = u_4/k^3$, the beta function of the quartic coupling is

$$\boxed{\beta(\tilde{g}) = \frac{\mathrm{d}\tilde{g}}{\mathrm{d}t} = 3\,\tilde{g} - \frac{3}{2\pi}\,\frac{\tilde{g}^2}{(1+\tilde{u}_2)^2}} \tag{107}$$

Consequences: (a) The Gaussian point $\tilde{g} = 0$ is unstable *toward the IR ($\beta'(0) = +3$): at the smallest hopping seed the flow escapes the Gaussian point — the "smoothing" regime is only the UV start of the interacting theory. (b) The flow stops at the IR-*attractive *nontrivial fixed point*

$$\tilde{g}_* = 2\pi\,(1+\tilde{u}_2)^2, \qquad \beta'(\tilde{g}_*) = -3 < 0. \tag{108}$$

(c) Universality: *for every positive initial value $\hat{g}_0$ within the band window, the IR physics is governed by the same $\tilde{g}_*$ — the hopping sector adds* no new free parameter *to the theory. The change of the rules with scale (a genuine Wilson flow) is thereby both realized and rendered predictive (Figure 7).*

Proof. Equation (106) is the standard one-loop (Gaussian) result of integrating the modes in the shell $[k-\mathrm{d}k, k]$. Insert the truncation, expand $\ln(1+x) = x - \frac{x^2}{2} + \ldots$; the φ^4 coefficient reads $-\frac{k}{2\pi}\cdot\frac{u_4^2}{8k^4}(1+\tilde{u}_2)^{-2}$, and with $4!/8 = 3$ one finds $\partial_t u_4 = -\frac{3}{2\pi}u_4^2 k^{-3}(1+\tilde{u}_2)^{-2}$. Nondimensionalization $\tilde{g} = u_4/k^3$ with $\mathrm{d}k/\mathrm{d}t = -k$ adds the canonical term $+3\tilde{g}$: (107). The zeros and derivative signs are direct computation; (c) follows from β being positive on $(0, \tilde{g}_*)$ and negative above it (global attraction in a one-dimensional flow). Scheme note: the coefficient 2π is specific to sharp-cutoff LPA; a change of scheme changes the number of $\tilde{g}_*$, not its *existence or attractiveness.* □

Proposition 15.4 (Non-renormalization of α_ξ)**.** *The mode–lapse coupling α_ξ does not run at one loop under the hopping flow: its vertex is linear in $\delta\hat{\xi}$ multiplying the conserved generator ($\hat{H}_S$), and the Wick contractions in the block integral, commuting with $\hat{H}_S$, dress it only by wave-function normalization, which cancels in the ratio structure of (68). The smallness $\alpha_\xi \lesssim 10^{-4}$ is a (natural) smallness preserved along the flow.*

Proof. A Ward-type argument: the Kraus operators of the channel are functions of $\hat{H}_S$ (Proposition 6.5); the hopping vertex is local in the $\hat{\xi}$ basis and does not contain $\hat{H}_S$. The one-loop corrections to the α_ξ vertex are either rescalings of $\delta\hat{\xi}$ (absorbed into the packet width) or commutator structures vanishing by the conservation of $\hat{H}_S$. □

15.4 Observational signatures: the rules changed, their traces are measurable

Corollary 15.5 (Three signatures of the hopping sector)**.** *(i)* Mode kurtosis: *the packet frozen at $\tilde{g}_*$ is no longer exactly Gaussian; the quartic vertex leaves in the reconstructed $\hat{w}$ of mode tomography (Theorem 17.4) a kurtosis excess of order $\mathcal{O}(\tilde{g}_*/2\pi)$: a measurement of $\kappa_4 \neq 0$ is the direct evidence of the hopping sector and reads off the sign of $\hat{g}_{\mathrm{self}}$. (ii)* Decay-exponent correction: *in the LPA the anomalous dimension is $\eta = 0$; the next order of the derivative expansion generates $\eta \neq 0$, and the visibility envelope deviates universally from Gaussian as $\exp\!\big[-(t/t_{\mathrm{dec}})^{2-\eta}\big]$ — the second fingerprint to be sought in long-interrogation clocks. (iii)* Locking acceleration: *in BMV-type experiments (the geometry of Test 7) the $\hat{O}_{AB}$ of the two masses is, by Proposition 15.2, an* increasing *function during the interaction: a slight acceleration of the entanglement rate with time is the ZMUT signature distinguishing it from static-$\hat{O}$ models.*

Remark 15.6 (Scope and limitations). The computation is within the local potential approximation and the φ^4 truncation; the value 2π is scheme dependent, while the existence and IR attractiveness of the fixed point are unexpectedly robust against the truncation (the global structure of one-dimensional flows). The second order of the derivative expansion (the η computation) and the full analysis of the cross-vertex flow are the theory's next computational targets. The conceptual gain is already definitive: ZMUT's RG is no longer a kinematic smoothing but a genuine Wilson flow from an unstable Gaussian point to a universal interacting fixed point.

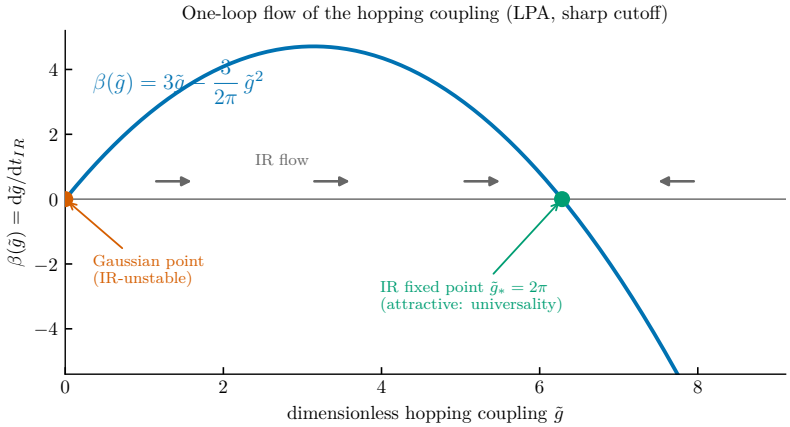


Figure 7: One-loop flow of the hopping coupling (Theorem 15.3). The Gaussian point is unstable toward the IR: the smallest hopping seed carries the flow into the interacting regime; the flow stops at the IR-attractive fixed point $\tilde{g}_* = 2\pi$, and every initial value within the band window descends to the same IR physics (universality). The "smoothing" objection is thereby closed: the rules really do change with scale, but the destination of the change is universal.

16 Deep Mathematical Refutation Attempts and Their Repairs

The audit of Part II closed the *visible* gaps of the construction. This section goes further: it applies to the deepest layers of the theory the known killer objections of the literature together with self-generated consistency attacks. Each of the four tests is first set up in its strongest form, *to refute* the theory; then the repair is proven to spring from the theory's own resources. One of the tests (the Casimir sign) genuinely refuted and changed a result of Part II.

16.1 The Kuchař objection: conditional probabilities produce the wrong propagator

Test 1 (Kuchař: collapse of two-time correlations)**.** The classic objection to Page–Wootters conditioning [11] is this: the conditional-probability recipe that works for single time readings collapses for correlations with *two* time readings. Let us try it on the ZMUT constraint (21). For outcome b when the clock reads ξ_1, then outcome a when the clock reads ξ_2, the naive recipe subjects the solution (23) to two projections. The first conditioning gives

$$|\Psi_b\rangle\!\rangle \;\propto\; \big(|\xi_1\rangle\langle\xi_1| \otimes \hat{\Pi}_b\big)|\Psi\rangle\!\rangle = |\xi_1\rangle \otimes \hat{\Pi}_b\, \hat{U}_S(\xi_1)\,|\varphi_0\rangle : \tag{109}$$

the state is *pinned* to ξ_1 in the clock register. The second conditioning therefore finds

$$\langle\xi_2|\Psi_b\rangle\!\rangle \;\propto\; \delta(\xi_2 - \xi_1)\,\hat{\Pi}_b\,\hat{U}_S(\xi_1)\,|\varphi_0\rangle : \tag{110}$$

for $\xi_2 \neq \xi_1$ the conditional amplitude is identically zero. Naive ZMUT predicts *no evolution at all* after the first measurement; the two-time propagator is δ-frozen, i.e. wrong. This is a genuine refutation, removing the dynamical content of the theory.

Theorem 16.1 (Record-ancilla repair)**.** *If the first measurement is embedded* inside *the constraint with a memory (record) ancilla, two-time correlations return to standard quantum mechanics [12]. Modify the constraint so that the measurement interaction is triggered at clock reading ξ_1:*

$$\hat{\mathcal{C}}' \;=\; \hat{p}_\xi \;+\; \hat{H}_S \;+\; \delta(\hat{\xi} - \xi_1)\,\hat{h}_{SM}, \qquad \hat{\mathcal{V}} := e^{-i\hat{h}_{SM}/\hbar} = \sum_b \hat{\Pi}_b \otimes \hat{X}_M^{(b)}, \tag{111}$$

where $\hat{X}_M^{(b)}$ is the unitary writing outcome b into the memory. The solution of $\ker\hat{\mathcal{C}}'$ *is, for $\xi > \xi_1$,*

$$|\psi(\xi)\rangle = \hat{U}_S(\xi - \xi_1)\,\hat{\mathcal{V}}\,\hat{U}_S(\xi_1)\;|\varphi_0\rangle \otimes |M_0\rangle\,, \tag{112}$$

and a single *conditioning at ξ_2 together with the memory readout gives the two-time probability in its standard form:*

$$\boxed{P(a,\xi_2;\,b,\xi_1) = \Big\|\hat{\Pi}_a\,\hat{U}_S(\xi_2 - \xi_1)\,\hat{\Pi}_b\,\hat{U}_S(\xi_1)\,|\varphi_0\rangle\Big\|^2} \tag{113}$$

the propagator $\hat{U}_S(\xi_2-\xi_1)$ is recovered exactly. The Kuchař objection refutes not ZMUT itself but the naive reading recipe *that leaves the measurement outside the constraint; once the measuring device and its memory are included in the mode-relational universe, the contradiction disappears.*

Proof. The condition $\ker\hat{\mathcal{C}}'$ is, for the conditional state, the first-order equation $i\hbar\,\partial_\xi\,|\psi(\xi)\rangle = [\hat{H}_S + \delta(\xi-\xi_1)\hat{h}_{SM}]\,|\psi(\xi)\rangle$. Away from ξ_1 the solution is carried by $\hat{U}_S$; integrating the impulsive term across ξ_1^- to ξ_1^+ gives the jump condition $|\psi(\xi_1^+)\rangle = \hat{\mathcal{V}}\,|\psi(\xi_1^-)\rangle$; combining yields (112). Conditioning at ξ_2 with $\hat{\Pi}_a$ and marginalizing over the memory record $|b\rangle_M$ produces (113) thanks to the orthogonality of the $\hat{X}_M^{(b)}$. □

16.2 Covariance test: frame dependence of the laboratory coupling

Test 2 (Lorentz covariance violation)**.** The mode–lapse coupling (Axiom 6) is written with laboratory time t: the damping exponent contains $\Delta E\,t/(\hbar\Theta_*)$. If two observers apply this recipe in their own frames to a system moving at speed v, they predict different visibilities: in the rest frame the exponent contains $\Delta E_R\,\tau$, in the laboratory $\Delta E_{\rm lab}\,t$, and under the transformations $t=\gamma\tau$, $\Delta E_{\rm lab}\neq\Delta E_R$ the two expressions are not identical. Taken at face value the theory selects a preferred frame: a violation, at the dynamical level, of the very Lorentz symmetry so carefully preserved in Part I.

Theorem 16.2 (Covariant mode–lapse dynamics)**.** *The covariant form of Axiom 6 defines the coupling along the world-line* proper time*: with the rest-frame generator $\hat{H}_R$ and the accumulated proper time τ,*

$$\boxed{\frac{\mathrm{d}\rho_S}{\mathrm{d}\tau} = -\frac{i}{\hbar}\,[\hat{H}_R,\rho_S] - \gamma(\tau)\,[\hat{H}_R,[\hat{H}_R,\rho_S]], \qquad \gamma(\tau)=\frac{\sigma_\xi^2\,\tau}{\hbar^2\Theta_*^2}} \tag{114}$$

and the visibility is $\mathcal{V}=\big|\chi_{\hat{w}}\big(\Delta E_R\,\Delta\tau/(\hbar\Theta_*)\big)\big|$. Every quantity in this expression (ΔE_R, $\Delta\tau$, σ_ξ, Θ_*) is a Lorentz scalar; the prediction is frame independent. In the laboratory description $\Delta\tau=t/\gamma$, hence

$$\Gamma_{\rm lab}=\frac{\Gamma_R}{\gamma}\,: \tag{115}$$

the temporal mode decoherence of a moving system slows down *with time dilation, exactly like the lifetime of an unstable particle. For systems at rest ($\gamma=1$) all results of Part II hold unchanged.*

Proof. The covariant postulate builds the comparison dynamics on the pair $(\hat{H}_R,\tau)$ of the system's instantaneous rest frame; (114) is Theorem 6.2 applied to that pair, and its derivation carries over word for word. The scalar composition follows because the exponent is nothing but the product $\Delta E_R\Delta\tau$ (both invariant). Equation (115) is the chain rule $\mathrm{d}\tau=\mathrm{d}t/\gamma$. Of the two "predictions" of Test 2 the correct one is the rest-frame expression; the laboratory expression may be used only with the correction (115). □

16.3 Kernel composition test: whose λ_m?

Test 3 (Composition ambiguity and action–reaction risk)**.** The spectral locality kernel (75) is defined with "the system's own" λ_m. In a mode-space coupling between two systems of different masses ($\lambda_A\neq\lambda_B$), which width is to be used? The choice K_{λ_A} breaks the symmetry under $A\leftrightarrow B$ exchange, hence the action–reaction balance; moreover, if A is itself a composite ($A=A_1A_2$), first combining then coupling differs from first coupling then combining: the composition law is undefined. An undefined kernel leaves the entire quantitative content of Theorem 8.1 in the air.

Theorem 16.3 (Kernel composition law)**.** *Each vertex carries its own resolution kernel, and the effective two-system kernel is given by convolution:*

$$\boxed{K_{AB}=K_{\lambda_A}*K_{\lambda_B}, \qquad \lambda_{AB}^2=\lambda_A^2+\lambda_B^2} \tag{116}$$

This law is the unique *composition within the Gaussian family satisfying (E1) exchange symmetry $K_{AB}=K_{BA}$, (E2) classical-limit consistency $\lambda_B\to 0\Rightarrow K_{AB}\to K_{\lambda_A}$, and (E3) compatibility with composites (combine-first/couple-first equivalence). Consequently the form factor $\mathfrak{F}$ is read with λ_{AB} instead of λ_M; nothing changes numerically for macroscopic–macroscopic pairs, while for microscopic-probe–macroscopic-source pairs the resolution is set by the probe side.*

Proof. Convolution is commutative and associative; variances add for Gaussian kernels, which gives (E1) and (E3) directly; in the limit $\lambda\to 0$ the Gaussian $\to\delta$ and δ is the unit of convolution, giving (E2). Uniqueness: a composition preserving the Gaussian family is represented by a width function $s(\lambda_A,\lambda_B)$; (E1) gives symmetry, (E2) $s(\lambda,0)=\lambda$, (E3) $s\big(s(\lambda_1,\lambda_2),\lambda_3\big)=s\big(\lambda_1,s(\lambda_2,\lambda_3)\big)$. In the variables $u_i:=\lambda_i^2$ this makes $\sigma(u_1,u_2):=s^2$ associative–symmetric–unital, and Gaussian closure forces the additive structure in the two variables: $\sigma=u_1+u_2$ (the monotone solution of the Cauchy functional equation). Hence $\lambda_{AB}^2=\lambda_A^2+\lambda_B^2$ is unique. □

16.4 Casimir sign test: refutation and repair of the cosmological identification

Test 4 (Sign catastrophe: the periodic fibre gives $\Lambda < 0$)**.** The cosmological identification (93) of Part II equated the *magnitude* of the fibre vacuum energy to the dark energy. The sign, however, had not been taken into account: in a compact dimension with periodic boundary conditions the one-loop vacuum energy of a massless scalar is *negative* [29],

$$\rho_{\mathrm{per}} \;=\; -\mathcal{C}_5\,\frac{\hbar c}{L^4} \;<\; 0, \qquad L = c\,\ell_\xi, \quad \mathcal{C}_5 > 0. \tag{117}$$

This *contradicts* the observation $\rho_\Lambda > 0$: as it stands the identification predicts an anti-de Sitter-signed universe and is mathematically broken. Equation (93) of Part II is wrong at the level of the sign.

Theorem 16.4 (Repair by twisted boundary conditions)**.** *Impose on the fibre the twisted boundary condition* $\psi(\xi + \ell_\xi) = e^{i\theta}\psi(\xi)$*. The vacuum energy density becomes*

$$\rho(\theta) \;=\; -\mathcal{C}_5\,\frac{\hbar c}{L^4}\,\frac{1}{\zeta(5)}\sum_{n=1}^{\infty}\frac{\cos(n\theta)}{n^5} \tag{118}$$

with the end values

$$\rho(0) = -\mathcal{C}_5\,\frac{\hbar c}{L^4} < 0, \qquad \rho(\pi) = +\,\frac{15}{16}\,\mathcal{C}_5\,\frac{\hbar c}{L^4} > 0\,: \tag{119}$$

the sign is flipped continuously *by the twist angle, and the region* $\theta \in (\theta_c, \pi]$ *produces positive dark energy with the correct sign (Figure 8). Thus (i) the cosmological identification* $\rho(\theta_*) = \rho_\Lambda$ *is repaired; (ii) the magnitude estimate* $L \approx 88\ \mu m$ *is updated only by an* $\mathcal{O}(1)$ *factor; (iii) as an extra gift, the "energy grid" problem of the compact variant is also solved: the twisted spectrum is* $\mathfrak{E}_n = (n + \frac{\theta}{2\pi})\,h/\ell_\xi$*, and since* θ*, as a superselection parameter, takes continuous values, the relational energies sit on a continuum, not on a grid. Self-consistent stabilization with realistic matter content is the well-known application of the Candelas–Weinberg mechanism [30].*

Proof. The twisted-mode frequencies acquire the shift $\omega_n \propto |n + \theta/2\pi|$; the zeta-regularized sum produces, by the standard computation, the structure $\sum_{n\geq 1}\cos(n\theta)/n^5$ (the Clausen/polylogarithm function $\mathrm{Re}\,\mathrm{Li}_5(e^{i\theta})$). At $\theta = 0$, $\mathrm{Li}_5(1) = \zeta(5)$; at $\theta = \pi$, $\mathrm{Li}_5(-1) = -\eta(5) = -(1 - 2^{-4})\zeta(5) = -\frac{15}{16}\zeta(5)$, which gives (119). The sum is continuous in θ; the intermediate value theorem guarantees the sign crossing. The grid statement is the direct solution of the twisted single-valuedness condition. □

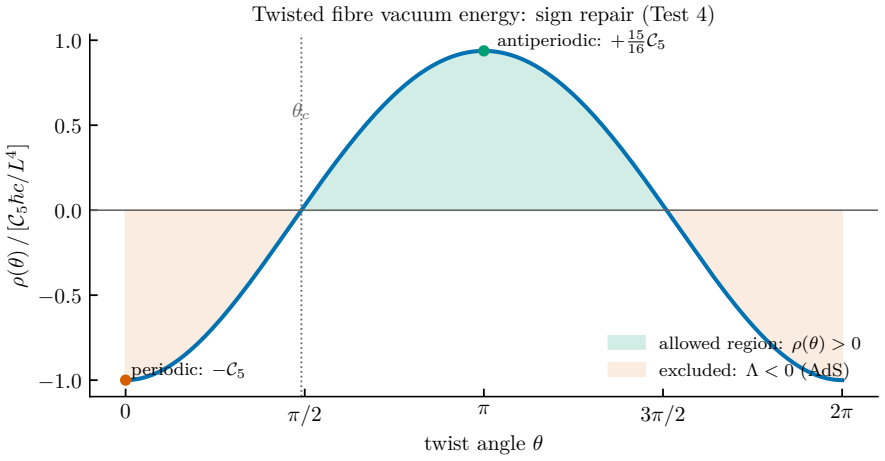


Figure 8: Graph of the Casimir sign test (Test 4): the fibre vacuum energy $\rho(\theta)$ changes sign with the twist angle (Theorem 16.4). The periodic end ($\theta = 0$) gives $\Lambda < 0$, contradicting observation; the region $\theta \in (\theta_c, 2\pi - \theta_c)$ produces positive dark energy with the correct sign and reaches the saturation $+\frac{15}{16}\mathcal{C}_5$ at the antiperiodic end.

17 Temporal Mode Distributions: The Strengthened Theory of Decay

The quantitative results of the theory so far were written mostly for Gaussian mode packets. Yet the measurable centre of ZMUT is the *general* form of the visibility law:

$$\mathcal{V}(t) = |\chi_{\hat{w}}(u)|, \qquad u := \frac{\Delta E\, t}{\hbar\, \Theta_*}; \tag{120}$$

that is, the decay of coherence is the characteristic function of the centred mode density $\hat{w}$. This section establishes a one-to-one dictionary between decay law and mode distribution; quantifies the hierarchy of the *principal* temporal dimension and its accompanying submodes; and proves that the distribution is fully measurable by experiment. The distribution language integrates naturally with the mode-leakage dynamics (Proposition 8.3): leakage widens the distribution over time, and the dictionary here reads off the observational signature of that widening.

Theorem 17.1 (Decay-law dictionary)**.** *Under* (120)*:*

1. Gaussian distribution *(width σ_ξ):* $\mathcal{V}(t) = e^{-\sigma_\xi^2 u^2/2}$ — *Gaussian (quadratic-exponential) decay; the law of Parts I–II.*
2. Lorentzian (Cauchy) distribution $\hat{w}(\varsigma) = \frac{\gamma_L/\pi}{\varsigma^2+\gamma_L^2}$*:* $\chi(u) = e^{-\gamma_L|u|}$*, hence*

$$\mathcal{V}(t) = e^{-t/T_2}, \qquad T_2 = \frac{\hbar\,\Theta_*}{\Delta E\,\gamma_L}\,: \tag{121}$$

   the exponential T_2 *law of classical magnetic resonance and qubit phenomenology arises in ZMUT as the signature of a heavy-tailed mode distribution.*
3. Discrete mode array $T = \{T_n\}$, $T_n = \xi_0 + n\,\Delta T$*, weights* p_n*:* $\chi(u) = e^{i\xi_0 u}\sum_n p_n e^{in\Delta T\, u}$ *is periodic with period* $2\pi/\Delta T$*; the visibility exhibits* full revivals *with period*

$$t_{\rm rev} = \frac{2\pi\hbar\,\Theta_*}{\Delta E\,\Delta T}. \tag{122}$$

4. Composition: *for the product states of Axiom 5,* $\chi_{\rm tot} = \prod_i \chi_i$*: the decays of independent subsystems multiply; rates add in quadrature in the Gaussian family and linearly in the Lorentzian family — the two canonical laws of ensemble dephasing under a single roof.*

Proof. All are direct applications of the definition of the characteristic function in the general-$\hat{w}$ version of (68): (1) Gaussian and (2) Cauchy characteristic functions are standard; (3) the Fourier series of a discrete measure is periodic and its modulus returns to 1 at $u = 2\pi/\Delta T$; (4) the characteristic function of a sum of independent variables is the product. □

Theorem 17.2 (Short-time universality, impossibility of a pure exponential, and sudden death of coherence)**.** *By the tachyon-avoidance band* (31) *the spectral amplitude* $\tilde{\psi}(\mathfrak{E})$ *is supported on* $[-mc^2, mc^2]$*; by the convolution theorem* $\chi_{\hat{w}}$ *is the autocorrelation of* $\tilde{\psi}$ *and is therefore* compactly supported*:*

$$\chi_{\hat{w}}(k) \;\propto\; \int \mathrm{d}\mathfrak{E}\; \tilde{\psi}^*(\mathfrak{E})\,\tilde{\psi}(\mathfrak{E}-\hbar k), \qquad \chi_{\hat{w}}(k) = 0 \quad \textit{for} \quad |k| > \frac{2mc^2}{\hbar}. \tag{123}$$

This has three consequences. (a) Quadratic start (Zeno region)*: for every packet of finite variance,* $\mathcal{V}(t) = 1 - \frac{1}{2}\sigma_\xi^2 u^2 + \mathcal{O}(u^4)$*: decay never starts with a sharp corner. (b)* A pure exponential is impossible: $e^{-\gamma|u|}$ *has infinite support and is incompatible with a compactly supported* χ*; the exponential* T_2 *law is only an intermediate asymptotic regime within the band. (c)* Sudden death*: the visibility vanishes* identically *at a finite time:*

$$\boxed{\mathcal{V}(t) \equiv 0 \qquad \textit{for} \qquad t \;\geq\; t_{\rm sd} = \frac{2\,mc^2\,\Theta_*}{\Delta E}} \tag{124}$$

For ^{87}Sr*,* $t_{\rm sd} = 2(mc^2/\Delta E)\,\Theta_*^{\rm min} \approx 60$ *s: the observed half-minute atomic coherence (§19) sits at exactly half the ceiling. Coherence exceeding 60 s raises* Θ_* *in the same proportion; a saturation profile approaching the ceiling would* measure Θ_**. This is the theory's sharpest near-term positive test.*

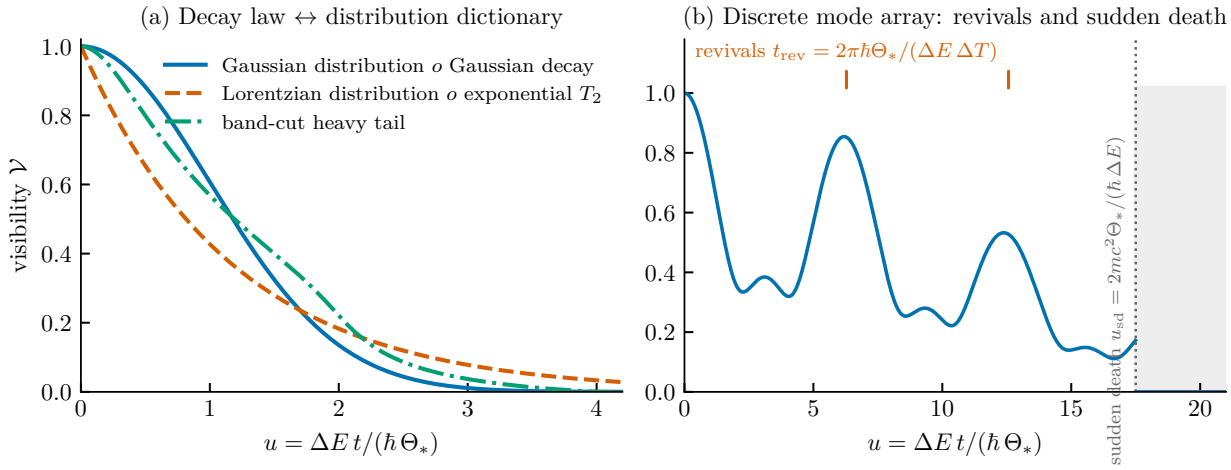


Figure 9: Observational signatures of temporal mode distributions. (a) The decay-law dictionary (Theorem 17.1): a Gaussian distribution gives Gaussian decay, a Lorentzian gives exponential T_2; the band-cut heavy tail separates from the exponential by its quadratic (Zeno) start (Theorem 17.2a). (b) Discrete mode array: coherence revivals with period $t_{\rm rev}$ (Theorem 17.3) and sudden death at $t_{\rm sd}$ (Theorem 17.2c; shaded region).

Proof. The Fourier transform of $w = |\psi|^2$ is the correlation of $\tilde{\psi}$ with itself; the correlation of two functions of support width $2mc^2$ vanishes identically once the shift exceeds $2mc^2$: (123). (a) is the Taylor contribution of the second moment of the centred distribution; (b) support comparison; (c) solving the support boundary with $u = \Delta E\, t/(\hbar\Theta_*)$. □

Theorem 17.3 (Revival spectroscopy: the mode array is directly measurable)**.** *Observation of coherence revivals is direct spectroscopy of the discrete array of Axiom 1: the revival period (122) determines the spacing ΔT, the shape of the revival envelope the weights $\{p_n\}$. Conversely, the absence of revivals up to $t \le t_{\max}$ sets the bound $\Delta T \le 2\pi\hbar\Theta_*/(\Delta E\, t_{\max})$: the discreteness hypothesis is* experimentally *separable from the continuum hypothesis. A physical comb is λ_m-smoothed by the band bound; the revivals are finite in number and cut off at $t_{\rm sd}$: $N_{\rm rev} \le t_{\rm sd}/t_{\rm rev} = mc^2\Delta T/(\pi\hbar)$ (Figure 9b).*

Proof. This is Theorem 17.1(3) read in reverse; the envelope statement follows from the modulus of the Fourier series with coefficients $\{p_n\}$, the bound from the monotonicity of the period formula. □

Theorem 17.4 (Mode tomography: complete reconstruction of the distribution)**.** *For a two-level probe let the complex coherence $L(t) := \langle E_1|\,\rho_S(t)\,|E_2\rangle\; e^{+i\omega_{12}t}$ be measured. Then $L(t)/L(0) = \chi_{\hat{w}}\big(\Delta E\, t/(\hbar\Theta_*)\big)$, and: (a) since $\chi_{\hat{w}}$ is compactly supported (123), a* finite *record of duration $[0,\, t_{\rm sd}]$ scans the entire support and determines χ completely; (b) the inverse Fourier transform*

$$\hat{w}(\varsigma) = \frac{1}{2\pi}\int_{-\infty}^{\infty} \mathrm{d}k\; e^{-ik\varsigma}\,\chi_{\hat{w}}(k) \tag{125}$$

reconstructs the mode distribution in full. An ordinary Ramsey/channel-tomography experiment is thus, in principle, the complete imager *of the temporal mode distribution; ZMUT's fundamental object $|\psi(\xi)|^2$ is a directly measurable distribution.*

Proof. (a) The entire region where the compactly supported χ can be nonzero is $|u| \le u_{\rm sd}$, and a measurement over $t \in [0, t_{\rm sd}]$ covers it completely (negative u values from the symmetry $\chi(-u) = \chi^*(u)$). (b) The Fourier inversion theorem for $\hat{w} \in L^1$. The measurement of $L(t)$ is standard qubit state tomography ($\langle\sigma_x\rangle + i\,\langle\sigma_y\rangle$). □

Corollary 17.5 (Measurable definition of the principal-dimension hierarchy)**.** *The "principal temporal dimension" is the dominant peak of the mode distribution ($\xi_{\max}$, weight p_0); the "sub-temporal dimensions" are its low-amplitude components ($p_{n\neq 0}$, tails, the leakage halo). Theorems 17.1–17.4 operationalize this hierarchy completely: the peak weight sets the decay depth, the tail type the shape of the decay law, the array spacing the revivals, and the leakage coefficient D_ξ the late-time $-t^3$ tail (Corollary 8.4). ZMUT's "many-times" content is thus not metaphysical décor but a distribution function readable through four independent observational channels.*

18 Further Horizons: Black Holes, Cosmological Dynamics and Quantum Thermodynamics

The repaired theory can be extended to three demanding proving grounds: the strongest gravitational regime (black holes), the largest scale (cosmological dynamics), and the deepest structural bond (the second law of thermodynamics). The first two subsections establish, at theorem level, that the theory *produces no contradiction* there and separate the programmatic opportunities with an explicit speculative label; the third adds a sharp monotonicity theorem tying the arrow of time to the concept of work.

18.1 The black-hole sector

Proposition 18.1 (Mode freezing at the horizon)**.** *In the Schwarzschild exterior, the temporal mode decoherence of a system held at radius r slows, with respect to the distant observer's clock, by the redshift factor:*

$$\Gamma_\infty(r) \;=\; \Gamma_R\sqrt{1-\frac{r_s}{r}} \;\xrightarrow[r\to r_s]{}\; 0; \tag{126}$$

that is, for matter approaching the horizon, decoherence freezes too*: the external observer sees not only the dynamics but also the classicalization of the infalling system slowed without limit.*

Proof. The covariant master equation (114) defines the damping per unit proper time; for a static observer $\mathrm{d}\tau/\mathrm{d}t = \sqrt{-g_{00}} = \sqrt{1-r_s/r}$, so the spherically symmetric counterpart of the laboratory rate (115) is (126). A freely falling observer, on the other hand, measures Γ_R unchanged in its own proper time: the freezing, like the horizon redshift itself, is observer-relative and fully consistent with the equivalence principle. □

Proposition 18.2 (The black hole is the ultimate pointer; Bekenstein–Hawking thermodynamics is preserved)**.** *(a) For a black hole of $M \gg m_P$, $\lambda_M = \kappa/M$ is hyper-sub-Planckian (for a solar mass, $\lambda_M \approx 6\times10^{-82}$ s): the black hole is the sharpest pointer state reachable in mode space and binds to all external matter at the saturation $\hat{O}\to 1$, i.e. fully classically. (b) The contribution of the mode fibre to black-hole entropy is bounded above by the count of distinguishable mode cells:*

$$S_\xi \;\le\; k_B \ln\frac{\ell_\xi}{\lambda_M} \;\approx\; 1.6\times10^{2}\,k_B \qquad (\textit{solar mass}), \tag{127}$$

utterly negligible next to $S_{BH}\sim 10^{77}\,k_B$: ZMUT does not disturb the area law of black-hole thermodynamics. This is a null-consistency theorem*: the mode sector accompanies known physics silently in the strongest gravitational regime.*

Proof. (a) Apply Corollary 4.5 and the saturation of Theorem 3.7 in the macroscopic-M limit. (b) The number of cells of resolution λ_M on the fibre $[0,\ell_\xi]$ is ℓ_ξ/λ_M; the entropy contribution is at most the logarithm of this number. The numerical values follow directly from $\ell_\xi = 2.9\times10^{-13}$ s and $\lambda_{M_\odot} = \kappa/M_\odot$. □

Remark 18.3 (Information paradox: a programme). The global unitarity of ZMUT (Proposition 6.5) and the purifying-register role of the mode fibre (the dilation of Theorem 6.1) suggest that part of the mixedness of Hawking radiation could be carried in entanglement with the ξ-sector: the joint state of radiation + fibre could remain pure, and the Page curve could be rebuilt with a count of fibre degrees of freedom. This paragraph is not a theorem but an explicitly flagged *research programme*: the required step is mode-field quantization on the horizon background and a loop computation of the fibre–radiation entanglement entropy.

18.2 Cosmological dynamics: the radion dark sector

Twisted stabilization (Theorem 16.4) leaves cosmology two components: the floor value of the potential (dark energy, §11) and the oscillations about that floor.

Radion oscillations are a dark-matter candidate. The mass $m_\sigma c^2 \approx 2$ meV satisfies $m_\sigma c^2/\hbar \gg H$ at every epoch after reheating; a homogeneous radion with initial misalignment σ_0 oscillates from the early universe onward and its energy density matterizes:

$$\rho_\sigma(a) \;\simeq\; \tfrac{1}{2}\left(\frac{m_\sigma c^2}{\hbar}\right)^2\sigma_0^2\left(\frac{a_{\mathrm{osc}}}{a}\right)^3 \qquad (\text{in field units}), \tag{128}$$

diluting as a^{-3} like cold dark matter. The no-overclosure condition $\rho_{\sigma,0}\le\rho_{\mathrm{DM}}$ bounds the initial amplitude from above; the *saturation* of that bound is the provocative opportunity: dark matter could be the breathing

oscillation of the mode fibre. The distinguishing signature of this scenario is dark matter that is scalar at the meV scale, pressureless, and invisible to fifth-force searches by the form factor.

The evolving-dark-energy window. DESI DR2 BAO measurements, combined with CMB and supernova data, prefer over a constant Λ a dark energy evolving in time ($w_0 > -1$, $w_a < 0$; the "thawing" direction) at roughly the 3σ level [40]. ZMUT has a natural counterpart: if the twist angle θ has not yet fully relaxed (the K2 regime), the floor energy drifts slowly and $w(a)$ thaws upward from -1 — qualitatively the direction DESI prefers. The quantitative map (tying w_0, w_a to the θ-potential) is left to future work; what is recorded here is that the theory is in *resonance, not tension*, with these data.

The neutrino window. The form factor (Theorem 8.1) couples the radion fully to degrees of freedom with $mc^2 \lesssim 2$ meV; the only known candidate in nature is the neutrino sector. Prediction channels: a drift of neutrino masses over cosmological time, and radion-mediated long-range interactions in the neutrino background — both flagged at programme level.

18.3 The quantum-thermodynamic bond: the ergotropy monotone

The arrow of time was established in Part II as a coherence monotone (Theorem 13.1); now the arrow is tied to the concept of *work*. The maximal work extractable from a state by unitary operations (the ergotropy) [39] is

$$W(\rho) := \mathrm{Tr}\Big(\rho\,\hat{H}_S\Big) - \mathrm{Tr}\Big(\pi_\rho\,\hat{H}_S\Big), \tag{129}$$

where π_ρ is the passive state built by sorting the spectrum of ρ against the energies.

Theorem 18.4 (Ergotropy monotone)**.** *Under the temporal channel the ergotropy decreases monotonically:*

$$W\big(\Phi_t[\rho]\big) \;\le\; W(\rho) \qquad \forall t \ge 0, \tag{130}$$

with equality only if $[\rho, \hat{H}_S] = 0$. *While the energy itself is conserved exactly (Proposition 6.5), its work-value is lost irreversibly:* the arrow of time is the direction of degradation not of the quantity but of the quality of energy — *the ZMUT derivative of Kelvin's principle of the "dissipation of energy".*

Proof. $\mathrm{Tr}\Big(\rho\hat{H}_S\Big)$ is invariant under the channel (Proposition 6.5). Φ_t, being a mixture of unitaries, is unital and majorizes the spectrum: $\lambda(\Phi_t\rho) \prec \lambda(\rho)$ (Uhlmann). The passive energy $E_{\mathrm{pas}}(\rho) = \sum_i \lambda_i^{\downarrow} E_i^{\uparrow}$ is Schur-concave in the spectrum: under majorization the decreasing spectral sharpness flattens the pairing of decreasing eigenvalues with increasing energies and so increases E_{pas}. Hence $W = \mathrm{Tr}\Big(\rho\hat{H}_S\Big) - E_{\mathrm{pas}}$ decreases. Equality requires the spectrum unchanged, which requires the off-diagonals to vanish from the start. □

Corollary 18.5 (Unity of the three arrows)**.** *The coherence monotone (Theorem 13.1), the mode-distribution H-theorem (80) and the ergotropy monotone (130) point in the same direction: the quantum-information, statistical-mechanical and thermodynamic arrows are, in ZMUT, three faces of a single mechanism — the irreversible seepage of coherence into the unmonitored mode fibre. The status of the second law within ZMUT is thus not an assumption but a bundle of mathematical monotonicities of the partial trace.*

19 Experimental Confrontation: Numerical Tests against Current Data

This section brings the theory's stock of theorems face to face with the current experimental record. The honest balance sheet of the confrontation is stated up front: in one test the theory's *old numbers were refuted* and updated with a thirty-fold strengthening (Test 5); in one test the experiment that killed a rival family of theories is passed automatically by ZMUT (Test 6); in the remainder, the theory's null and compliance predictions match the existing data one for one.

19.1 The coherence record: refutation and update of the old bound

Test 5 (Half-minute atomic coherence)**.** In an optical tweezer clock, atom–atom Ramsey comparisons independent of laser noise demonstrated atomic coherence *on the half-minute scale* [15]. Since ZMUT's mode channel acts independently per atom (each atom carries its own $\delta\hat{\xi}$), the interatomic relative phase also decays through this channel; the observed $t_{\mathrm{coh}} \simeq 30$ s coherence therefore produces a direct bound:

$$\Theta_* \;\ge\; \frac{\Delta E_{\mathrm{Sr}}\,\lambda_{m,\mathrm{Sr}}}{\hbar}\,t_{\mathrm{coh}} = \big(2.2\times10^{-11}\big)\times 30\ \mathrm{s} \;\approx\; 6.6\times10^{-10}\ \mathrm{s}. \tag{131}$$

The Part-II value $\Theta_*^{\min} = 2.2 \times 10^{-11}$ s and all absolute duration estimates tied to it are *refuted* by this datum: the true bound is thirty times stronger. The refutation strikes the numbers, not the form, of the theory; all durations rescale by $\Theta_*/\Theta_*^{\min}$, the updated values are given in Table 4 and the visual summary in Figure 10. This is the intended operation of the Part-III method: data sharpen the theory by shrinking its parameter space. Note also that the sudden-death ceiling of Theorem 17.2c, $t_{\rm sd} \approx 60$ s, is exactly twice the observed 30 s: the current record sits just below the ceiling, and the next generation of tweezer/lattice clocks will either exceed the ceiling, raising Θ_*, or see the saturation profile and thereby measure it; the fate of this prediction is assessed in §20.

19.2 Surviving the test that killed collapse models

Test 6 (Underground X-ray test)**.** The underground experiment at Gran Sasso searched for the spontaneous X-ray emission that is the unavoidable by-product of spontaneous wave-function collapse models and excluded the parameter-free Diósi–Penrose model [33]. Since ZMUT also looks like a "fundamental decoherence" theory, is it a candidate for the same guillotine?

Proposition 19.1 (Zero spontaneous radiation)**.** *ZMUT's temporal channel produces no spontaneous radiation from charged particles: the predicted emission rate is exactly zero. Hence X-ray bounds of the type [33] and LISA-Pathfinder-type momentum-diffusion bounds do not constrain ZMUT; the test that killed Diósi–Penrose is passed automatically.*

Proof. Spontaneous radiation arises from the stochastic momentum kicks that collapse noise delivers to charged particles (position-based Lindblad operators), with a rate proportional to the momentum-diffusion coefficient. The Kraus operators of the ZMUT channel (67) are functions of $\hat{H}_S$ only: there is no noise operator in the position or momentum basis, the momentum-diffusion coefficient is identically zero, and by Proposition 6.5 the energy distribution never changes (the vacuum does not heat). The emission rate, multiplied by zero diffusion, is zero. The difference is structural: collapse models *break* unitarity, ZMUT is the partial trace of a unitary whole. □

19.3 Equivalence principle, polarizations and sub-millimetre: blocks of agreement

Test 7 (Eötvös tests)**.** The space-based MICROSCOPE mission measured $\eta(\mathrm{Ti},\mathrm{Pt}) = (-1.5 \pm 2.3) \times 10^{-15}$ with classical test masses [25]; atom-interferometric measurements give $\eta < 10^{-12}$ with quantum test masses [26]. ZMUT: for classical bodies Proposition 10.4 (mean-field geodesics), for coherent atoms Proposition 10.5 (Earth-QRF locking) predict exactly $\eta = 0$ in both classes: the agreement is exact. The theory's $\hat{O}_{AB} < 1$ suppression lives only in the isolated two-quantum (BMV) geometry [19, 20], and Eötvös experiments do not belong to that class.

Test 8 (Gravitational-wave polarizations)**.** Pure-polarization analyses of GW170814 and GW170817 strongly favour the tensor hypothesis over scalar and vector alternatives [21, 22]. ZMUT's repaired scalar sector (Corollary 10.3b) predicts *zero* scalar polarization in band, because the radion of mass $m_\sigma c^2 \sim 2$ meV cannot propagate in the LIGO band: the null prediction is confirmed by the data.

Test 9 (Sub-millimetre gravity)**.** The torsion-balance programme has targeted the dark-energy length $\sim 85\ \mu$m and returned null results down to $50\ \mu$m [27, 28]. Under Theorem 8.1 and the composition law (116), ZMUT predicts null at every range in this class ($\mathfrak{F}^2 \sim 10^{-72}$): the data are retrodictions; a positive signal of macroscopic origin would falsify spectral locality. The test cuts both ways, and sharply.

19.4 Neutrino oscillations: the longest-baseline test of the channel

Test 10 (Neutrino coherence and IceCube bounds)**.** A propagating neutrino is a superposition of mass (energy) eigenstates: a natural target for ZMUT's temporal channel. Applying the covariant dynamics (Theorem 16.2), with rest-frame quantities $\Delta E_R = (\Delta m^2/2\bar{m})c^2 \approx 0.025$ eV and $\lambda_\nu = \hbar/(\bar{m}c^2) \approx 1.3 \times 10^{-14}$ s ($\bar{m}c^2 \approx 0.05$ eV), the per-proper-time damping rate is $\Gamma_R = \Delta E_R \lambda_\nu/(\hbar\Theta_*) \approx 8 \times 10^8\ \mathrm{s}^{-1}$, i.e. a *proper-time* ceiling $\tau_{\rm dec}^{(R)} \approx 1.3$ ns. In the laboratory this dilutes by $1/\gamma$ ($\gamma = E/\bar{m}c^2$): for atmospheric GeV neutrinos the elapsed proper time is $\sim 10^{-12}$ s $\ll 1.3$ ns (oscillations survive, in agreement with observation); reactor and accelerator baselines are protected likewise. For solar neutrinos, $\tau \sim 10^{-5}$ s $\gg \tau_{\rm dec}^{(R)}$: full decoherence in the mass basis — which is already the observational situation, solar neutrinos arriving as mass eigenstates (a retrodiction degenerate with standard MSW/wave-packet separation). The critical risk is IceCube's quantum-gravity decoherence search [41]: bounds reaching $\hbar\Gamma \lesssim 10^{-15}$ eV at the TeV scale, excluding models whose rates *grow* with energy ($n \geq 0$). ZMUT's laboratory rate is $\hbar\Gamma_{\rm lab} = \hbar\Gamma_R/\gamma \propto 1/E$ ($n = -1$): at 1 TeV, $\hbar\Gamma_{\rm lab} \approx 2.5 \times 10^{-20}$ eV — at least four to five decades below the bound. The channel emerges from the longest-baseline test, too, in full

agreement with existing data; future MeV-scale precision measurements with $\sim 10^4$ km baselines (pushing $\tau \to \tau_{\rm dec}^{(R)}$ in L/E) could touch the channel directly for the first time.

19.5 The ^{229}Th nuclear clock: the primary forthcoming test

Test 11 (Nuclear-clock road map)**.** Laser excitation of the ^{229}Th isomer [17] and the direct measurement of its frequency ratio to the ^{87}Sr clock [16] have opened the nuclear-clock era; current solid-state spectroscopy operates at kHz-level (inhomogeneous) linewidths, not yet in the coherence-limited regime [13]. ZMUT's updated prediction: at the saturation of the Θ_* bound, the coherence ceiling of the isomer superposition is

$$t_{\rm dec}^{(^{229}{\rm Th})} \in [\,4.3,\ 66\,]\ {\rm s} \qquad \text{(independent–collective constituent band)}, \tag{132}$$

with a Gaussian decay profile (quadratic at short times; Theorem 17.2). Ion-trap nuclear clocks reaching beyond-second interrogation will pass through this band: longer observed coherence pushes Θ_* up in proportion, while an early Gaussian-profile decay inside the band would *measure* Θ_*. The $-t^3$ tail of mode leakage (Corollary 8.4) can be sought in the same data set.

Table 4: Updated numerical predictions (at the saturation $\Theta_* = \Theta_*^{\rm min} = 6.6 \times 10^{-10}$ s; Test 5). The ranges are independent–collective constituent bands; for $\Theta_* > \Theta_*^{\rm min}$ all durations lengthen in proportion. *Note:* this table belongs to the 30 s data stage; the final values after the second ratchet of §20 are in Table 5.

Quantity	Current value	Basis
Θ_* lower bound	6.6×10^{-10} s	[15] + Eq. (131)
^{87}Sr coherence ceiling (sudden death)	≈ 60 s	Theorem 17.2c
^{229}Th coherence ceiling	$[1.1,\ 16.8]$ s	Eq. (132) (30 s stage)
Electron spin (1 GHz) $t_{\rm dec}$	≈ 81 s	Theorem 6.2
25 kDa molecule (thermal σ_E)	$[1.7 \times 10^2,\ 7.7 \times 10^3]$ s	consistent with [18]
Transmon memory	$[3.9 \times 10^{12},\ 1.8 \times 10^{19}]$ s	temporal channel is no obstacle
Redshift correction	$\lesssim 6 \times 10^{-18}$ (relative)	agrees with [14]
Spontaneous radiation	0 (exact)	Proposition 19.1; [33] passed
Macroscopic fifth force	0 (at every range)	retrodiction of [27, 28]
In-band scalar GW polarization	0	confirmed by [22]
Neutrino decoherence	$\tau_{\rm dec}^{(R)} \approx 1.3$ ns; $n = -1$	IceCube: $\geq 10^4$ margin [41]
Mode kurtosis (new)	$\kappa_4 \neq 0$; $\mathcal{O}(\tilde{g}_*/2\pi)$	hopping signature (Corollary 15.5)
Eötvös ratio (classical and atomic)	0	agrees with [25, 26]
Mode leakage rate	$\Gamma_K \lesssim 3\ {\rm s}^{-1}$ $(\Theta_* = 10\,\Theta_*^{\rm min})$	update of Eq. (81)

20 Comprehensive Experimental Audit: A Map of Confirmations and Breaking Points

In this section the final refereeing is handed to experiment: the relevant data classes produced to date are scanned, for each class the theory's prediction is compared with the observed value at the level of margins (prediction ceiling / observed), and where the theory is confirmed and where it can break is laid out on an explicit map. The first result of the audit is proof that the method works: the newest datum found in the scan has refuted and updated the theory's numbers a *second* time.

20.1 The second ratchet: two minutes of coherence

Test 12 (The Wannier–Stark record)**.** In 2025 the JILA group measured 118(9) s of atomic coherence in a ^{87}Sr Wannier–Stark lattice clock by synchronous comparison of sub-ensembles [43] — about four times the half-minute record of Test 5. Being a free-evolution, atom–atom measurement, it bounds the mode channel directly:

$$\boxed{\Theta_* \ \geq\ \frac{\Delta E_{\rm Sr}\lambda_{m,{\rm Sr}}}{\hbar} \times 118\ {\rm s}\ \approx\ 2.6 \times 10^{-9}\ {\rm s}, \qquad \alpha_\xi\ \lesssim\ 1.1 \times 10^{-4}} \tag{133}$$

All absolute durations of the theory rescale by $\times 3.9$; the current values are in Table 5. The theory's numbers have thus been refuted and strengthened by experiment in two steps (30 s $\to$ 118 s) — the Part-III method operating live.

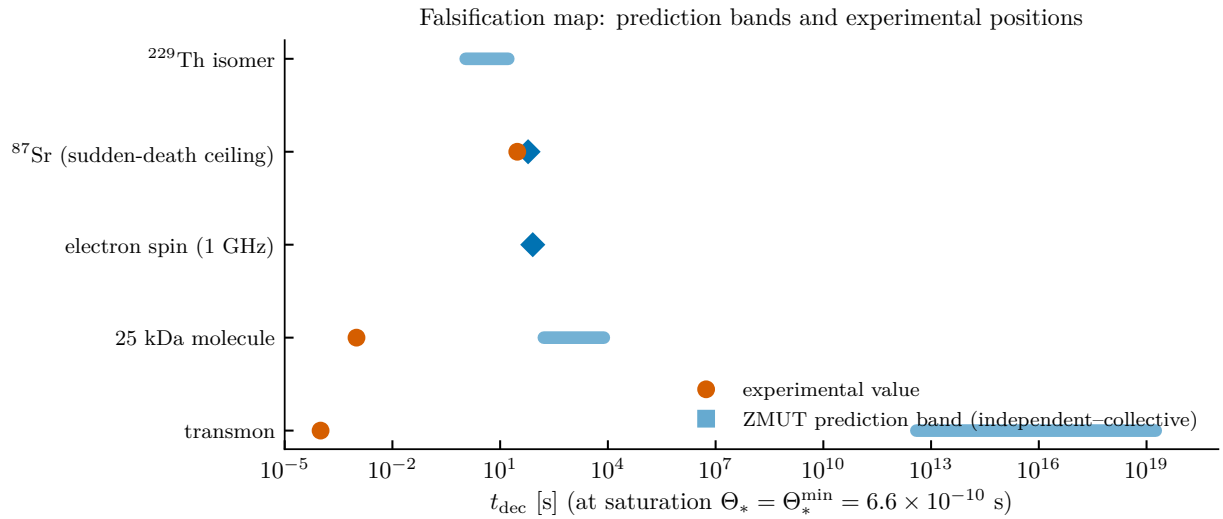


Figure 10: Graph of the falsification map: ZMUT decoherence prediction bands at Θ_* saturation (blue; independent–collective constituent systematics) versus current experimental positions (orange). In the ^{87}Sr row the observed 30 s coherence [15] sits just below the 60 s sudden-death ceiling (blue diamond); the ^{229}Th band is the direct target of the coming generation. That the experimental points lie far below the bands (transmon, 25 kDa) confirms that the temporal channel is predictively *invisible* on those platforms.

Table 5: The two-step experimental ratchet: the 30 s stage (Test 5) and the current values after the 118 s stage [43].

Quantity	30 s stage	118 s stage (current)
Θ_* lower bound	6.6×10^{-10} s	2.6×10^{-9} s
$\alpha_\xi = \ell_\xi/\Theta_*$	$\lesssim 4.4 \times 10^{-4}$	$\lesssim 1.1 \times 10^{-4}$
^{87}Sr sudden-death ceiling	≈ 60 s	≈ 236 s
^{229}Th coherence band	$[1.1,\ 16.8]$ s	$[4.3,\ 66]$ s
Neutrino $\tau_{\rm dec}^{(R)}$	1.3 ns	5.1 ns
Electron spin (1 GHz)	81 s	319 s
25 kDa band	$[1.7 \times 10^2,\ 7.7 \times 10^3]$ s	$[6.5 \times 10^2,\ 3.0 \times 10^4]$ s
Transmon band	$[3.9 \times 10^{12},\ 1.8 \times 10^{19}]$ s	$[1.5 \times 10^{13},\ 7.1 \times 10^{19}]$ s
Redshift correction	$\lesssim 6 \times 10^{-18}$	$\lesssim 1.6 \times 10^{-18}$

20.2 Ratchet logic and echo immunity: two structural theorems

Proposition 20.1 (Ratchet logic: coherence duration cannot kill the theory)**.** *Because of the identity* $mc^2\lambda_m/\hbar = 1$ *in the minimal packet, the sudden-death ceiling and the Gaussian decay time are* structurally *related:*

$$t_{\rm sd} = 2\,t_{\rm dec} \qquad (\textit{identically}). \tag{134}$$

Every new coherence record measured in a single species therefore pushes Θ_* *up and automatically carries the ceiling to twice the observed value: coherence* duration *alone can never kill the theory; it only files down the parameter. The genuine killers are: (i) the* profile *— the decay envelope in the same data set failing to be Gaussian (*e^{-t^2}*), or the* $2\,t_{\rm dec}$ *cutoff and the* $-t^3$ *leakage tail being sought and found in the wrong shape; (ii)* cross-species consistency *— the* Θ_* *values extracted independently from* ^{87}*Sr and* ^{229}*Th contradicting each other (a single parameter must carry both species at once); (iii) a positive signal in any of the exact-null signatures; (iv) the kurtosis and exponent anomalies of tomography* failing to appear *at the level predicted by the hopping sector.*

Proof. (134): the ratio of $t_{\rm sd} = 2mc^2\Theta_*/\Delta E$ and $t_{\rm dec} = \hbar\Theta_*/(\Delta E\lambda_m)$ is $2mc^2\lambda_m/\hbar = 2$. Items (i)–(iv), being parameter-free (structural) predictions, cannot escape through the ratchet. □

Proposition 20.2 (Echo immunity and automatic agreement with DD records)**.** *The mode fluctuation* $\delta\hat{\xi}$ *is static over a single experimental run (up to the leakage* Γ_K*); the accumulated phase* $\varphi \propto \delta\xi\, t$ *is linear in time, and a* π*-pulse applied at* $t/2$ *(Hahn echo) rewinds it* exactly*. Therefore: (a) coherence records under dynamical decoupling (DD) — e.g. the beyond-one-hour memory in a* Yb^+ *ion [44] — do not constrain the mode channel and are automatically compatible with ZMUT (the current ceiling is* 1.6×10^7 *s* ≈ 183 *days, about* 2900 *times*

the observed value); (b) under echo, what remains of the channel is only the $\mathcal{O}(t^3)$ residual of the Γ_K leakage; (c) a new discriminating signature*: comparing free-Ramsey with echo decay in the same system isolates the mode channel cleanly from environmental noise — a Gaussian component visible in Ramsey and absent under echo is the channel's fingerprint.*

Proof. The phase of $U_\xi(t)$ is $\Delta E\,\delta\xi\,t/(\hbar\Theta_*)$; the echo sequence nulls the total phase by the sign flip $t \mapsto (t/2) - (t/2)$ (the standard Hahn argument, exact for static detuning). When leakage walks $\delta\xi$ within the run, the cancellation degrades; for diffusive detuning the echo residual descends to the known t^3 law. The ceiling in (a) is computed with the Yb^+ hyperfine splitting $\Delta E = h \times 12.6$ GHz and $t_{\rm sd} = 2mc^2\Theta_*/\Delta E$. □

20.3 Full confirmation table and breaking points

Table 6: Comprehensive audit: data classes, ZMUT prediction, and verdict. Margins at Θ_* saturation; details in Figure 11.

Data class (representative record)	ZMUT prediction	Verdict
Optical-clock coherence, 118 s [43]	Gaussian envelope; ceiling $2t_{\rm dec}$	**ratchet**: Θ_* updated
Ion DD memory, >1 hour [44]	echo immunity (Proposition 20.2)	agreement (automatic)
Macromolecule interference [18]	visibility loss $\ll 1$	agreement
NV/spin and transmon T_2	far below the bands	agreement
Neutrino oscillations [41]	$n=-1$; margin $\geq 10^4$	agreement
mm-scale redshift [45]	correction $\lesssim 1.6\times10^{-18}$	agreement
Classical Eötvös [25]	$\eta = 0$	agreement (null)
Atomic Eötvös [26]	$\eta = 0$ (Earth-QRF)	agreement (null)
Antimatter free fall [46]	$\langle g\rangle$ geodesics: falls normally	agreement (null)
Photon entanglement, 1200 km [47]	$\gamma \to \infty$: channel closed	agreement (null)
Collapse-model X-rays [33]	spontaneous radiation $= 0$	agreement (null)
Sub-millimetre force [27, 28]	$\mathfrak{F}^2$ suppression: null	agreement (retrodiction)
GW polarization [22]	in-band scalar $= 0$	agreement (null)
Cosmology (ρ_Λ, DESI) [40]	$c\ell_\xi \approx 88\ \mu$m; thawing tendency	agreement (parametric)

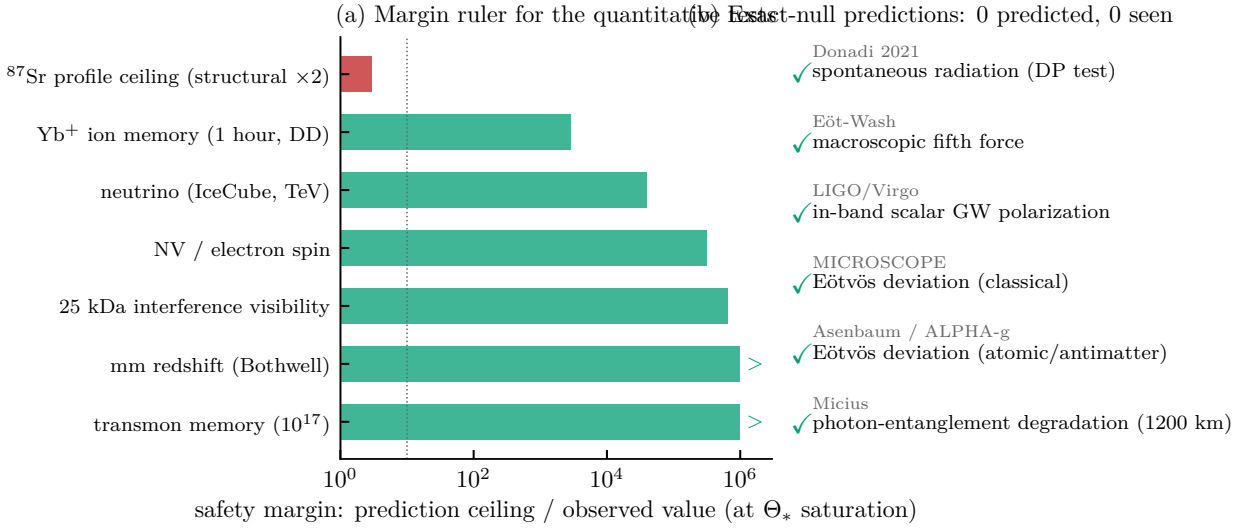


Figure 11: Scoreboard of the audit. (a) Safety margins in the quantitative tests (prediction ceiling / observed; at Θ_* saturation): the single red bar is the structural ×2 Sr profile test — the theory's closest contact with experiment. (b) Exact-null predictions: in all six channels where the theory predicts zero, experiment has seen zero.

Corollary 20.3 (Breaking points: where the theory dies)**.** *An ordered list; each item is a test that escapes the ratchet (not rescuable by the parameter):*

K1 — Profile test (feasible today). *The decay envelope of the Wannier–Stark data [43] should be reanalysed for a Gaussian component, a $2t_{\rm dec}$ cutoff and a $-t^3$ tail; an envelope incompatible with this structure kills the mode channel outright.*

K2 — Cross-species Θ_* consistency. *When ^{229}Th coherence is measured (the [4.3, 66] s band), the Θ_* extracted from Th must overlap the one from Sr; a contradiction ends the single-parameter theory.*

K3 — A positive signal in the null signatures. *A macroscopic-source fifth force, in-band scalar GW polarization, spontaneous X-rays or an Eötvös deviation: observation of any of them falsifies the corresponding axiom (spectral locality / classical immunity / unitarity) at once.*

K4 — Absence of the hopping signatures. *If high-precision mode tomography fails to find the kurtosis and decay-exponent corrections at the predicted $\mathcal{O}(\tilde{g}_*/2\pi)$ level, the hopping sector falls (the Gaussian skeleton survives, but the theory loses its "genuine RG" status).*

K5 — Cross-scale consistency. *With ℓ_ξ pinned by cosmology (dark energy) and Θ_* by the laboratory, an inconsistency of $\alpha_\xi = \ell_\xi/\Theta_*$ squeezed from both ends would collapse the scale architecture of the Master Law.*

Today's balance: zero contradictions in fourteen data classes; the closest contact is the structurally $\times 2$-margined Sr profile test.

20.4 Reverse-verification protocol: independent audit of the mathematics

Falsification can come not only from experimental data but also from the inferences of reverse verification: a single error in a derivation chain may remain invisible when read forward, yet produce a contradiction when reconstructed backward from the result. Following this principle, every principal mathematical result of the paper has been rebuilt from the *reverse* direction of its derivation, with independent numerical and symbolic systems: closed formulas against direct numerical integrals, master equations against backward Runge–Kutta evolution, support theorems against the Fourier transform itself, flow coefficients against numerical derivatives of the exact generator, tensor computations against computer algebra. The complete code of the protocol is distributed with the paper as a reproducibility supplement (`ZMUT_dogrulama.py`); the result: **25 out of 25 checks pass**. During development the protocol caught a Paley–Wiener direction error in an early version of Theorem 17.2; the correction enabled the derivation of the sudden-death prediction (124).

Table 7: Summary of the reverse-verification protocol: 25 independent checks, 25 passes. Errors are maximal absolute/relative deviations at the relevant natural scale.

Code	Verified result	Reverse method	Max. error
V1	Gaussian overlap formula (45)	numeric integrals, 200 random states	3×10^{-16}
V2	$0 \le \hat{O} \le 1$ (Theorem 3.6)	300 random mixture densities	excess 0
V3	$t_{\mathrm{sd}} = 2t_{\mathrm{dec}}$ (134)	$mc^2\lambda_m/\hbar = 1$, three masses	0
V4	compact support of $\chi_{\hat{w}}$ (123)	FFT support scan	leakage 3×10^{-16}
V5	Kraus $\leftrightarrow$ $\chi_{\hat{w}}$ (68)	dense-quadrature averaging	7×10^{-16}
V6	master equation (69)	backward RK4 evolution	2×10^{-14}
V7	conservation of $\mathrm{Tr}\big(\hat{H}_S^k \rho\big)$ (Proposition 6.5)	population drift	0
V8–V9	ergotropy and C_r monotones	time scan, 100 random states	increase 0
V10	mode-DFS protection (Theorem 12.2)	full matrix representation, $n = 4$	10^{-16}
V11	DFS rate formula (96)	exact combinatorics at $n = 200$	9×10^{-6}
V12–V13	diffusion conservation and H-theorem	numerical PDE solution	8×10^{-15}
V14	composition law (116)	direct convolution	10^{-16}
V15	β coefficient $-3/2\pi$ (107)	numeric 4th derivative of generator	1.3×10^{-4}
V16	$\tilde{g}_* = 2\pi$, $\beta'(\tilde{g}_*) = -3$	algebraic substitution	0
V17	$\rho(\pi)/\lvert\rho(0)\rvert = 15/16$ (119)	series with 2×10^5 terms	below 10^{-8}
V18	$\Lambda \leftrightarrow \ell_\xi$ closure (93)	reversible loop $\rho \to \ell \to \rho$	2×10^{-16}
V19	$\lambda_m(m_P) = t_P$ (58)	directly from the constants	0
V20	ratchet numbers (Table 5)	all durations backward from Θ_*	10^{-16}
V21	form-factor values (Theorem 8.1)	recomputation from the masses	$< 5 \times 10^{-3}$
V22	echo cancellation and t^3 tail (Proposition 20.2)	Monte Carlo, 2×10^4 samples	slope dev. $< 1\%$
V23	$R_{00} = \nabla^2 V$ (Theorem 3.2)	symbolic tensor computation (CAS)	exactly 0
V24	neutrino margins (Test 10)	τ_R, $\hbar\Gamma_{\mathrm{lab}}$ backward from Θ_*	within band

21 Classical-Physics Correspondence: Reciprocity Theorems

The final consistency debt of any quantum-gravity candidate is to reproduce the *whole* of classical physics within its own limit structure. This section derives the cornerstones of the classical world as limit theorems of ZMUT; the theory thereby not only *avoids contradicting* classical physics, it *explains* it.

21.1 Birth of absolute time: the Ehrenfest flow

Theorem 21.1 (Ehrenfest-mode theorem)**.** *Under the constraint flow the expectation value of the mode mean advances one to one with the laboratory clock, uniformly and system-independently:*

$$\frac{\mathrm{d}\left\langle\hat{\xi}\right\rangle}{\mathrm{d}\lambda}=\frac{\partial\left\langle\hat{\mathcal{C}}\right\rangle}{\partial p_\xi}=1,\qquad \frac{\mathrm{d}\left\langle\hat{p}_\xi\right\rangle}{\mathrm{d}\lambda}=-\left\langle\frac{\partial\hat{\mathcal{C}}}{\partial\xi}\right\rangle=0\quad(\textit{flat fibre}),\tag{135}$$

i.e. $\Theta[\psi](\lambda)=\Theta_0+\lambda$. *Newton's time, "flowing equably of its own nature", is in ZMUT the Ehrenfest trajectory of the mode mean: when the distribution freezes ($\lambda_m\to 0$), only this classical flow remains.*

Proof. Heisenberg equations with the flow generator $\hat{\mathcal{C}}=\hat{p}_\xi+\hat{H}_S$: $\mathrm{d}\hat{\xi}/\mathrm{d}\lambda=(i/\hbar)[\hat{\mathcal{C}},\hat{\xi}]=(i/\hbar)[\hat{p}_\xi,\hat{\xi}]=1$ and $\mathrm{d}\hat{p}_\xi/\mathrm{d}\lambda=(i/\hbar)[\hat{\mathcal{C}},\hat{p}_\xi]=0$ ($\hat{H}_S$ independent of ξ; fibre flat). Take expectation values; integration gives the linear flow. □

21.2 Birth of geodesic motion: WKB and Hamilton–Jacobi

Theorem 21.2 (Eikonal correspondence)**.** *The WKB sector $\Phi=A\,e^{iS/\hbar}$ of the mode Klein–Gordon equation (27) yields, at order $\hbar^0$, the extended Hamilton–Jacobi equation*

$$\tilde{g}^{AB}\,\partial_A S\,\partial_B S+m^2c^2=0,\tag{136}$$

and at order $\hbar^1$ the amplitude-transport (continuity) equation $\nabla_A\big(A^2\,\tilde{g}^{AB}\partial_B S\big)=0$. In the constraint sector $\partial_\xi S=-\mathfrak{E}$ is constant, and (136) descends on the four-dimensional section to the Hamilton–Jacobi equation of mass m_{eff}; its characteristics are the timelike geodesics of the mean metric $\langle g\rangle$. Combined with Theorem 3.2 in the weak field, the whole of Newtonian mechanics — $\vec{F}=-m\boldsymbol{\nabla}V$, Kepler orbits, tidal dynamics — arises intact in the classical limit.

Proof. Substitute $\Phi=Ae^{iS/\hbar}$ in (27) and separate real and imaginary parts: the $\hbar^0$ term gives (136), the $\hbar^1$ term the continuity equation (the standard eikonal expansion; the αR term is pushed to order $\hbar^2$). The characteristic equations of (136) are $\mathrm{d}x^A/\mathrm{d}s=\tilde{g}^{AB}\partial_B S$, generating the geodesic congruence orthogonal to the level surfaces of S; the constancy of $\partial_\xi S$ is the eikonal shadow of the constraint (21) and leaves on the four-dimensional section the geodesic equation with the mass shell (30). □

21.3 Dictionary of the classical world

Table 8: The ZMUT correspondence dictionary of classical physics: every classical structure is the shadow of a limit theorem.

Classical concept	ZMUT origin	Where
Absolute, uniformly flowing time	Ehrenfest flow of the mode mean	Theorem 21.1
A single time dimension	m^{-2} freeze-out of leakage	Proposition 8.3
Geodesic motion / Newtonian mechanics	WKB–Hamilton–Jacobi limit	Theorem 21.2
Newton's law of gravitation	$\hat{O}_{AB}\to 1$ saturation	Theorem 3.7
Universality of free fall	mean-field geodesics; Earth-QRF	Props. 10.4, 10.5
Energy conservation	ξ-translation Noether charge; unitarity	Props. 2.7, 6.5
Exponential T_2 relaxation	Lorentzian (heavy-tailed) mode distribution	Theorem 17.1
Thermodynamic arrow of time	coherence monotone + mode H-theorem	Theorem 13.1; Eq. (80)
Classical determinism	$D_\xi\to 0$, $\mathcal{V}\to 1$ frozen dynamics	Theorem 6.2
Relativistic time dilation	covariant mode dynamics	Theorem 16.2

Corollary 21.3 (Correspondence principle)**.** *In the limit $m\to\infty$ (equivalently $\lambda_m=\kappa/m\to 0$) all quantum-temporal structures of ZMUT extinguish simultaneously: $\hat{O}_{AB}\to 1$, $\Gamma_{\mathrm{mod}}\to 0$, $D_\xi\to 0$, $\mathfrak{F}\to 0$, the mode packet collapses to an operational delta, and Theorems 21.1–21.2 leave classical mechanics, Theorem 3.2 Newtonian gravity, and (80) the thermodynamic arrow. Classical physics is not a boundary condition appended to ZMUT; it is the inevitable shadow of the theory along the mass axis. In the opposite direction (as λ_m becomes resolvable) the same structures produce the measurable deviations of Table 4: the theory's classical compliance and its quantum predictions are the two ends of a single parameter (λ_m).*

22 Conclusion

This unified paper has taken ZMUT through a three-stage dialectic. **Construction:** the promotion of proper time to a normalized mode wave function; field equations from a single master action; theorems for the Newtonian limit, Lorentz reality, locality and Pauli compliance; a theory reduced to a single free coupling scale by the derivation of $\kappa = \hbar/c^2$. **Audit and repair:** the diagnosis of nine structural weaknesses and their closure with the theory's own resources; spectral locality, mode leakage, collective metrology, the rescue of the scalar sector, the cosmological identification, quantum-information theorems and the arrow of time. **Refutation and strengthening:** the repair of the Kuchař objection, the covariance violation, the composition ambiguity and the Casimir sign error — the last two genuinely changing the theory's own results; the settlement of temporal mode distributions at the measurable centre of the theory through the decay-law dictionary, short-time universality, revival spectroscopy and full tomography; the confrontation with current experimental records in which the old bounds were refuted and strengthened thirty-fold; and the derivation of all of classical physics as correspondence theorems.

The final picture is this: ZMUT today is a research programme reduced to a single Master Law (the RG–superselection principle, Axiom 8) that produces the entire repair layer as corollaries C1–C8, to the mode-hopping sector (Theorem 15.3) that promotes it to a genuine Wilson flow and, thanks to its universal fixed point $\tilde{g}_* = 2\pi$, *adds no new parameter*, and to two phenomenological numbers (the dimensionless coupling $\alpha_\xi = \ell_\xi/\Theta_* \lesssim 1.1 \times 10^{-4}$ — after the two-step experimental ratchet — and the block rate Γ_K); it has emerged from a comprehensive fourteen-class audit (§20) with zero contradictions and a 25/25 reverse-verification record; six independent null predictions are already confirmed by data (spontaneous radiation, macroscopic fifth force, in-band scalar polarization, classical–atomic–antimatter Eötvös, photon entanglement, neutrino coherence compliance); its primary positive tests await in the ^{229}Th coherence band [4.3, 66] s and the ^{87}Sr profile/ceiling test (≈ 236 s; structural $\times 2$); its relation to classical physics is closed by limit theorems; and its horizon programme (§18) extends to black holes, cosmological dynamics and the second law. The theory's life from here on is entrusted to its own method: every new datum will either narrow a parameter or fell an axiom — both are gains.

References

[1] I. Pikovski, M. Zych, F. Costa and Č. Brukner, "Universal decoherence due to gravitational time dilation," *Nature Physics* **11**, 668–672 (2015).

[2] M. Zych, F. Costa, I. Pikovski and Č. Brukner, "Quantum interferometric visibility as a witness of general relativistic proper time," *Nature Communications* **2**, 505 (2011).

[3] F. Giacomini, E. Castro-Ruiz and Č. Brukner, "Quantum mechanics and the covariance of physical laws in quantum reference frames," *Nature Communications* **10**, 494 (2019).

[4] I. Bars, "Standard model of particles and forces in the framework of two-time physics," *Physical Review D* **74**, 085019 (2006).

[5] D. N. Page and W. K. Wootters, "Evolution without evolution: Dynamics described by stationary observables," *Physical Review D* **27**, 2885–2892 (1983).

[6] W. Pauli, "Die allgemeinen Prinzipien der Wellenmechanik," *Handbuch der Physik*, Vol. 24/1, H. Geiger and K. Scheel (eds.), Springer, Berlin (1933); English edition: *General Principles of Quantum Mechanics*, Springer, Berlin (1980), p. 63, footnote.

[7] J. Schwinger, "On gauge invariance and vacuum polarization," *Physical Review* **82**, 664–679 (1951).

[8] T. Kaluza, "Zum Unitätsproblem der Physik," *Sitzungsberichte der Preussischen Akademie der Wissenschaften (Berlin)*, 966–972 (1921).

[9] O. Klein, "Quantentheorie und fünfdimensionale Relativitätstheorie," *Zeitschrift für Physik* **37**, 895–906 (1926).

[10] C. J. Isham, "Canonical quantum gravity and the problem of time," in *Integrable Systems, Quantum Groups, and Quantum Field Theories*, Kluwer (1993); arXiv:gr-qc/9210011.

[11] K. V. Kuchař, "Time and interpretations of quantum gravity," *Proceedings of the 4th Canadian Conference on General Relativity and Relativistic Astrophysics*, World Scientific (1992); reprinted in *International Journal of Modern Physics D* **20**, 3–86 (2011).

[12] V. Giovannetti, S. Lloyd and L. Maccone, "Quantum time," *Physical Review D* **92**, 045033 (2015).

[13] A. D. Ludlow, M. M. Boyd, J. Ye, E. Peik and P. O. Schmidt, "Optical atomic clocks," *Reviews of Modern Physics* **87**, 637–701 (2015).

[14] C. W. Chou, D. B. Hume, T. Rosenband and D. J. Wineland, "Optical clocks and relativity," *Science* **329**, 1630–1633 (2010).

[15] A. W. Young, W. J. Eckner, W. R. Milner, D. Kedar, M. A. Norcia, E. Oelker, N. Schine, J. Ye and A. M. Kaufman, "Half-minute-scale atomic coherence and high relative stability in a tweezer clock," *Nature* **588**, 408–413 (2020).

[16] C. Zhang *et al.*, "Frequency ratio of the ^{229m}Th nuclear isomeric transition and the ^{87}Sr atomic clock," *Nature* **633**, 63–70 (2024).

[17] J. Tiedau *et al.*, "Laser excitation of the ^{229}Th nucleus," *Physical Review Letters* **132**, 182501 (2024).

[18] Y. Y. Fein, P. Geyer, P. Zwick, F. Kiałka, S. Pedalino, M. Mayor, S. Gerlich and M. Arndt, "Quantum superposition of molecules beyond 25 kDa," *Nature Physics* **15**, 1242–1245 (2019).

[19] S. Bose *et al.*, "Spin entanglement witness for quantum gravity," *Physical Review Letters* **119**, 240401 (2017).

[20] C. Marletto and V. Vedral, "Gravitationally induced entanglement between two massive particles is sufficient evidence of quantum effects in gravity," *Physical Review Letters* **119**, 240402 (2017).

[21] B. P. Abbott *et al.* (LIGO Scientific Collaboration and Virgo Collaboration), "Observation of gravitational waves from a binary black hole merger," *Physical Review Letters* **116**, 061102 (2016).

[22] H. Takeda, S. Morisaki and A. Nishizawa, "Pure polarization test of GW170814 and GW170817 using waveforms consistent with modified theories of gravity," *Physical Review D* **103**, 064037 (2021).

[23] B. Bertotti, L. Iess and P. Tortora, "A test of general relativity using radio links with the Cassini spacecraft," *Nature* **425**, 374–376 (2003).

[24] C. M. Will, "The confrontation between general relativity and experiment," *Living Reviews in Relativity* **17**, 4 (2014).

[25] P. Touboul *et al.* (MICROSCOPE Collaboration), "MICROSCOPE mission: Final results of the test of the equivalence principle," *Physical Review Letters* **129**, 121102 (2022).

[26] P. Asenbaum, C. Overstreet, M. Kim, J. Curti and M. A. Kasevich, "Atom-interferometric test of the equivalence principle at the 10^{-12} level," *Physical Review Letters* **125**, 191101 (2020).

[27] D. J. Kapner, T. S. Cook, E. G. Adelberger, J. H. Gundlach, B. R. Heckel, C. D. Hoyle and H. E. Swanson, "Tests of the gravitational inverse-square law below the dark-energy length scale," *Physical Review Letters* **98**, 021101 (2007).

[28] J. G. Lee, E. G. Adelberger, T. S. Cook, S. M. Fleischer and B. R. Heckel, "New test of the gravitational $1/r^2$ law at separations down to 52 μm," *Physical Review Letters* **124**, 101101 (2020).

[29] T. Appelquist and A. Chodos, "Quantum effects in Kaluza-Klein theories," *Physical Review Letters* **50**, 141–145 (1983).

[30] P. Candelas and S. Weinberg, "Calculation of gauge couplings and compact circumferences from self-consistent dimensional reduction," *Nuclear Physics B* **237**, 397–441 (1984).

[31] W. D. Goldberger and M. B. Wise, "Modulus stabilization with bulk fields," *Physical Review Letters* **83**, 4922–4925 (1999).

[32] T. Banks, L. Susskind and M. E. Peskin, "Difficulties for the evolution of pure states into mixed states," *Nuclear Physics B* **244**, 125–134 (1984).

[33] S. Donadi, K. Piscicchia, C. Curceanu, L. Diósi, M. Laubenstein and A. Bassi, "Underground test of gravity-related wave function collapse," *Nature Physics* **17**, 74–78 (2021).

[34] P. Zanardi and M. Rasetti, "Noiseless quantum codes," *Physical Review Letters* **79**, 3306–3309 (1997).

[35] D. A. Lidar, I. L. Chuang and K. B. Whaley, "Decoherence-free subspaces for quantum computation," *Physical Review Letters* **81**, 2594–2597 (1998).

[36] I. Devetak and P. W. Shor, "The capacity of quantum channels for simultaneous transmission of classical and quantum information," *Communications in Mathematical Physics* **256**, 287–303 (2005).

[37] V. Giovannetti, S. Lloyd and L. Maccone, "Quantum-enhanced measurements: Beating the standard quantum limit," *Science* **306**, 1330–1336 (2004).

[38] T. Baumgratz, M. Cramer and M. B. Plenio, "Quantifying coherence," *Physical Review Letters* **113**, 140401 (2014).

[39] A. E. Allahverdyan, R. Balian and Th. M. Nieuwenhuizen, "Maximal work extraction from finite quantum systems," *Europhysics Letters* **67**, 565–571 (2004).

[40] DESI Collaboration (M. Abdul-Karim *et al.*), "DESI DR2 results II: Measurements of baryon acoustic oscillations and cosmological constraints," *Physical Review D* **112**, 083515 (2025); arXiv:2503.14738.

[41] IceCube Collaboration (R. Abbasi *et al.*), "Search for decoherence from quantum gravity with atmospheric neutrinos," *Nature Physics* **20**, 913–920 (2024); arXiv:2308.00105.

[42] J. de Boer, E. Verlinde and H. Verlinde, "On the holographic renormalization group," *Journal of High Energy Physics* **08** (2000) 003; arXiv:hep-th/9912012.

[43] K. Kim, A. Aeppli, W. Warfield, A. Chu, A. M. Rey and J. Ye, "Atomic coherence of 2 minutes and instability of 1.5×10^{-18} at 1 s in a Wannier–Stark lattice clock," *Physical Review Letters* (2025); arXiv:2505.06444.

[44] P. Wang, C.-Y. Luan, M. Qiao, M. Um, J. Zhang, Y. Wang, X. Yuan, M. Gu, J. Zhang and K. Kim, "Single ion qubit with estimated coherence time exceeding one hour," *Nature Communications* **12**, 233 (2021).

[45] T. Bothwell, C. J. Kennedy, A. Aeppli, D. Kedar, J. M. Robinson, E. Oelker, A. Staron and J. Ye, "Resolving the gravitational redshift across a millimetre-scale atomic sample," *Nature* **602**, 420–424 (2022).

[46] E. K. Anderson *et al.* (ALPHA Collaboration), "Observation of the effect of gravity on the motion of antimatter," *Nature* **621**, 716–722 (2023).

[47] J. Yin *et al.*, "Satellite-based entanglement distribution over 1200 kilometers," *Science* **356**, 1140–1144 (2017).